

Aus dem Biomedizinischen Zentrum  
Institut für Chirurgische Forschung (Walter-Brendel-Zentrum  
für experimentelle Medizin)  
der Ludwig-Maximilians-Universität München  
Kommissarischer Vorstand: Prof. Dr. med. dent. Reinhard Hicklel

***In vivo* pharmacological profiling in *Xenopus* embryos  
defines a subset of A<sub>1</sub> adenosine receptor-selective  
antagonists with potent anti-angiogenic activities**

Dissertation zum Erwerb  
des Doktorgrades der Naturwissenschaften  
an der Medizinischen Fakultät der Ludwig-Maximilians-Universität  
München



**vorgelegt von  
Mazhar Gull  
aus Pakistan  
2016**

Mit Genehmigung der Medizinischen Fakultät  
der Universität München

Erstgutachter:

Prof. Dr. phil. André W. Brändli

Zweitgutachter:

Prof. Dr. Ralph A.W. Rupp

Dekan:

Prof. Dr. med. dent. Reinhard HICKEL

Tag der mündlichen Prüfung: 07.07.2017



“You never change things by fighting the existing reality.  
To change something, build a new model that makes the existing model  
obsolete.”

R. Buckminster Fuller

## Table of Contents:

Table of figures.....	IX
Table of tables.....	XI
Abstract.....	XIII
Zusammenfassung .....	XIV
Introduction .....	1
A chemical genetic screen in <i>Xenopus</i> embryos defines adenosine receptor antagonists as modulators of the vasculature .....	2
G-protein coupled receptors constitute key mediators of cellular response .....	7
Structural diversity of the GPCR superfamily .....	8
Guanosine nucleotide-binding proteins.....	12
GPCR activation and signaling.....	14
Adenosine .....	16
The adenosine receptor family of GPCRs .....	18
AR signaling and biological functions .....	19
Crystal structures of adenosine receptors.....	23
Expression of adenosine receptors .....	29
Genetic analysis of adenosine receptor functions.....	31
Roles for adenosine receptors in angiogenesis and lymphangiogenesis.....	33
Adenosine receptors as therapeutic targets .....	37
Hypothesis and Aims .....	40

Materials and methods.....	41
Obtaining <i>Xenopus</i> embryos .....	42
Pharmacological treatments of <i>Xenopus</i> embryos.....	43
Whole mount <i>in situ</i> hybridizations.....	45
Marker genes for antisense probe synthesis .....	49
Microinjection of morpholino oligonucleotides .....	49
Mammalian cell culture .....	49
Chemical treatments and immunostaining of cell cultures .....	50
FACS analysis of A <sub>1</sub> AR antagonist treated cells.....	50
Proliferation and sprouting assays.....	51
Results .....	53
Reanalysis of an <i>in vivo</i> chemical library screen defines AR-subtype specific antagonists for testing in <i>Xenopus</i> embryos .....	54
Widespread expression of ARs in <i>Xenopus</i> embryos.....	59
Antagonists with selectivity for A <sub>1</sub> ARs are effective at inducing edema in <i>Xenopus</i> embryos .....	61
Combination treatments with antagonists targeting A <sub>2A</sub> , A <sub>2B</sub> or A <sub>3</sub> ARs were ineffective at inducing edema formation.....	65
AR antagonists affecting blood and lymph vessel morphogenesis .....	68
DEPX and 7CN treatments disrupt lymph vessel morphogenesis.....	70
7CN and DEPX specific antagonists did not affect hematopoiesis, erythrocyte dispersal and muscle differentiation.....	73

Effects of DEPX and 7CN on endothelial cell proliferation and sprouting <i>in vitro</i> .....	75
Structure-activity relationship studies .....	78
The <i>in vivo</i> activity of DEPX is influenced by side chain length .....	78
Endothelial cell proliferation is not affected by DEPX derivatives.....	84
The <i>in vivo</i> activity of 7CN requires the presence of a phenyl ring .....	85
7MN inhibits endothelial cell proliferation and sprouting .....	89
7MN and 7CN cause mitotic arrest <i>in vitro</i> .....	91
7MN and 7CN disrupt the microtubular cytoskeleton.....	93
Discussion.....	96
<i>In vivo</i> identification of vascular disruptive agents .....	97
<i>Xenopus</i> embryos as a powerful model to identify the vascular disruptive agents <i>in vivo</i> .....	98
AR agonists fail to induce edema in <i>Xenopus</i> embryos .....	100
Pharmacological inhibition of A <sub>2A</sub> , A <sub>2B</sub> or A <sub>3</sub> AR signaling does not affect vascular development.....	101
A <sub>1</sub> AR antagonists induce edema <i>in vivo</i> .....	102
Only a subset of A <sub>1</sub> AR antagonists affect blood and lymph vessel development <i>in vivo</i> .....	104
Structure-activity relationship studies reveal critical molecular determinants for bioactivity <i>in vivo</i> .....	105
Physicochemical properties and <i>in vivo</i> bioactivities of AR antagonists .....	108
Endothelial cells are direct targets of 7CN and 7MN .....	109

DEPX and DPPX exert their anti-angiogenic activities via an indirect mechanism .....	109
7CN and 7MN inhibit endothelial cell proliferation and sprouting by destabilization of the microtubular cytoskeleton .....	111
Tissue and cell-type selectivities of the active compounds .....	112
Conclusions .....	115
Outlook.....	116
Bibliography .....	119
Acknowledgements .....	132
Deklaration .....	134
Appendix .....	135
Abbreviation.....	135
Curriculum Vitae .....	138

## Table of figures

Figure 1. Schematic illustration of the relationship between the blood circulation and the lymphatic system. ....	2
Figure 2. Two-step whole-organism based chemical library screening strategy to identify modulators of vascular development in <i>Xenopus</i> embryos.....	5
Figure 3. Human GPCR superfamily sequence homology tree.....	10
Figure 4. GPCR subfamilies and their ligands. ....	11
Figure 5. Classification, expression, and function of G protein $\alpha$ subunit family members. ....	13
Figure 6. Diversity of GPCRs activation and signaling.....	15
Figure 7. Structures and extracellular degradation of ATP to adenosine.....	17
Figure 8. Overview of the intracellular signaling pathways activated by ARs. ...	22
Figure 9. Agonist bound crystal structure of $A_{2A}$ AR. ....	26
Figure 10. Comparison of the ligand binding sites of $A_{2A}$ adenosine receptors bound to various ligands. ....	28
Figure 11. General structural architecture of $A_{2A}$ adenosine receptors highlighting the binding sites for orthosteric and allosteric ligands.....	28
Figure 12. Model explaining the functions of different AR subtypes in the stimulation of angiogenesis. ....	35
Figure 13. Proposed disease targets for selective adenosine receptor ligands...	38
Figure 14. Expression of AR genes in <i>Xenopus</i> embryos. ....	60
Figure 15. Procedure to assess the potency of AR antagonists to induce edema formation in <i>Xenopus</i> embryos. ....	61
Figure 16. Distinct edema phenotypes induced by subtype-specific AR antagonists in <i>Xenopus</i> embryos.....	62
Figure 17. Dose-response relationships of phenotypes induced in <i>Xenopus</i> embryos by AR antagonist treatment.....	64
Figure 18. Summary of the phenotypes observed after treatment of <i>Xenopus</i> embryos with AR antagonist combinations. ....	66

Figure 19. AR antagonists interfering with blood vessel morphogenesis.....	69
Figure 20. AR antagonists interfering with lymph vessel morphogenesis.....	71
Figure 21. AR antagonist treatments do not affect pronephric kidney development. ....	72
Figure 22. Effects of DEPX and 7CN treatments on erythropoiesis, hemangiopoiesis, and myogenesis in <i>Xenopus</i> embryos. ....	74
Figure 23. Effects of DEPX and 7CN on endothelial cell proliferation.....	76
Figure 24. Effects of DEPX and 7CN on endothelial cell sprouting. ....	77
Figure 25. Selected derivatives of DEPX. ....	78
Figure 26. Dose-response relations of phenotypes induced by AR antagonists in <i>Xenopus</i> embryos. ....	80
Figure 27. Edema phenotypes induced by DPPX in <i>Xenopus</i> embryos.....	81
Figure 28. DPPX disrupts vascular development in developing embryos. ....	82
Figure 29. Effects of DPPX on selected tissues and organs of <i>Xenopus</i> embryos. .....	83
Figure 30. DEPX derivatives did not affect endothelial cell proliferation. ....	84
Figure 31. Compound structurally related to 7CN. ....	85
Figure 32. Dose-response relationship of phenotypes induced by 7MN. ....	86
Figure 33. Edema phenotypes induced by 7MN in <i>Xenopus</i> embryos.....	87
Figure 34. 7MN interfered with vasculature development in <i>Xenopus</i> embryos.	87
Figure 35. Effects of 7MN treatment on selected organs in <i>Xenopus</i> embryos. .	88
Figure 36. Human endothelial cell proliferation is inhibited by 7MN.....	89
Figure 37. 7MN inhibited on endothelial sprout formation. ....	90
Figure 38. 7MN and 7CN induce mitotic arrest with increased DNA content.....	92
Figure 39. Effects on the microtubular cytoskeleton of HUVECs after a 2-hour treatment with 7MN and 7CN. ....	94
Figure 40. Effects on the microtubular cytoskeleton of HUVECs after a 16-hour treatment with 7MN and 7CN. ....	95

## Table of tables

Table 1. Number of human GPCR genes by class.....	9
Table 2. Primary sequence and key properties of human ARs.....	19
Table 3. Crystal structures of the A <sub>2A</sub> adenosine receptor .....	25
Table 4. Expression domains of AR subtypes in zebrafish, mouse, and human .	30
Table 5. Selection of phenotypes observed in AR knockout mice .....	32
Table 6. Summary of AR involvement in angiogenesis using human cell cultures .....	34
Table 7. AR antagonists selected for the pharmacological studies .....	44
Table 8. Protocol for whole mount <i>in situ</i> hybridization of <i>Xenopus</i> embryos....	47
Table 9. AR agonists tested in <i>Xenopus</i> embryos by Kalin <i>et al.</i> (2009).....	56
Table 10. AR antagonists tested in <i>Xenopus</i> embryos by Kalin <i>et al.</i> (2009) ....	57
Table 11. AR-subtype selective antagonists chosen for <i>in vivo</i> testing in <i>Xenopus</i> embryos .....	58
Table 12. Compilation of pharmacological parameters obtained from <i>Xenopus</i> embryos after AR antagonist treatment .....	65
Table 13. Frequencies of phenotypes observed in <i>Xenopus</i> embryos treated with AR antagonist combinations .....	67
Table 14. DEPX derivatives and their AR subtype selectivities .....	79
Table 15. Pharmacological values obtained from <i>Xenopus</i> embryos after treatment with DEPX derivatives .....	80
Table 16. 7CN derivatives and their AR subtype selectivities.....	85
Table 17. Pharmacological values of 7CN derivatives obtained from the treatment of <i>Xenopus</i> embryos.....	86

Table 18. Comparison between $K_i$ values and selected pharmacological parameters of $A_1$ AR antagonists .....	103
Table 19. Chemical properties of 7CN, DEPX, and their derivatives .....	107

## Abstract

The purine nucleoside adenosine is an important intermediate metabolite, which is released from most cells. It mediates signaling through activation of four distinct adenosine receptors (ARs): A<sub>1</sub>, A<sub>2A</sub>, A<sub>2B</sub>, and A<sub>3</sub>. ARs have been recognized as therapeutic targets for a wide range of physiological processes and pathophysiological conditions, including epilepsy, chronic pain, ischemia, inflammation, and cancer. This has led to the development of various subtype-specific AR antagonists. By screening a chemical library *in vivo*, we had previously recovered AR antagonists as inhibitors of blood and lymph vessel angiogenesis in *Xenopus* embryos [Kalin *et al.* 2009 Blood 114, 1110-1122]. Here, we assessed the role of adenosine signaling in vascular development in *Xenopus* embryos by testing a panel of subclass-selective AR antagonists for anti-(lymph) angiogenic activities. Compound-treated embryos were assessed phenotypically for evidence of edema formation, which is a reliable pathophysiological indicator of anti-angiogenic activity. Quantitative pharmacological parameters, such as EC<sub>50</sub>, EC<sub>max</sub>, and LC<sub>50</sub> values, were established for each compound. While antagonists selective for A<sub>2A</sub>, A<sub>2B</sub>, or A<sub>3</sub> ARs were typically inactive, all A<sub>1</sub> AR antagonists were found to induce edema with EC<sub>50</sub> values ranging from 0.3 to 6.7 μM. However, only two compounds, 7-chloro-4-hydroxy-2-phenyl-1, 8-naphthyridine (7CN) and 1,3 Diethyl-8-phenylxanthine (DEPX), had potent anti-angiogenic activities *in vivo*. Subsequently, structure-activity relationship studies led to the identification of two additional compounds, 7-methyl-2-phenyl-1, 8-naphthyridine (7MN) and 1,3-dipropyl-8-phenylxanthine (DPPX), equally capable of disrupting vascular development in *Xenopus* embryos. Treatment of primary human endothelial cell cultures demonstrated that only 7CN and 7MN but not DEPX and DPPX disrupted cell proliferation and VEGF-induced sprouting *in vitro*. Gene expression and knockdown studies in *Xenopus* embryos failed however to provide evidence for a central role of A<sub>1</sub> ARs in vascular development. This suggests that the antiangiogenic activities of 7CN and 7MN may be due to polypharmacology involving inhibition of other targets than A<sub>1</sub> ARs alone. In fact, we found that 7CN and 7MN induced destabilization of microtubules, mitotic arrest, and excess DNA replication in endothelial cell cultures. Taken together, phenotypic compound profiling in *Xenopus* embryos has led to the identification of 7CN and 7MN as promising drug candidates that act as potent anti-angiogenic compounds interfering with essential endothelial cell functions.

## Zusammenfassung

Das Purinnukleosid Adenosin ist ein wichtiger Metabolit, der von vielen Zellen freigesetzt wird. Adenosin wirkt als Signalmolekül mittels Aktivierung von vier verschiedenen Adenosinrezeptoren (AR): A<sub>1</sub>, A<sub>2A</sub>, A<sub>2B</sub> und A<sub>3</sub>. AR dienen als vielversprechende Angriffspunkte für die Entwicklung von Arzneimitteln zur Modulation einer breiten Palette von physiologischen Prozessen und pathophysiologischen Zuständen, einschliesslich Epilepsie, chronischen Schmerzen, Ischämie, Entzündungen und Krebs. In der Folge wurden verschiedene subtypspezifische AR-Antagonisten entwickelt. Mittels eines *In Vivo* Screening-Verfahrens hatte unsere Arbeitsgruppe zuvor mehrere AR-Antagonisten einer chemischen Bibliothek als Inhibitoren der Blut- und Lymphgefässangiogenese in *Xenopus* Embryonen identifiziert [Kalin et al. 2009 Blood 114, 1110-1122]. In der vorliegenden Arbeit untersuchten wir mittels einer Reihe von subklassenselektiven AR-Antagonisten die Rolle der Signalwirkung von Adenosin bei der Bildung des Gefässsystems in *Xenopus* Embryonen. Insbesondere wurde nach anti-lymphatischen bzw. -angiogenetischen Aktivitäten *in vivo* gesucht. Wirkstoff-behandelte Embryonen wurden phänotypisch beurteilt und auf Ödembildung als zuverlässigen pathophysiologischen Indikator für anti-angiogenetische Aktivitäten untersucht. Für jede Verbindung wurden quantitative pharmakologische Parameter, wie EC<sub>50</sub>, EC<sub>max</sub> und LC<sub>50</sub>, ermittelt. Typischerweise waren A<sub>2A</sub>-, A<sub>2B</sub>- oder A<sub>3</sub>-AR-selektive Antagonisten inaktiv. Hingegen waren alle A<sub>1</sub> AR-Antagonisten aktiv und induzierten Ödeme mit EC<sub>50</sub>-Werten von 0.3 bis 6.7 µM. Allerdings besaßen nur zwei Verbindungen, 7-Chloro-4-hydroxy-2-phenyl-1, 8-naphthyridin (7CN) und 1,3 Diethyl-8-phenylxanthin (DEPX), starke anti-angiogenetische Aktivitäten *in vivo*. Anschliessend wurden Studien zur Struktur-Wirkungs-Beziehung durchgeführt. Diese führten zur Identifizierung von zwei zusätzlichen Verbindungen, 7-Methyl-2-phenyl-1, 8-naphthyridin (7MN) und 1,3-Dipropyl-8-phenylxanthin (DPPX), die in der Lage waren, die Gefässbildung in *Xenopus* Embryonen zu stören. Die Behandlung von primären humanen Endothelzellkulturen zeigte dann, dass nur 7CN und 7MN, aber nicht DEPX und DPPX, in der Lage waren die Proliferation und das VEGF-induzierte Sprouting *in vitro* zu unterbinden. Umfangreiche Genexpressions- und Knockdown-Studien lieferten keine Hinweise für eine zentrale Rolle von A<sub>1</sub> AR bei der vaskulären Gefässbildung in *Xenopus* Embryonen. Dies weist darauf hin, dass die anti-angiogenetischen Aktivitäten von 7CN und 7MN vermutlich auf Polypharmakologie zurückzuführen sind und sich nicht durch die alleinige

Hemmung von A<sub>1</sub> ARs erklären lassen. In der Tat fanden wir, dass die Behandlung von endothelialen Zellkulturen mit 7CN und 7MN zu einer Destabilisierung des mikrotubulären Zytoskeletts, einer Blockierung der Mitose und zu übermässiger DNA Replikation führten. Zusammengenommen hat die phänotypische Charakterisierung von AR Antagonisten in *Xenopus* Embryonen zur Identifizierung von 7CN und 7MN als viel versprechende Wirkstoffkandidaten geführt. Beide Verbindungen haben potente anti-angiogenetische Aktivitäten, welche wesentliche endotheliale Zellfunktionen stören.



## A chemical genetic screen in *Xenopus* embryos defines adenosine receptor antagonists as modulators of the vasculature

The vasculature comprises of an extensively branched network, and is among the first organ systems to develop within the developing embryo. In vertebrates, two vascular systems exist, namely the blood vasculature and the lymphatic vasculature, which are hierarchical networks of vessels lined by endothelial cells (Schuermann et al., 2014, Neufeld et al., 2014). The blood vasculature is comprised of arterial vessels carrying oxygenated blood from the lungs via the heart to the periphery, whereas venous vessels return oxygen-depleted blood to the lungs to discharge CO<sub>2</sub>. The lymphatics represent a separate vessel system that permeates the body and communicates with the blood vasculatures via thoracic duct, which drains lymph into the blood circulation (Fig. 1). Besides the transport of oxygen and CO<sub>2</sub>, the physiological roles of the blood vasculature include the transport of nutrients, signaling molecules, and immune cells to all tissues and organs of the vertebrate body. Key functions attributed to the lymphatic vasculature include roles in immune regulation, tissue fluid homeostasis, the uptake of dietary fats, and the absorption of excess extravasated protein-rich fluids from the interstitial spaces and their return to the blood circulation (Stacker et al., 2014, Schuermann et al., 2014).

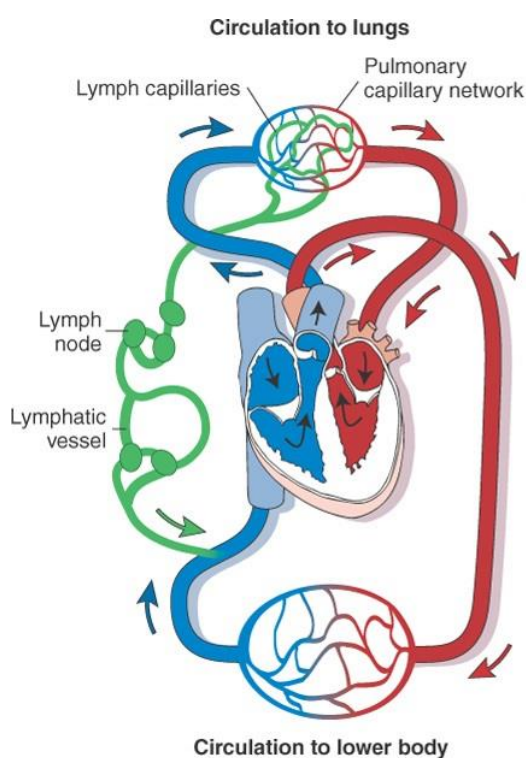


**Figure 1. Schematic illustration of the relationship between the blood circulation and the lymphatic system.** The blood vessels form a closed circulatory system composed of arteries (red) and veins (blue). The lymphatic system (green) forms a one-way conduit for tissue fluid and leukocytes. Tissue fluids are drained by lymph capillaries and transported by a series of larger lymphatic vessels into the venous blood circulation. Picture is modified from [www.softchalk.com](http://www.softchalk.com).

Unlike most other organs of the adult body, the vasculature has a remarkable capacity to grow and extend also in adult organism. This can occur as a natural process, for example as a response to hypoxia to meet increased needs for oxygenation, during the female menstrual cycle, or as part of the wound healing process (Guo and Dipietro, 2010, Demir et al., 2010). By contrast, misregulation of vessel growth is observed as a hallmark of several different pathological conditions and human diseases. For example, an involvement of blood and lymph vessel has been found in chronic inflammatory diseases, like psoriasis, inflammatory bowel disease, and rheumatoid arthritis (Carmeliet, 2003, Roudnicky et al., 2013). Furthermore, tumor growth is usually accompanied by the release of vascular endothelial growth factor (VEGF) triggering the sprouting of new blood vessels from existing vascular beds to fulfill the increased requirements for nutrients and oxygen in the expanding tumor tissue (Dome et al., 2007). Finally, the tumors induce lymphangiogenesis to promote tumor metastasis via lymph nodes by releasing vascular endothelial growth factors (VEGFB, VEGFC) and the activation of VEGF receptor signaling through VEGFR2 and VEGFR3 (Makinen et al., 2001). The ability to influence or modulate blood and lymph vessel growth using small organic molecules or specific antibodies could therefore be beneficial in tumor therapy or any other disease, where pathological blood or lymph vessel growth is observed. For example, Bevacizumab, commercially known as Avastin, is a humanized anti-VEGF monoclonal antibody that was the first anti-angiogenic therapeutic agents approved for cancer treatment. Avastin inhibits all isoforms of VEGF to reduce angiogenesis, tumor growth, and metastasis. Avastin is currently used in chemotherapy against different types of cancers including colorectal, lung, breast, and brain cancer (Greillier et al., 2016, Shih and Lindley, 2006).

A better understanding of vascular and lymphatic development may provide novel drug targets to treat various pathologies associated with dysregulated vascular growth and function. Over the years, different approaches have therefore been used to define molecular determinants and signaling pathways regulating angiogenesis and lymphangiogenesis (Corada et al., 2014). This includes the identification of genes underlying hereditary diseases of the vasculature and lymphatics in the human population, the study of candidate genes using reverse-genetics approaches, and genetic screens in model organisms, such as zebrafish (Habeck et al., 2002, Jin et al., 2007). Chemical genetics uses small organic molecules to perturb biochemical pathways and to identify potential drug targets with efficacy in modulating biological processes

(Schenone et al., 2013). Larvae of aquatic organisms, such as fish and amphibians, are particularly attractive for chemical genetic screening approaches (Wheeler and Brandli, 2009). First, they represent whole organisms with fully functional organs. Second, they are small enough to be cultured in multiwell dishes. Finally, they are sufficiently abundant to envisage the screening of thousands of chemical compounds for suitable bioactivity *in vivo*. Chemical genetics therefore represents an interesting alternative to the above-mentioned genetic approaches in order to define drug candidates targeting the vasculature in living organisms.

Our laboratory had developed in the past an unbiased chemical genetic screening strategy to identify small organic molecules that could interfere with blood and/or lymph vessel development or function *in vivo* (Kalin et al., 2009). About 36 hours post fertilization, *Xenopus* embryos initiate the development of blood and lymphatic vessel systems, which subsequently become fully functional (Ny et al., 2005, Helbling et al., 2000). Edema formation, i.e. abnormal fluid accumulation in tissue and organs, was selected as a pathophysiological read-out indicating an imbalance of fluid homeostasis caused by disruption of blood and/or lymphatic vessel functions. Edema formation is a simple phenotypic trait that can be easily scored in *Xenopus* embryos and tadpoles using a stereomicroscope. The whole-organism based screening strategy was comprised of two steps (Fig. 2).

First, *Xenopus* embryos were arrayed in 48-well dishes and treated with compounds from a chemical library. Compounds inducing edema or late lethality were identified and selected for a secondary screen. In the secondary screen, whole-mount *in situ* hybridization was used to visualize the integrity of the blood and lymphatic vessel systems of compound-treated embryos. Using this 2-step screening strategy, a commercial chemical library of 1280 pharmacologically active compounds (LOPAC<sup>1280</sup>, Sigma-Aldrich) were tested at a concentration of 20  $\mu$ M. In total, 32 bioactive compounds emerged that interfered with angiogenesis and/or lymphangiogenesis *in vivo* from the chemical screen (Kalin et al., 2009). They could be grouped into three distinct categories. Compounds that affected blood vessel development only; compounds selectively interfering with lymph vessel formation; and those interfering with both blood and lymphatic vessel. Importantly, two known VEGFR inhibitors (SU4312, SU5416) were identified as bioactive compounds, which validated the phenotypic *in vivo* screening strategy.

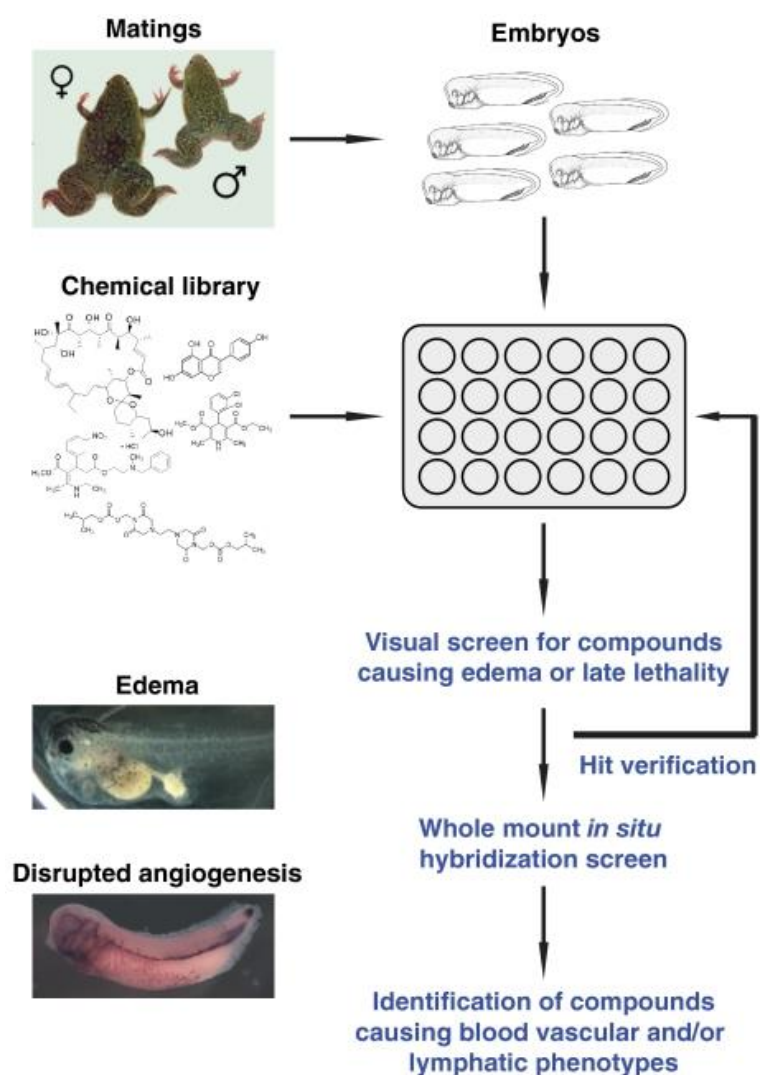


**Figure 2. Two-step whole-organism based chemical library screening strategy to identify modulators of vascular development in *Xenopus* embryos.** In first step, embryos are cultured in multi-well dishes, which contain per well a single compound from a chemical library. Embryos are visually scored for late lethality or the presence of edema. In a second step, whole-mount *in situ* hybridization of compound-treated embryos was performed to identify those compounds interfering with vascular development. Figure taken from Kalin *et al.* (2009).

The study also identified novel compounds, not previously known to interfere with blood and/or lymph vessel development. For example, this included two compounds (1, 3-Diethyl-8-Phenylxanthine, DEPX; 7-Chloro-4-hydroxy-2-phenyl-1,8-naphthyridine, 7CN) known as antagonists that disrupted signaling of G-protein coupled receptors (GPCRs) of the adenosine receptor (AR) subfamily. DEPX and 7CN were effective at disrupting both blood and lymphatic vessel development in *Xenopus* embryos. Furthermore, 7CN blocked proliferation

and tube formation of human endothelial cells *in vitro*. Finally, 7CN inhibited VEGF-induced angiogenesis and lymphatic vessel enlargement in the mouse (Kalin et al., 2009). Collectively, these findings indicate a role for members of the AR family of GPCRs in vascular development and function in *Xenopus*, mouse, and humans. The fact that the *in vivo* chemical screening strategy led to the identification of two chemically distinct AR antagonists (DEPX, 7CN) further strengthens this notion.

Many open questions still remain. What are the half-effective doses of DEPX and 7CN that cause edema formation in *Xenopus* embryos? Are there other than vascular defects observed in DEPX- or 7CN-treated embryos? What are the doses causing lethality in 50% of the treated embryos? What are the molecular targets of DEPX and 7CN? Are there other AR that antagonists disrupt vascular development *in vivo*? The present thesis is aimed at providing answers to the questions raised here.

## **G-protein coupled receptors constitute key mediators of cellular response**

The anti-angiogenic compounds DEPX and 7CN identified by phenotypic drug screening in *Xenopus* embryos (Kalin et al., 2009) target the adenosine receptor (AR) family of G protein-coupled receptors (GPCRs), which are important sensors of extracellular signals. In all living organisms, cell-cell communication represents a vital process for the regulation of various physiological functions. Cells respond to signals from the extracellular environment, through activation of membrane receptors. These receptors convert the external cues into intracellular signals that activate or suppress specific biochemical pathways. Ultimately, this will trigger cell-specific responses, such as morphological changes and differential gene expression. Guanylyl-nucleotide-binding protein-coupled receptors, also known as G protein-coupled receptors (GPCRs), represent the largest superfamily of cell surface receptors present in vertebrate genomes (Fredriksson et al., 2003, Lagerstrom and Schioth, 2008). They are able to respond to a wide range of chemically diverse signals, which includes ions, amines, amino acids, hormones, lipids, peptides, organic odorants, and even photons. GPCRs play vital roles in regulating numerous aspects of human physiology such as vision, smell, and taste, the immune response, cellular metabolism, signal transmission in the nervous system, angiogenesis, endocrine signaling, reproduction, and many others. Given their central role in cellular signaling and in the regulation of important physiological functions of the human body, GPCRs have become important therapeutic targets (Salon et al., 2011, Overington et al., 2006). Currently, about 30-50% of all approved drugs act through modulating GPCR function (Lagerstrom and Schioth, 2008).

The human genome encodes more than 800 distinct GPCR genes and they constitute the largest gene family of cell surface receptors (Jassal et al., 2010, Fredriksson et al., 2003). GPCRs are embedded in the cell membrane and they all share a common topology consisting of a seven transmembrane (7TM) alpha-helical fold. The seven transmembrane (7TM) helices form a bundle that is interlinked by three extracellular (ECL) and three intracellular loops (ICL). The extracellular (EC) region, which may include a sizeable amino terminus, plays an important role in the activation of the receptor. It is responsible for the recognition and binding of ligands and participates in transmitting signals across the membrane (Schulte and Levy, 2007, Ji et al., 1998). Ligand binding induces conformational changes in the EC region and in the 7TM bundle. This will

subsequently lead to structural reorganizations affecting the three ICLs and the C-terminus on the cytoplasmic side enabling the binding of intracellular effectors, such as heterotrimeric G proteins (Unal and Karnik, 2012).

### **Structural diversity of the GPCR superfamily**

More than 4% of all genes present in the human genome encode for GPCRs, which comprise the largest superfamily of integral membrane proteins. GPCRs are characterized by a similar 7TM topology and they share highest sequence homology in the TM domains. Structural diversity is mainly confined to the amino- and carboxy-terminal domains (Kobilka, 2007). The overall sequence identity between GPCRs is low and even for the TM domains it is typically less than 20%. On the basis of sequence and structural similarities, the GPCR superfamily is commonly divided into five major classes and numerous subfamilies (Cobanoglu et al., 2011, Fredriksson and Schiöth, 2005, Fredriksson et al., 2003). A phylogenetic tree of the human GPCR superfamily is shown in Fig. 3. Class A, also known as *Rhodopsin* family, is the largest family of GPCRs comprising approximately 700 human receptor proteins (Krishnan et al., 2012, Jassal et al., 2010). They bind a diverse range of ligands, including amines, purines and peptides. Furthermore, they are targets for the majority of drugs in clinical use that interfere with GPCR functions (Tyndall and Sandilya, 2005). Class A is further divided in four subgroups:  $\alpha$ ,  $\beta$ ,  $\gamma$ , and  $\delta$ ; and they consist of many prominent GPCR genes. Rhodopsin (RHO), cannabinoid (CNR) and adenosine receptors (ADORA) belong to subgroup  $\alpha$ ; endothelin (EDNRA, EDNRB) and neuropeptide Y (NPY1R, NPY2R, NPY5R) receptors are part of  $\beta$  group; subgroup  $\gamma$  contains chemokine receptors (CCR, CXCR), angiotensin receptors (AGTR) and melanin-concentrating hormone receptors (MCHR1, MCHR2); and  $\delta$  group harbors follicle stimulating hormone receptor (FSHR) and purinergic receptors (P2Y) among others. With 388 distinct genes, olfactory receptors represent the biggest gene cluster in  $\delta$  group of the *Rhodopsin* family of GPCRs (Lagerstrom and Schiöth, 2008, Krishnan et al., 2012). Class B is the second largest GPCRs family and it contains two subfamilies: the *Secretin* and *adhesion* receptor families. The *Secretin* receptor family (15 genes) is characterized by an extracellular hormone-binding domain, which mainly recognizes peptides hormones. *Adhesion* receptor family is comprised of 33 members, which contain GPCR proteolytic (GPS) domains. *Secretin* receptor family members do not have GPS domains and they differ in the N-termini from

Adhesion receptors. For these reasons, they are classified separately (Fredriksson et al., 2003).

The classification of GPCRs put forward by Fredriksson *et al.* in 2003 has to date been largely upheld. With the improvements in annotating the human genome, the total number of human GPCRs has however increased to 836 genes (Cvacek et al., 2016). Furthermore, vomeronasal receptors (VNR) have been recognized as a separate class, since they have little similarity to other families of GPCRs. They appear to be distantly related to TAS2 and rhodopsin-like GPCRs. Table 1 provides the current gene numbers by GPCR class.

**Table 1. Number of human GPCR genes by class**

<b>Class</b>	<b>Genes</b>	<b>Class</b>	<b>Genes</b>
A - alpha	88	B - Secretin	16
A - beta	33	B - Adhesion	33
A - gamma	57	C - Glutamate	22
A - delta	58	Frizzled/TAS2	36
A - other	51	Vomeronasal	5
A - Olfactory	418	Other	11

Class A and class B are comprised of 705 and 49 genes, respectively. "Other" refers to currently unclassified GPCRs. Table adapted from Cvacek *et al.* (2016).

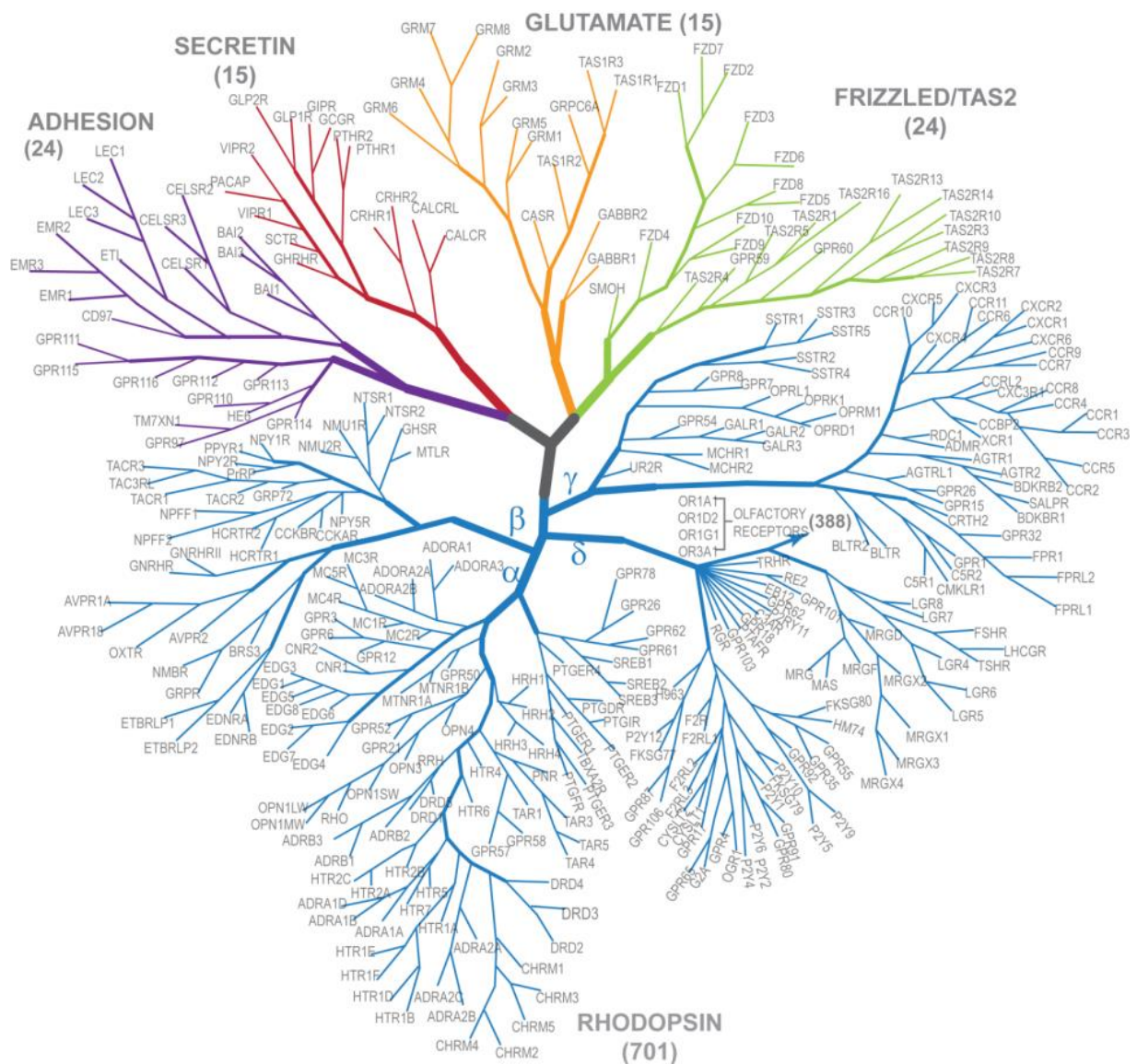


**Figure 3. Human GPCR superfamily sequence homology tree.** The phylogenetic tree was constructed based on sequence similarity in the seven transmembrane domains. The tree shows the five major families of GPCRs: *Rhodopsin* family (class A); *Secretin* and *Adhesion* families (class B); *Glutamate* family (class C) and *Frizzled/taste 2* receptors (TAS2) family. The *Rhodopsin* family is further divided into subfamilies: the  $\alpha$ -group, the  $\beta$ -group, the  $\gamma$ -group, and the  $\delta$ -group as indicated. The  $\delta$ -group also contains the olfactory receptors. Only four olfactory receptors are shown, but they comprise the largest distinct group with 388 receptors. Figure was adapted from Stevens *et al.* (2013).

The class C or *Glutamate* receptor family is comprised of 22 human GPCR proteins, which includes GPRC6A, eight metabotropic glutamate receptors (GRMs), two GABBRs, seven orphan receptors and the calcium-sensing receptor (CASR) (Lagerstrom and Schiöth, 2008). Most members of the *Glutamate* family have long N-termini with contain cysteine rich domains (CRD), which distinguish

them from other GPCR families. The *Frizzled/Taste 2* receptor (TAS2) family includes two distinct clusters, the frizzled receptors and the TAS2 receptors. The *frizzled* branch contains the smoothed receptor (SMO) and the ten frizzled receptors (FZD1-10). SMO acts in a ligand-independent manner in the regulation of the hedgehog signaling pathway (Amakye et al., 2013). By contrast, the binding of Wnt glycoprotein family members activates FZD signaling (MacDonald and He, 2012). Finally, the *Taste2 receptor (TAS2)* family embraces 25 distinct TAS2 genes in human genome; with all of them confined to chromosomes 9 and 12. Fig. 4 provides an overview of the key structural features of the different GPCR families and their ligands. Diversity is associated with the extracellular domains, while the characteristic arrangement of the TM domains is shared. The ability of their extracellular domains to interact with small organic molecules has rendered GPCRs the targets of a substantial proportion of the currently approved drugs on the market (Tesmer, 2016, Wise et al., 2002).

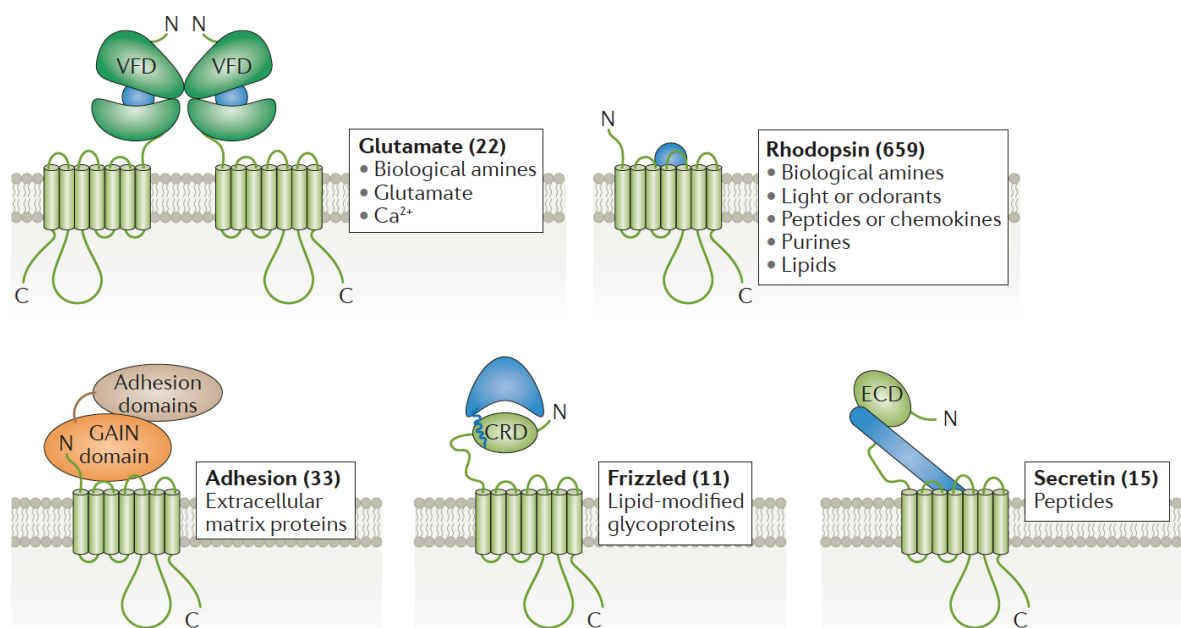


**Figure 4. GPCR subfamilies and their ligands.** The diversity of extracellular domains is evident, whereas the topology of the TM domains is conserved. Numbers in parentheses correspond to the number of GPCR genes identified for each family shown in the human genome. Olfactory GPCRs are included in the rhodopsin family. Members of the TAS2 and vomeronasal families are not shown, as they lack analogous extracellular domains (ECD). Complete listing of the human GPCR gene numbers is provided in Table 1. The Venus fly trap domains (VFD) mediate dimerization of glutamate receptors. Adhesion receptors contain GPCR autoproteolysis-inducing domains (GAIN) that cleave the ECD. The mature receptors exist therefore as two non-covalently associated subunits. GPCR ligands are shown in blue and the location of their binding sites are shown. Wnts are ligands for GPCRs of the Frizzled subfamily. These ligands are modified covalently by palmitoylation (jagged line) and bind to the cysteine-rich domains (CRD) of the receptors. Figure adapted and modified from Tesmer (2016).

### **Guanosine nucleotide-binding proteins**

GPCRs transduce signals by activating effector proteins, called guanosine nucleotide-binding proteins or G proteins, which are members of a group of enzymes known as GTPases (Ross and Wilkie, 2000, Oldham and Hamm, 2008). G proteins are heterotrimeric protein complexes containing three subunits:  $G\alpha$ ,  $G\beta$ , and  $G\gamma$ . Typically, mammalian genomes harbor genes for 16 distinct  $G\alpha$  subunits, 7  $G\beta$  subunits, and 11  $G\gamma$  subunits (Hurowitz et al., 2000). The  $G\alpha$  subunit genes encode for GTP-binding proteins and comprise the biggest family of G protein subunits (Fig. 5). They are further divided into four classes:  $G\alpha_s$ ,  $G\alpha_i/G\alpha_o$ ,  $G\alpha_q/G\alpha_{11}$ , and  $G\alpha_{12}/G\alpha_{13}$ . They are widely expressed throughout the body and interfere with different signaling pathways and ion channels.  $G\alpha_s$  is responsible for the stimulation of adenylyl cyclase.  $G\alpha_i$  inhibits adenylyl cyclase and is also responsible for the activation of G-protein-coupled inwardly rectifying potassium (GIRK) channels.  $G\alpha_q$  acts by regulating phospholipase C (PLC), which converts phosphatidylinositol bisphosphate ( $PIP_2$ ) into diacylglycerol and inositol triphosphate ( $IP_3$ ). Finally,  $G\alpha_{12}$  activates Rho guanine-nucleotide exchange factors (GEFs). The biochemical functions and primary gene expression domains of  $\alpha$  subunits of trimeric G proteins are compiled in Fig. 5. The G protein  $\beta$  and  $\gamma$  subunits are important for the formation of the heterotrimeric protein complex (Smrcka, 2008, Worzfeld et al., 2008). After GPCR activation, the  $G\alpha$  subunit harboring the GTPase activity dissociates from heterotrimeric complex, but  $G\beta\gamma$  remains composed and is called the  $G\beta\gamma$  complex.  $G\beta\gamma$  complexes do not contain catalytic activity, they exert their downstream effects through regulation of ion channels by protein-protein interaction. Furthermore, they regulate second messenger signaling.

Name	Expression	Effector
<b>G<sub>αs</sub> class</b>		
G <sub>αs</sub>	Ubiquitous	AC↑
G <sub>αolf</sub>	Olfactory epithelium, brain	AC↑
<b>G<sub>αi</sub>/G<sub>αo</sub> class</b>		
G <sub>αi1</sub>	Widely distributed	} AC↓ (directly regulated)
G <sub>αi2</sub>	Ubiquitous	
G <sub>αi3</sub>	Widely distributed	
G <sub>αo</sub>	Neuronal, neuroendocrine	VDCC↓, GIRK ↑
G <sub>αz</sub>	Neuronal, platelets	AC↓, Rap1GAP
G <sub>αgust</sub>	Taste cells, brush cells	Unknown
G <sub>αt-r</sub>	Retinal rods, taste cells	PDE ↑
G <sub>αt-c</sub>	Retinal rods	PDE ↑
<b>G<sub>αq</sub>/G<sub>α11</sub> class</b>		
G <sub>αq</sub>	Ubiquitous	} PLC-β↑
G <sub>α11</sub>	Almost ubiquitous	
G <sub>α14</sub>	Kidney, lung, spleen	
G <sub>α15/16</sub>	Hematopoietic cells	
<b>G<sub>α12</sub>/G<sub>α13</sub> class</b>		
G <sub>α12</sub>	Ubiquitous	PDZ-RhoGEF/LARG, others
G <sub>α13</sub>	Ubiquitous	Lsc, PDZ-RhoGEF/LARG, others

**Figure 5. Classification, expression, and function of G protein  $\alpha$  subunit family members.** The primary expression domains of the different  $\alpha$  subunits and the key effectors are listed. Abbreviations: AC, adenylyl cyclase; GIRK, G-protein-regulated inward-rectifier potassium channel; PDE, phosphodiesterase; PDZ, PSD95-Disc-large-ZO-1; PLC, phospholipase C; RhoGEF, Rho guanine nucleotide exchange factor; VDCC, voltage-dependent Ca<sup>2+</sup>-channel. The figure is taken from Worzfeld *et al.* (2008).

## **GPCR activation and signaling**

GPCRs are activated by ligand binding (Dorsam and Gutkind, 2007, Conn et al., 2009, Kenakin, 2010). While the endogenous GPCR ligands can come in many different flavors, such as ions, biogenic amines, amino acids, peptides, hormones, and lipids (Fig. 4), they all activate GPCR signaling by occupying a receptor-specific extracellular ligand-binding pocket, known as the orthosteric site. This causes subtle conformation changes in the GPCR structure triggering activation of trimeric G protein signaling on the intracellular side. GPCR ligands can work in two ways (Wootten et al., 2013). As classical agonists, they stimulate GPCR signaling by binding to the orthosteric binding site. In contrast, the binding of antagonists blocks GPCR activation. Antagonists that do so by binding to the orthosteric site, where they may displace the activating agonist, are known as inverse agonists. The detailed knowledge about the interaction of GPCR ligands with their orthosteric binding sites has been essential for the development of therapeutics targeting GPCR signaling (Katritch et al., 2012).

A single GPCR can couple to one or more distinct trimeric G proteins. In their resting stage, trimeric G proteins interact with GPCRs and they have GDP bound to the  $G\alpha$  subunit. Agonist-induced GPCR activation triggers the exchange of GDP for GTP and the dissociation of the  $G\alpha$  subunit from the  $G\beta\gamma$  subunits. After dissociation,  $G\alpha$ -GTP and the  $G\beta\gamma$  heterodimers have the capability to interfere with different effectors to regulate intracellular signaling pathways. This is achieved by regulating enzymatic effectors, like phospholipase C (PLC) isoforms, adenylate cyclase or ion channels, which in turn triggers the generation or release of small molecules (cAMP,  $Ca^{2+}$ ) referred to as second messengers. They control intermediary metabolism by modulating the activities of protein kinases, such as PKA (via cAMP) and PKC (via  $Ca^{2+}$ ) (Luttrell, 2008). Typically,  $G\alpha_s$  family members cause an increase in intracellular cAMP concentration by stimulation of adenylyl cyclase, whereas members of  $G\alpha_i$  /  $G\alpha_o$  class lower cAMP levels by inhibition of adenylyl cyclase or stimulation of phosphodiesterases (PDE) (Fig. 5, 6). The  $G\alpha_q$  /  $G\alpha_{11}$  class activates phospholipase C, which cleaves  $PIP_2$  to diacylglycerol and  $IP_3$ , ultimately increasing intracellular  $Ca^{2+}$  levels. Besides the regulation of the classical second-messenger generating pathways, members of the  $G\alpha_{12}$  /  $G\alpha_{13}$  class and  $G\beta\gamma$  subunits control key intracellular signal-transducing effectors, including small GTP-binding proteins of the Ras and Rho classes, guanine nucleotide exchange factors (GEF) and various serine-threonine kinases (MAPK, ERK, JNK),

which remain to be fully elucidated. Ultimately, the activation of GPCR-regulated signaling networks controls many cellular functions, such as proliferation, differentiation, migration, and survival. Importantly, dysregulation of GPCR signaling can contribute to pathophysiological processes, such as cancer progression and metastasis (Dorsam and Gutkind, 2007).

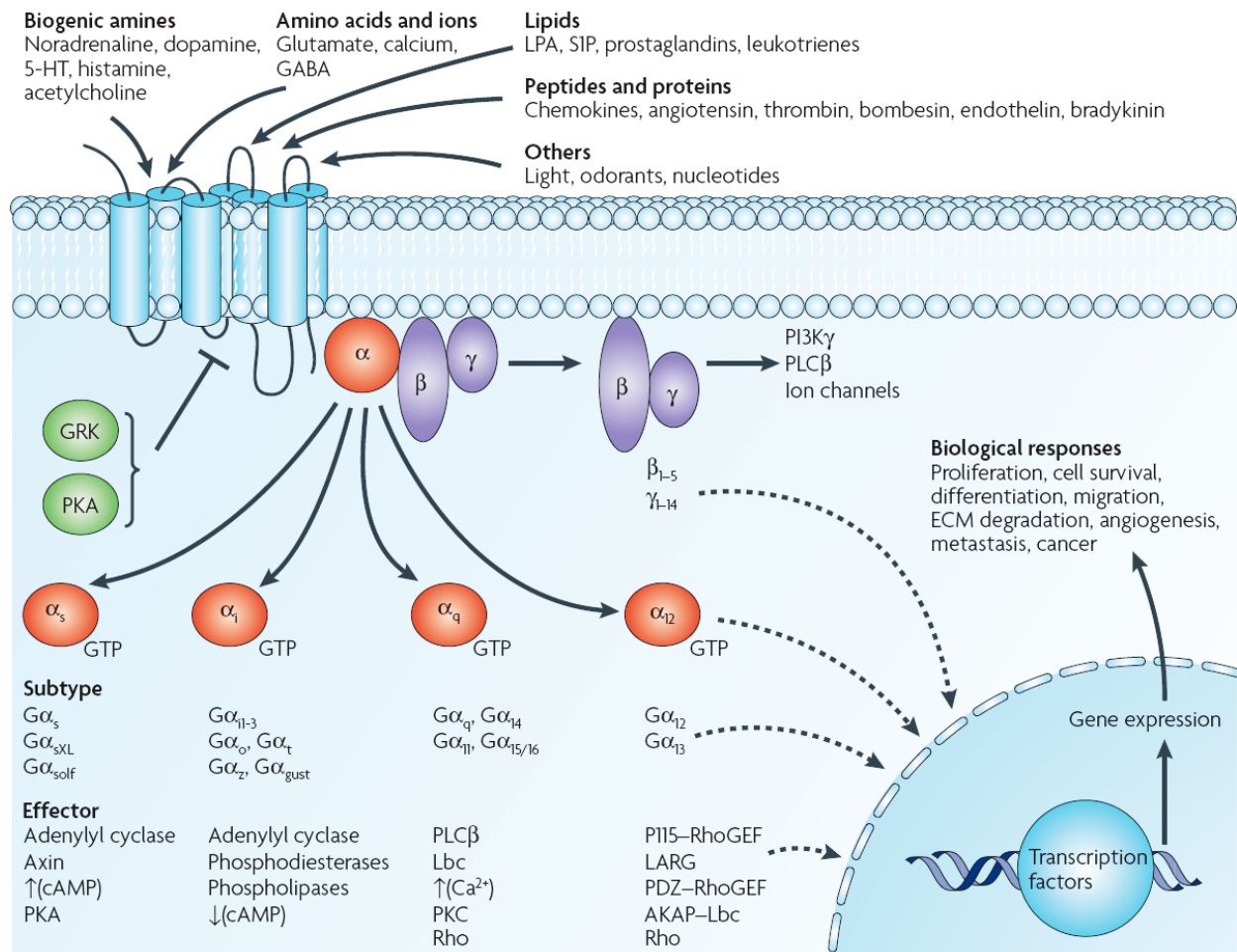


**Figure 6. Diversity of GPCRs activation and signaling.** Various ligands use GPCRs to transmit extracellular signals into the cell to regulate membrane, cytoplasmic, and nuclear targets. This will elicit a wide range of biological responses, such as cell proliferation, survival, differentiation, and migration. Abbreviations: 5-HT, 5-hydroxytryptamine; ECM, extracellular matrix; ERK, extracellular signal-regulated kinase; JNK, c-jun N-terminal kinase (JNK); GABA, gamma-aminobutyric acid; GEF, guanine nucleotide exchange factor; GRK, G protein receptor kinase; IP3, inositol triphosphate; LPA, lysophosphatidic acid; PI3K, phosphatidylinositol 3-kinase; PIP, phosphatidylinositol bisphosphate; PKA, protein kinase A; PKC, protein kinase C; PLC, phospholipase C; S1P, sphingosine-1-phosphate. Figure taken from Dorsam and Gutkind (2007).

### **Adenosine**

The endogenous purine nucleoside adenosine is an important intermediate metabolite, composed of adenine and ribose. It is a component of the biological energy currency ATP and serves as building block for nucleic acids (Chen et al., 2013, Borea et al., 2016). In addition, extracellular adenosine acts as a signaling molecule to mediate various physiological and pathological effects through activation of a family of GPCRs, known as adenosine receptors (AR). Intracellular adenosine is primarily produced by ATP breakdown to AMP followed by hydrolysis, which can occur during physical exercise and ischemic conditions. ATP can be released from cells via multiple processes, where it can activate its own receptors, such as P2X ionotropic ion channels and P2Y metabotropic GPCRs. Furthermore, it serves as an important source for extracellular adenosine. ATP release mechanisms include vesicular exocytosis, passage through channels, and cell lysis. Fig. 7 shows the pathway of ATP and ADP breakdown to adenosine (Roberts et al., 2014, Chen et al., 2013). In a first step, the extracellular enzyme ectonucleoside triphosphate diphosphohydrolase 1 (ENTPD1, CD39) breaks ATP as well as ADP down to AMP. The final critical step is the conversion of AMP to adenosine by ecto-5' nucleotidase (NTSE, CD73). The action of these enzymes will rapidly and efficiently shift signaling of released adenine nucleotides to adenosine-mediated GPCR signaling. An alternative source of extracellular adenosine is the release of intracellularly generated adenosine via the equilibrative nucleoside transporters ENT1 and ENT2. Once generated, adenosine can be removed from extracellular spaces by adenosine deaminase (ADA) to form inosine. Typically, reasonable high levels of adenosine are present in cells because of its involvement in several different metabolic pathways, and therefore intracellular concentrations of adenosine can never reach zero (Chen et al., 2013).

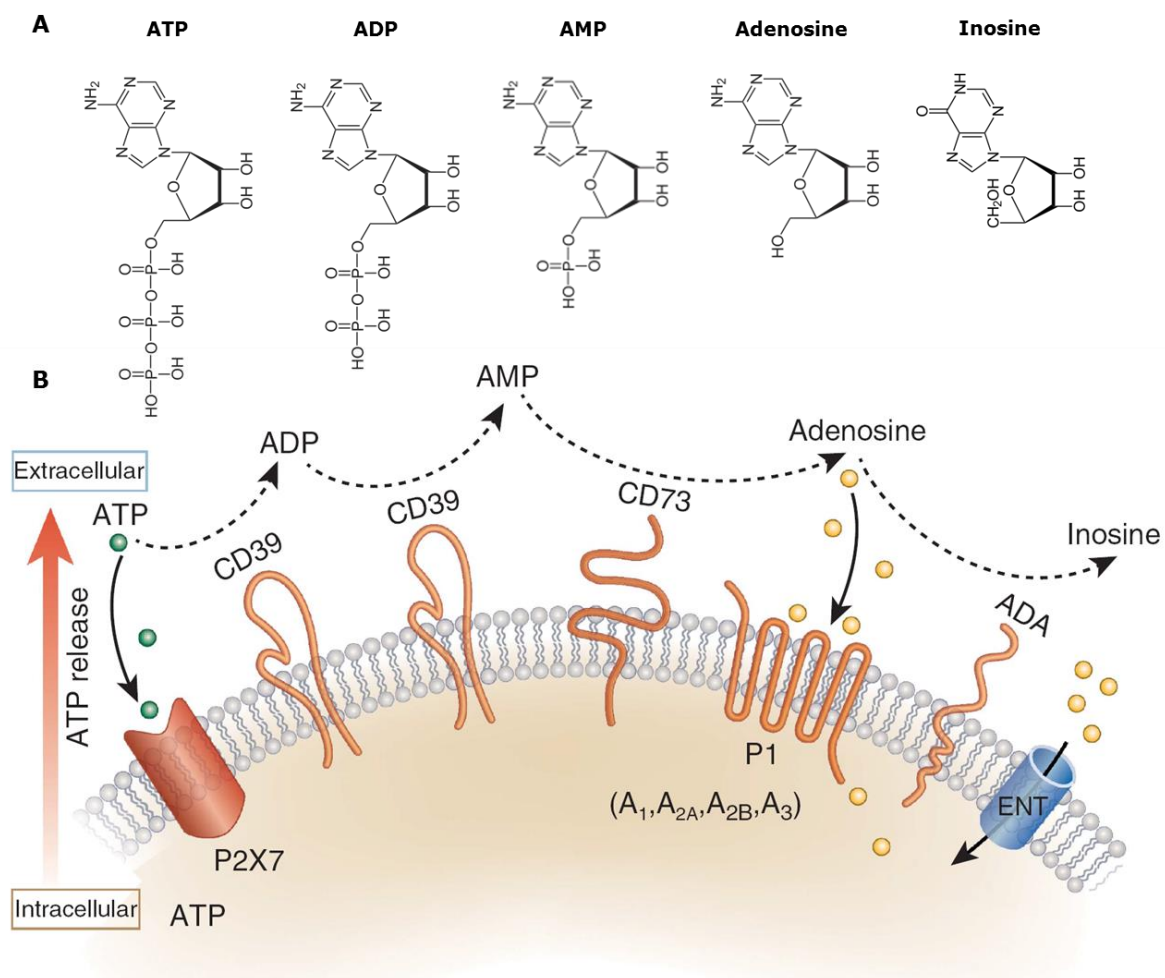


**Figure 7. Structures and extracellular degradation of ATP to adenosine.** (A) Structures of ATP and the breakdown products leading to adenosine and inosine. (B) Schematic representation of extracellular ATP catabolism. See main text for abbreviations. Panel B is a modified version a figure taken from Roberts *et al.* (2014).

### **The adenosine receptor family of GPCRs**

Adenosine serves as a signaling molecule by exerting its influence through the activation of four distinct GPCRs of the adenosine receptor (AR) subfamily: A<sub>1</sub>, A<sub>2A</sub>, A<sub>2B</sub>, and A<sub>3</sub> (Fredholm et al., 2011). Each AR has a unique ligand selectivity, activation profile, tissue distribution, and G protein binding preference. The corresponding human genes encoding the four ARs are denoted ADORA1, ADORA2A, ADORA2B, and ADORA3, respectively. All vertebrate genomes, including amphibians, harbor a complement of four AR genes. The key properties and biochemical features of the human AR subtypes are summarized in Table 2. ARs, as GPCRs, share the structural motif of a single polypeptide chain forming seven transmembrane (7TM) helices, with the N-terminus being extracellular and the C-terminus located in the cytoplasm. The primary sequence lengths vary between 318 to 412 amino acids and they share a relatively high degree of overall amino acid sequence identity ranging between 31 to 46% (Pirainen et al., 2011). For example, the A<sub>1</sub> AR has higher sequence identity to A<sub>3</sub> (46%) than to either A<sub>2B</sub> (42%) or A<sub>2A</sub> (37%). Three intracellular (ICL) and three extracellular (ECL) loops connect the seven TM helices, consisting of 25-30 residues each. Helix 8 is located on the cytoplasmic side and does not cross the membrane. The variation in sequences length between ARs can be attribute to differences in the length of the C-terminal segment. The A<sub>2A</sub> AR has C-terminus of more than 120 amino acids. The C-terminal domain is not required for coupling to trimeric G proteins, but may serve as a binding site of accessory proteins modulating AR-subtype specific activities (Zezula and Freissmuth, 2008). All ARs harbor potential N-linked glycosylation sites located in the ECLs, but the glycosylation state does not appear to alter the ligand binding properties (Pirainen et al., 2011). Furthermore, several tyrosine and serine/threonine phosphorylation sites have been predicted in both the cytoplasmic domains and the C-termini of all four ARs. Apart from A<sub>2A</sub>, all ARs have potential palmitoylation sites at the end of helix 8. Removal of palmitoylation sites by mutagenesis appears to influence receptor degradation and phosphorylation, whereas no effects were seen with G protein binding (Pirainen et al., 2011). For example, depalmitoylation of A<sub>1</sub> AR increases the phosphorylation of the receptor by GPCR kinases (GRKs) resulting in rapid desensitization of receptor (Gao et al., 1999).

**Table 2. Primary sequence and key properties of human ARs**

Subtype	Gene	Chromosomal location	G protein $\alpha$ subunits	Length [Residues]	Predicted MW [Da]	Adenosine Potency* [nM]
A <sub>1</sub>	ADORA1	1q32.1	G <sub>i</sub> , G <sub>o</sub>	326	36,512	1-10
A <sub>2A</sub>	ADORA2A	22q11.23	G <sub>s</sub> , G <sub>olf</sub>	412	44,707	30
A <sub>2B</sub>	ADORA2B	17p12-p11.2	G <sub>s</sub> , G <sub>q</sub>	332	36,333	1000
A <sub>3</sub>	ADORA3	1p13.2	G <sub>i</sub> , G <sub>o</sub> , G <sub>q</sub>	318	36,185	100

\*Adenosine potency is approximately EC<sub>50</sub>. Table adapted from Piirainen *et al.* (2011), Chen *et al.* (2013) and Jacobson & Müller (2016).

### AR signaling and biological functions

The basal physiological levels of extracellular adenosine have been estimated to range between 30-200 nM (Ballarin *et al.*, 1991). From the baseline levels, adenosine concentrations can vary substantially as a consequence of many biological variables, such as tissue type and stress experienced, which can affect adenosine production from intracellular adenosine sources, adenosine metabolism to inosine or AMP, extracellular adenosine production or adenosine transport (Smrcka, 2008, Jacobson and Gao, 2006, Chen *et al.*, 2013). Extreme physiology, such as strenuous exercise, will raise extracellular adenosine to the low micromolar range and under pathological conditions of ischaemia they can increase to 30  $\mu$ M (Chen *et al.*, 2013, Jacobson, 2009). The affinity of ARs for their natural ligand adenosine varies with the subtype (Table 2). In addition, inosine can also act as a partial agonist for A<sub>1</sub> and A<sub>3</sub> ARs (Fredholm *et al.* 2011). Highest affinities for adenosine (1-30 nM) are observed for the A<sub>1</sub> and the A<sub>2A</sub> ARs. For A<sub>3</sub> AR, adenosine affinity is intermediate (100 nM) and A<sub>2B</sub> has the lowest at about 1  $\mu$ M. Basal extracellular adenosine levels would therefore only be sufficient to partially activate the ARs present. Apart from varying affinities, the ability of adenosine to stimulate ARs is dependent on the number of ARs present on the cell surface, and this number can change depending on the circumstances (Chen *et al.* 2013; Jacobson & Müller 2016).

ARs participate in many normal physiological functions, which include the regulation of renal blood flow, immune functions, blood circulation, cardiac rhythm, angiogenesis, sleep, and neuromodulation. On the other hand they also play important roles in pathological processes, such as neurodegenerative

disorders, inflammatory diseases, ischemia-reperfusion, and tumor growth (Chen et al., 2013, Fredholm et al., 2005, Eltzschig, 2009, Hasko et al., 2008). Given the differences in adenosine affinities, tissue distribution, and gene expression levels, it is likely that AR subtypes participate to various degrees in the different physiological and pathological effects of ARs. Importantly, ARs also exert subtype-specific intracellular effects (Fig. 8).

### A<sub>1</sub> AR

The A<sub>1</sub> AR is the most conserved AR subtype across different vertebrate species (Chen et al., 2013). The highest expression levels of A<sub>1</sub> AR are found in brain, particularly at excitatory nerve endings (Yamaguchi et al., 2014). A<sub>1</sub> AR signaling has traditionally been linked to G<sub>i</sub>-mediated inhibition of adenylyl cyclase activity. It also stimulates potassium channels, such as K<sub>ATP</sub> channels in neurons and myocardium. Furthermore, it blocks transient calcium channels, which raises intracellular calcium levels. Finally, the activation of phospholipase C (PLC) elevates intracellular inositol-triphosphate (IP<sub>3</sub>) concentrations (Smrcka, 2008, Chen et al., 1999, Jacobson and Gao, 2006).

### A<sub>2A</sub> AR

A<sub>2A</sub> ARs are highly expressed in immune cells, blood platelets, thymus, and the striatum of the brain. Intermediate levels of A<sub>2A</sub> AR expression are found in heart, lungs, and blood vessel (Fredholm et al., 2001). A<sub>2A</sub> ARs stimulate the AMP-protein kinase pathway, and interact with G<sub>s</sub> and G<sub>oif</sub> proteins to upregulate the PKA pathway. Furthermore, A<sub>2A</sub> ARs regulate various processes in the central nervous system, such as motor activities, neuronal cell death, the sleep-awake cycle, and psychiatric behaviors by interacting with a number of neurotransmitters in the brain. Apart from brain activities, A<sub>2A</sub> ARs play vital roles in peripheral tissues, where they modulate angiogenesis, inflammation, and coronary blood flow, and they are implicated in the control of cancer progression (Eltzschig et al., 2012, Jacobson and Gao, 2006, Chen et al., 2013).

### A<sub>2B</sub> AR

A<sub>2B</sub> ARs are widely expressed in many tissues of the body, but the expression levels are generally low when compared to other AR family members (Smrcka, 2008, Chen et al., 2013). A<sub>2B</sub> AR stimulation triggers adenylyl cyclase activation via G<sub>s</sub> and PLC activation via G<sub>q</sub>. Furthermore, stimulatory effects on mitogen-activated protein kinase (MAPK) activities are observed. Among all ARs, A<sub>2B</sub> AR receptors are most insensitive to adenosine concentration requiring

micromolar adenosine concentrations for activation (Table 2). Such concentrations of extracellular adenosine are typically only encountered under pathological conditions, like ischemia, inflammation or hypoxia. It is believed that  $A_{2B}$  ARs play vital roles in attenuating acute inflammation, increasing ischemia tolerance, and adaptation to hypoxia (Rosenberger et al., 2009, Eckle et al., 2012, Eckle et al., 2008, Hart et al., 2011).

### $A_3$ AR

In humans,  $A_3$  ARs are expressed at very low levels under normal physiological conditions. This can however change dramatically under pathological conditions. For example, the blood cells of patients suffering from rheumatoid arthritis, Crohn's disease, or colon cancer, express elevated levels of  $A_3$  ARs when compared to healthy individuals. The functional significance of these observations remain however still elusive. Among different vertebrate species, the pharmacology and distribution of  $A_3$  ARs is subject to considerable variation. In mice, for example,  $A_3$  AR signaling has been implicated in the degranulation of mast cells, but the situation may be different in humans. The classical signaling pathways associated with  $A_3$  AR activation comprise  $G_i$ -mediated inhibition of adenylate cyclase and  $G_q$ -mediated stimulation of PLC. Despite the apparent species-specific differences,  $A_3$  ARs are considered as significant drug targets and some  $A_3$ AR-specific agonists have entered clinical testing for anti-tumor and anti-inflammatory indications (Ochaion et al., 2009, Gessi et al., 2004).

With regard to intracellular signaling, the following picture emerges. After stimulation AR subtypes have shared and divergent effects on second messenger pathways (Fig. 8). All ARs play a central role in the regulation of cyclic AMP (cAMP) levels by modulating the activity of adenylyl cyclase through distinct sets of G proteins (Table 2). In general,  $A_1$  and  $A_3$  ARs are coupled with G proteins of the  $G_i$ ,  $G_q$ , and  $G_o$  families to exert an inhibitory effect on adenylate cyclase activity (Ardura and Friedman, 2011, Sheth et al., 2014). The activation of  $A_1$  and  $A_3$  ARs will also increase activity of PLC raising intracellular  $Ca^{2+}$  levels, which will stimulate PKC.  $A_1$  ARs also modulate voltage-sensitive  $K^+$  and  $Ca^{2+}$  channels. In contrast, the canonical signaling mechanisms activated by  $A_{2a}$  and  $A_{2B}$  ARs rely on the stimulation of adenylate cyclase activity by  $G_s$  and  $G_{olf}$  to raise intracellular cAMP levels and activate PKA (Borea et al., 2016, Headrick et al., 2013). Furthermore,  $A_{2B}$  but not  $A_{2A}$  ARs activate PLC through  $G_q$ . Finally, all four subtypes of ARs can couple to mitogen-activated protein kinase (MAPK),

giving them a role in cell growth, survival, death and differentiation (Jacobson and Gao, 2006, Eisenstein and Ravid, 2014).

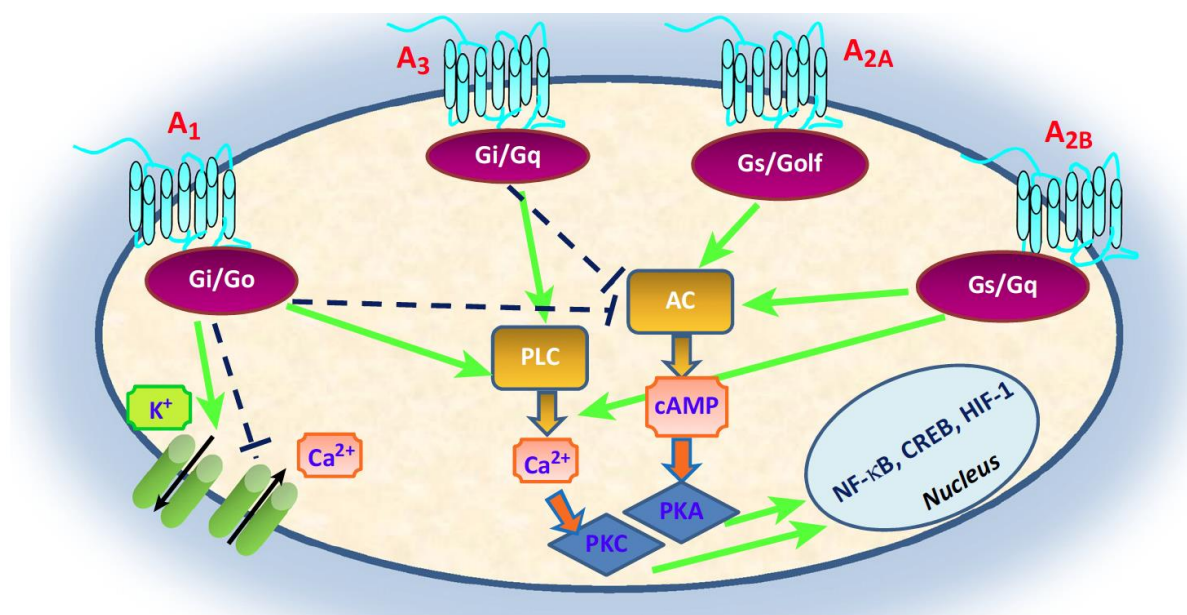


**Figure 8. Overview of the intracellular signaling pathways activated by ARs.** ARs have common and subtype-specific effects on intracellular second messenger pathways. Figure adapted from Borea *et al.* (2016).

### **Crystal structures of adenosine receptors**

Until 2007, the structural information on GPCRs was limited to crystal structures of rhodopsin, which were used to infer the structures of other GPCRs (Rosenbaum et al., 2009, Katritch et al., 2013, Salon et al., 2011). Breakthrough developments in protein engineering and microcrystallography have resulted in the exponential growth of reported crystal structures for GPCRs. By 2013, structures of 16 GPCRs had been determined covering a range of different GPCR subfamilies with distinct ligand recognition and functional characteristics. They include the structures of the beta-adrenergic,  $A_{2A}$  adenosine, chemokine CXCR4, dopamine D3, histamine  $H_1$ , muscarinic, and opioid receptors (Katritch et al., 2013). In addition, several GPCRs have been co-crystallized in complexes with different ligands: agonists, inverse agonists and antagonists. The intrinsic structural flexibility of GPCRs, which had been a major source for the problems encountered in GPCR crystallography, was overcome by a number of protein engineering strategies with the aim of decreasing protein heterogeneity and trapping a stable GPCR conformation (Katritch et al., 2013, Salon et al., 2011). For example, the third intracellular loop (ICL3) was replaced with a highly crystallizable protein, such as T4 lysozyme or apocytochrome  $B_{562}$ RIL. Alternatively, monoclonal antibodies were used to assist the crystallization process by mimicking  $G\alpha$  interactions on the intracellular loop domains of GPCRs. In the thermostabilization approach, point mutations would be introduced to improve the thermostability and to trap stable agonist or antagonist-bound GPCR conformations. Importantly, all non-rhodopsin GPCR structures reported to date have truncated or modified N- and C-termini, and frequently lack glycosylation sites. Despite these modifications, the engineered GPCRs were shown to retain ligand-binding properties similar to their unmodified counterparts. Furthermore, the conformational differences between multiple structures of the same receptor obtained with different engineering approaches were found to be rather minor (Xu et al., 2011). While corroborating the common seven transmembrane  $\alpha$ -helical GPCR fold, the structures provide first insights into the scope of structural diversity in the GPCR superfamily. Diversity is observed mainly in the extracellular and intracellular loops. Furthermore, size, shape and amino acid composition of the ligand binding pockets are unique for each GPCR type. Finally, there is growing evidence that GPCRs can adopt multiple conformations that include more than one active state (Katritch et al., 2013). In the simplest model, there is an equilibrium between inactive (R) and active (R\*) states. The inactive R state represents the ground

state and binds inverse agonists. The activated state R\* signals by coupling and activation of trimeric G proteins. Various biochemical studies and the structural information gained from the crystallization of GPCRs indicate a more complex situation supporting the existence of intermediate conformational states. Katritch *et al.* (2013) suggest a more refined model with five distinct conformational states: R (inactive, inverse agonist-bound state), R' (inactive, agonist-bound state), R'' (active, agonist-bound state), R\* (active, with G $\alpha$  mimic), and R\*<sup>G</sup> (active, G protein signaling state). To date, there is however, no representative series of crystal structures supporting all five conformational states for a given GPCR. Overall, the GPCR crystal structures have been crucial for improving our understanding of the mechanisms by which various ligands induce conformational changes leading to GPCR activation, G protein coupling, and cytoplasmic signal transduction.

With regard to X-ray crystallography, ARs are currently among the most comprehensively covered GPCR family members enabling detailed structure-based studies and in-depth understanding of ligand-binding pockets (Lebon *et al.*, 2015, Yuan *et al.*, 2015). The crystallization efforts have focused so far solely on the human A<sub>2A</sub> AR. Since 2008, a total of 15 structures of A<sub>2A</sub> ARs cocrystallized in complex with a variety of natural and artificial ligands have been reported (Table 3).

**Table 3. Crystal structures of the A<sub>2A</sub> adenosine receptor**

Ligand	Type	Comments	Engineering strategy	Activation state	PDB ID	Reference
ZM241385	Inverse agonist	A <sub>2A</sub> selective non-xanthine derivative	ICL3 replacement by T4L	R	3EML	Jaakola <i>et al.</i> 2008
			Point mutations	R	3PWH	Dore <i>et al.</i> 2011
			Antibody complex	R	3VGA 3VG9	Hino <i>et al.</i> 2012
			ICL3 replacement by BRIL	R	4EYI	Liu <i>et al.</i> 2012
UK-432097	Agonist	A <sub>2A</sub> selective xanthine derivative	ICL3 replacement T4L fusion	R''	3QAK	Xu <i>et al.</i> 2011
Adenosine	Agonist	Nonselective endogenous xanthine derivative	Point mutations	R''	2YDO	Lebon <i>et al.</i> 2011
NECA	Agonist	Nonselective xanthine derivative	Point mutations	R''	2YDV	Lebon <i>et al.</i> 2011
				R*	5G53	Carpenter <i>et al.</i> 2016
CGS21680	Agonist	A <sub>2A</sub> selective xanthine derivative	Point mutations	R''	4UG2 4UHR	Lebon <i>et al.</i> 2015
XAC	Antagonist	Nonselective xanthine derivative	Point mutations	R	3REY	Dore <i>et al.</i> 2011
Caffeine	Antagonist	Low affinity, nonselective xanthine derivative	Point mutations	R	3RFM	Dore <i>et al.</i> 2011
Compound 4e	Antagonist	A <sub>2A</sub> selective non-xanthine derivative	Point mutations	R	3UZC	Congreve <i>et al.</i> 2012
Compound 4g	Antagonist	A <sub>2A</sub> selective nonxanthine derivative	Point mutations	R	3UZA	Congreve <i>et al.</i> 2012

Abbreviations: BRIL, apocytochrome b<sub>562</sub>RIL; ICL3, intracellular loop 3; PDB ID, Protein Data Bank ID; R (inactive state); R'' (active state); T4L, T4 lysozyme.

At present, the A<sub>2A</sub> AR structures represent three (R, R'', R\*) of the five proposed confirmation states of GPCRs (Katritch *et al.*, 2013). The structure of the A<sub>2A</sub> AR bound to an engineered G protein, mini-G<sub>s</sub>, is the most recent entry (Carpenter

et al., 2016). The mini-G<sub>s</sub> is a truncated variant containing point mutations to stabilize the protein in absence of the fully assembled trimeric G protein. The A<sub>2A</sub>R-mini-G<sub>s</sub> structure was obtained after co-crystallization with the agonist NECA and GDP bound to the mini-G<sub>s</sub>. The transition to an active G-protein bound state affects primarily the cytoplasmic end of TM helix 6 without affecting the extracellular domains of the receptor around the ligand-binding domain. The structure of the fully activated receptor coupled to the trimeric G protein is still lacking and may provide additional insights. Surprisingly, the use of different protein engineering strategies had no significant impact on the obtained crystal structures overall (Yuan et al., 2015, Lebon et al., 2015). Collectively, the different A<sub>2A</sub> AR structures confirm the canonical membrane topology of GPCRs with seven transmembrane  $\alpha$ -helix domain (7TM) spanning the lipid bilayer (Massink et al., 2015). The extracellular regions include the N-terminus and three extracellular loops (ECL 1-3), which are responsible for ligand recognition and binding. The cytoplasmic side consists of three intercellular loops (ICL 1 - 3), which interact with G-proteins and other downstream effectors. Furthermore, the helix 8 and the C-terminus are also present (Fig. 9A).

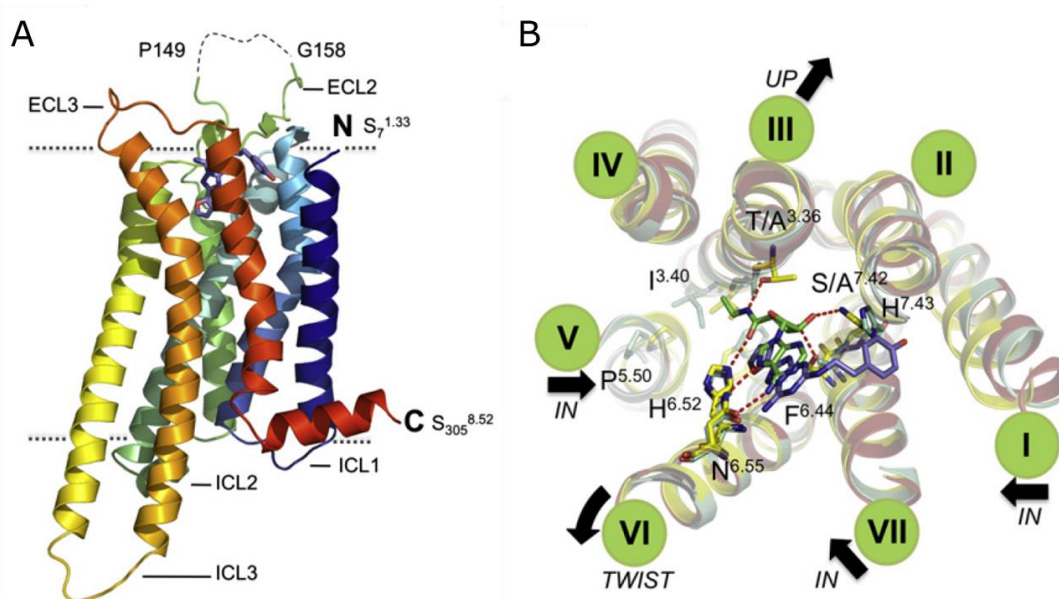


**Figure 9. Agonist bound crystal structure of A<sub>2A</sub> AR.** (A) Structure of A<sub>2A</sub> AR in complex with the inverse agonist ZM241385. The visible extracellular and intracellular loops are labeled. The disordered portion of ECL2 is shown as a dashed line. Dotted lines denote the boundaries of the lipid bilayer. (B) Close-up view of the superimposed orthosteric ligand binding sites for ZM241385 (blue) and the agonist NECA (green). Transmembrane helices are shown as green discs. The black arrows show transmembrane helical movements occurring on A<sub>2A</sub> AR activation. Pictures is taken and modified from Dore *et al.* (2011).

Agonist binding to the A<sub>2A</sub> AR appears to induce a series of stereotypical movements of the TM helices in the lipid bilayer. More specifically, the helices 1, 3, 5, 6 and 7 go through following conformational changes: TM7 and TM1 shift towards the center of the receptor, TM3 moves upward in the direction of extracellular region of the receptor, and the inward movement of TM5 leads to the rotational movement of TM4 (Fig. 9B). At the same time, it is believed that the IC regions undergo large conformation changes as part of the A<sub>2A</sub> AR activation mechanism. This will allow for interactions with trimeric G proteins and intracellular signaling. Precise structural insights will require cocrystallization of activated A<sub>2A</sub> AR with trimeric G protein complexes (Dore et al., 2011).

A comparison of the different A<sub>2A</sub> crystal structures has revealed details on the orthotopic ligand-binding pocket and the binding mode of the core adenosine moieties of A<sub>2A</sub> AR agonists (Fig. 10). While remarkable similarity in the binding mode was observed, the shape of the binding pocket at the extracellular surface differs significantly between the different ligand-bound structures. These changes can be mainly attributed to the differences in the length of the side groups extending from the core structure occupying the adenosine-binding pocket. For example, the (2-carboxyethyl) phenylethylamino extension of CGS21680, an agonist protrudes into a pocket formed by ECL2, ECL3 and the extracellular portions of TM2 and TM7. As these regions are the most divergent between different ARs, they may help to determine subtype-specific ligand binding. Furthermore, the entrance to the ligand-binding pocket appears to be very open as the inverse agonist ZM241385 can bind in two different manners.

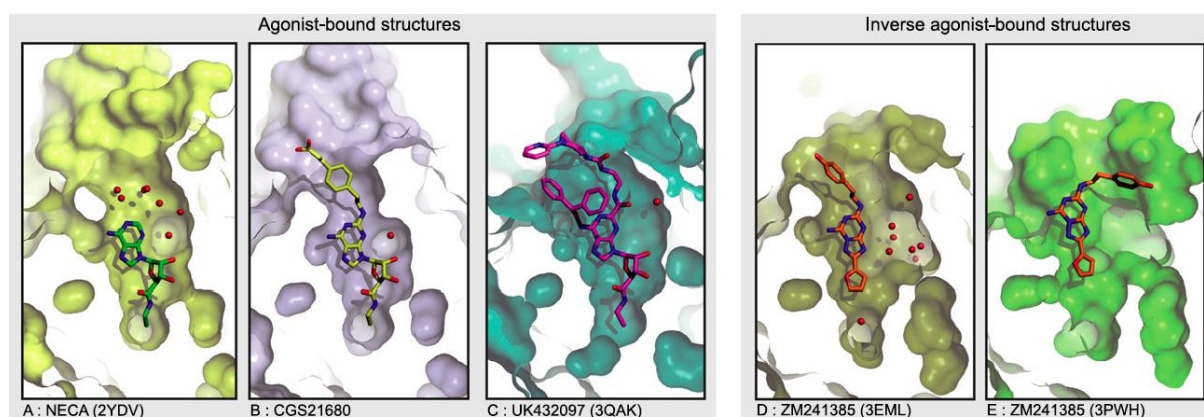


**Figure 10. Comparison of the ligand binding sites of A<sub>2A</sub> adenosine receptors bound to various ligands.** The PDB IDs are shown in parentheses. The PDB ID for CGS21680 is 4UG2. The receptor is viewed as a slice perpendicular to the membrane plane through the binding pocket. The surfaces are shown in color and water molecules are represented as red spheres. The figure was taken from Lebon *et al.* (2015).

The recently reported 1.8-Å high-resolution structure of the inactive A<sub>2A</sub> AR has revealed structured water molecules, sodium ions, lipids, and cholesterol bound to the receptor (Liu *et al.*, 2012). Importantly, the allosteric regulatory site, which binds a sodium ion and 10 water molecules, was identified (Fig. 11). It is localized deep in the middle of 7TM bundle. Upon receptor activation, the inward movement of TM7 collapses the pocket and does not provide sufficient space for the sodium ion.

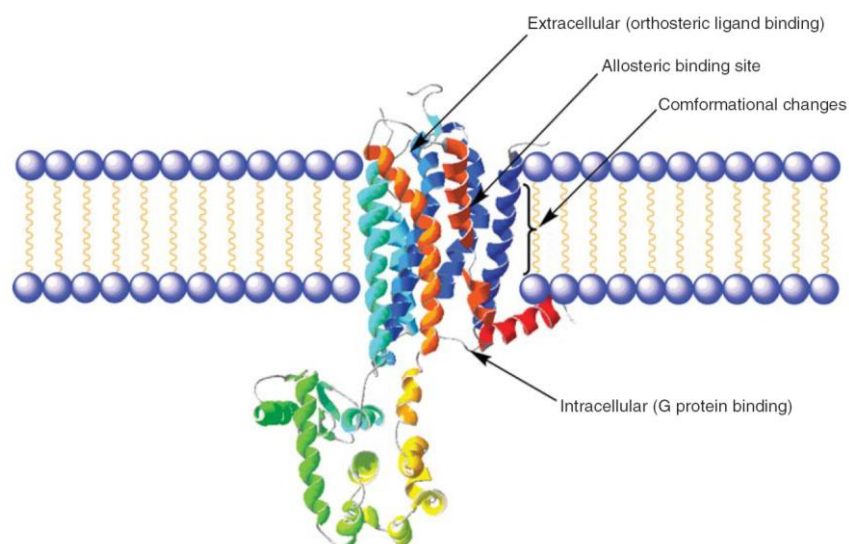


**Figure 11.** General structural architecture of A<sub>2A</sub> adenosine receptors highlighting the binding sites for orthosteric and allosteric ligands. Figure taken and adapted from Yuan *et al.* (2015).

The various crystal structures of A<sub>2A</sub> AR have provided information at atomic resolution about orthosteric and allosteric ligand binding sites, which will guide the rational design of novel compounds targeting the A<sub>2A</sub> AR. Many questions, for example about the precise structural determinants for ligand affinity, specificity and stability, remain however unresolved. Further insights into AR function will require the determination of the structures of the closely related A<sub>1</sub>, A<sub>2B</sub>, and A<sub>3</sub> ARs.

### **Expression of adenosine receptors**

Adenosine is ubiquitously present throughout the human body and involved in various physiological and pathological processes as outlined above. The effects of extracellular adenosine are mediated via four distinct AR subtypes, which are generally widely expressed in various tissue and organs of the body. Nevertheless, each AR subtype has its own characteristic gene expression profile. Table 4 provides an overview of main expression domains for the four AR subtypes in human and two model organisms (zebrafish embryos; adult mice). It is evident that there is extensive overlap in gene expression of AR subtypes in different organs of the vertebrate body. This is particularly true for brain, heart, kidney, and liver. While AR subtypes may share gene expression in the same organ, expression of each AR subtype may be confined to distinct structures or tissues of the organ. These differences are at present poorly understood. The main expression domains for each AR subtype are similar across species, but there also appear to be species-specific differences. For instance, the brain is one of the main organs expressing A<sub>3</sub> AR in humans, whereas this is not the case for mice (Table 4). These apparent differences warrant a more systematic comparative analysis of AR gene expression across model organisms in the future.

**Table 4. Expression domains of AR subtypes in zebrafish, mouse, and human**

AR subtype	Main expression domains		
	Zebrafish	Mouse	Human
<b>A<sub>1</sub></b>	-	Brain (hippocampus, cerebellum), Spinal cord, Eye, Adrenal gland, Atria	Brain (hippocampus, striatum, thalamus), Spinal cord, Kidney, Muscle, Adrenals, Atria, Heart, Liver, Bladder, Testis, Lung
<b>A<sub>2A</sub></b>	Heart, Brain (hindbrain, hypothalamus), Ventral hematopoietic mesoderm	Brain (cerebellum, cortex), Spleen, Thymus, Heart, Leukocytes, Lung, Blood vessels	Brain (cerebellum, prefrontal cortex, temporal lobe), Lung, Olfactory tubercle, Heart, Kidney, Liver, Vasculature, Testis, Spleen
<b>A<sub>2B</sub></b>	Vasculature, Brain (telencephalon, hindbrain, neurons), Eye (retina), Yolk syncytial layer	Intestine (colon, cecum), Bladder, Blood vessels, Brain, Kidney, Liver, Adrenal gland, Pituitary gland	Brain (cerebellum, prefrontal cortex, frontal lobe, temporal lobe), Intestine, Heart, Kidney, Liver, Testis
<b>A<sub>3</sub></b>	-	Lung, Liver, Spleen, Testis, Thyroid, Heart, Arteries, Mast cells	Brain, Heart, Kidney, Lungs, Eyes, Adrenal gland, Blood, Muscle, Liver

Table summarizes gene expression data for zebrafish embryos (Boehmler *et al.* (2009), adult mice (Wei *et al.* 2011), and humans (Fredholm *et al.* 2001; Jacobson & Müller 2016). Abbreviations: -; unknown.

### **Genetic analysis of adenosine receptor functions**

Adenosine signaling has been implicated in many physiological processes, such as neuromodulation, immune regulation, vascular functions, and metabolic control. Over the last twenty years, various mouse strains deficient in the four AR subtypes have been generated by targeted mutagenesis in embryonic stem cells with the aim of uncovering the normal physiological roles of ARs. The phenotypes have been extensively reviewed elsewhere (Fredholm et al., 2011, Chen et al., 2013, Wei et al., 2011, Jacobson and Muller, 2016). The most striking finding from the loss of function experiments is the fact that none of the AR subtype knockouts had lethal effects and all the mutant mouse strains were viable and fertile. In line with the findings in AR knockout mice, there are presently also no reports of AR mutations causing disease phenotypes in the human population (Online Mendelian Inheritance in Man; [www.omim.org](http://www.omim.org); November 2016). This indicates that there is extensive functional redundancy of AR gene functions in mice and probably also in humans, which is not surprising given the broad and extensive overlap of gene expression domains of AR subtypes (Table 4). Many organs, such as brain, heart and kidney, express at least two or more AR subtypes. Alternatively, the lack of severe phenotypes in the AR knockout mouse strains could indicate the existence of compensation mechanisms. Indeed, up-regulation of A<sub>2B</sub> AR expression was observed in coronary arteries of A<sub>2A</sub> AR knockout mouse (Teng et al., 2008). In future, it will be important to generate double, triple and quadruple knockout mouse lines of the four AR subtypes. For example, A<sub>1</sub> AR and A<sub>2A</sub> AR double knockout mice have a lower body temperature than wild-type mice (Yang et al., 2009). The systematic and coordinated generation of mutant mouse lines carrying multiple AR gene mutation may reveal further insights into physiological processes regulated by AR signaling.

While general phenotypes of the single AR knockout mice are not significantly different to wild-type mice, minor differences have been observed, particularly under special physiological and/or pathologic conditions. This encompasses behavioral abnormalities (aggression, anxiety), cardiovascular changes, alteration in homeostasis, and immune system deficiencies (Wei et al., 2011, Belikoff et al., 2011, Yaar et al., 2005). A selection of these subtle phenotypes are shown in Table 5. Given the mild and modest phenotypes seen in AR-deficient mice, it will be important that mutant and control mice share the same genetic background.

**Table 5. Selection of phenotypes observed in AR knockout mice**

<b>A<sub>1</sub> AR</b>	<b>A<sub>2A</sub> AR</b>	<b>A<sub>2B</sub> AR</b>	<b>A<sub>3</sub> AR</b>
Hyperalgesia	Acute pain response ↓	Leukocyte adhesion to blood vessels ↑	Airway responsiveness ↓
Blood pressure and renin activity ↑	Anxiety ↑	Inflammation ↑	Mast cell degranulation ↓
Anxiety ↑	Aggression ↑	Vascular leakiness ↑	Intraocular pressure ↓
Heart rate ↓	Heart rate ↑	Myocardial preconditioning	Resistance to cardiac ischemia-reperfusion injury
Tubuloglomerular feedback ↓	Blood pressure ↑		
	Focal brain ischemia damage ↓		
	Neonatal brain ischemia damage ↑		

Table adapted from Fredholm *et al.* (2011), Chen *et al.* (2013) and Jacobson & Müller (2016).

### **Roles for adenosine receptors in angiogenesis and lymphangiogenesis**

Adenosine is an ubiquitous and endogenous purine nucleoside which controls several physiological processes, including angiogenesis and vasculogenesis. During metabolic stress such as hypoxia and cancer, the secretion of adenosine is increased. Furthermore, adenosine has been reported as a master regulator of angiogenesis during (Lenoir et al., 2014, Escudero et al., 2014). In the vasculature, adenosine induces vasodilation of preexisting vasculature and it stimulates angiogenesis in order to increase blood flow and thereby increasing nutrient and oxygen delivery (Feoktistov et al., 2009, Adair, 2005). First evidence for a role of adenosine in the stimulation of angiogenesis was provided by experiments using the chicken chorioallantoic membrane (CAM) system (Dusseau and Hutchins, 1988, Dusseau et al., 1986). Administration of adenosine led to a dose-dependent increase in vascular density supporting an angiogenic role for adenosine. In *Xenopus* tadpoles, long-term treatment with the adenosine agonist NECA causes dilation of brain blood vessels and increased blood flow (Jen and Rovainen, 1994). The effect of adenosine on angiogenesis appears to involve the modulation of multiple steps, including vascular endothelial cell proliferation, migration, and tube formation (Feoktistov et al., 2009, Adair, 2005). Adenosine activates all AR subtypes ( $A_1$ ,  $A_{2A}$ ,  $A_{2B}$ ,  $A_3$ ) and endothelial cells are known to express ARs. Table 6 provides a summary of the postulated involvement of AR subtypes in the modulation of angiogenesis. There are however conflicting reports on the presence of specific AR subtypes in endothelial cells. For example, human umbilical vein endothelial cells (HUVEC) express preferentially  $A_{2A}$  ARs, whereas microvascular endothelial cells (HMEC) have a preference for  $A_{2B}$  ARs (Feoktistov et al., 2002).

**Table 6. Summary of AR involvement in angiogenesis using human cell cultures**

AR	Angiogenic process	Cell type
A <sub>1</sub>	Migration ↑	EPC
A <sub>2A</sub>	VEGF expression ↑	Macrophages
	Thrombospondin 1 expression ↓	HMVEC
	sFlt-1 release ↓	Macrophages
	mFlt-1 expression ↑	Macrophages
	Proliferation/migration and VEGF expression ↑	HUVEC
A <sub>2B</sub>	Permeability ↑	HUVEC-PMN
	VEGF expression ↑	HMVEC
	Migration ↑	HREC
	VEGF, IL-8 and bFGF expression ↑	HMEC-1
	IL-8 secretion ↑	Melanoma cells, HT29
	VEGF expression ↑	HUVEC under hypoxia
	Proliferation/migration and tube formation and VEGF expression ↑	HREC
A <sub>3</sub>	Migration and tube formation ↓	HUVEC
	VEGF and IL-8 expression ↑	Melanoma cells
	VEGF expression ↑	HT29
	Angiopoietin-2 expression ↑	HMEC-1

VEGF, vascular endothelial growth factor; sFlt-1, soluble Flt1; mFlt-1, membrane-linked Flt1; IL-8, Interleukin 8; bFGF, basic fibroblast growth factor; HMVEC, human microvascular endothelial cells; HUVEC, human umbilical vein endothelial cells; PMN, polymorphonuclear leukocyte; HREC, human retinal endothelial cells; HMEC-1, human microvascular endothelial cell line 1; EPC, endothelial progenitor cells; HT-29, human colon adenocarcinoma. Increase (↑) and decrease (↓) of pro- or anti-angiogenic processes; AR, adenosine receptor. Table adapted from Escudero *et al.* (2014), where the primary references can be found.

Multiple pieces of evidence suggests that the proangiogenic activities of adenosine can be furthermore attributed to its ability to modulate the release of pro- and anti-angiogenic factors (Feoktistov *et al.*, 2009). During ischemia or hypoxia, the heart produce adenosine as negative feedback signal to retain oxygen supply. The released adenosine activates A<sub>2A</sub> ARs, which will inhibit production of the antiangiogenic factor thrombospondin-1. At the same time adenosine activates A<sub>2B</sub> ARs on endothelial cell, which will stimulate the release

of vascular endothelial growth factors (VEGF), fibroblast growth factor (bFGF), and interleukin-8 (IL-8) (Feigl, 2004, Feoktistov et al., 2002, Linden, 2005). During wound repair and in inflammation, adenosine stimulates angiogenesis by activation of  $A_{2A}$  ARs on macrophages resulting in the production of VEGF instead of IL-6 and tumor necrosis factor (Olah and Caldwell, 2003). Expression of ARs in different types of leukocytes, such as macrophages, mast cells, and neutrophils, has been demonstrated in the past (Feoktistov et al., 2003, Thiele et al., 2004, Salmon and Cronstein, 1990). Taken together, the indirect stimulation of angiogenesis via adenosine involves two distinct mechanisms: the increased production and release of proangiogenic factors, like VEGF and angiopoietin 2 (Ang2), and downregulation of the production of antiangiogenic factors, like thrombospondin-1 (Tsp1). Overall, the effects of adenosine signaling on blood vessels is complex as it involves direct and indirect modes of action. Direct effects are mediated by endothelial ARs, whereas in the indirect effects are triggered by ARs on smooth muscle cells and different leukocytes. Figure 12 shows the model of Clark *et al.* (2007) describing the complex involvement of ARs in angiogenesis.

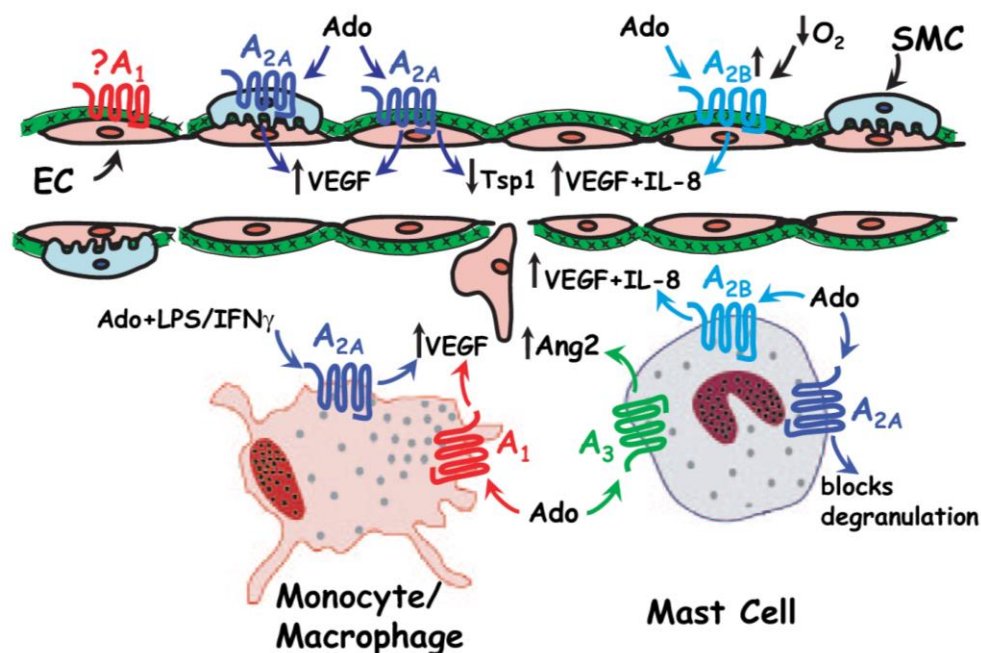


**Figure 12. Model explaining the functions of different AR subtypes in the stimulation of angiogenesis.** In monocytes and macrophages, extracellular adenosine (Ado) activates  $A_1$  and  $A_{2A}$  ARs to stimulate the release of VEGF. Lipopolysaccharides (LPS) or interferon  $\gamma$  ( $IFN\gamma$ ) synergize with adenosine to activate  $A_{2A}$  ARs. Stimulation of mast cells by adenosine blocks degranulation (via  $A_{2A}$  AR) and promotes release of interleukin-8 (IL-8) and angiopoietin-2 (Ang2) via  $A_{2B}$  and  $A_3$  ARs, respectively. In smooth muscle cells (SMC),  $A_{2A}$  AR activation stimulates VEGF

release. In endothelial cells,  $A_{2A}$  AR activation inhibits thrombospondin 1 (Tsp1) and promotes VEGF synthesis. Furthermore, hypoxia-induced upregulation of endothelial  $A_{2A}$  and  $A_{2AB}$  ARs triggers IL-8 and VEGF release. The role of  $A_1$  ARs, which is present in endothelial cells remains unclear. Figure taken from Clark *et al.* (2007).

While there is ample evidence supporting a role for adenosine signaling in regulating blood vessel angiogenesis, the effects of adenosine on lymphangiogenesis remain poorly understood. Kalin *et al.* (2009) provided first evidence indicating a role for adenosine signaling in modulating lymphangiogenesis. The  $A_1$  AR-selective antagonists 7-chloro-4-hydroxy-2-phenyl-1,8-naphthyridine (7CN) and 1,3-diethyl-8-phenylxanthine (DEPX) were identified as chemical agents not only affecting blood vessel formation, but also causing hypoplasia of lymphatics in *Xenopus* embryos. 7CN inhibited both cell proliferation and tube formation of human lymphatic endothelial cells *in vitro*. Furthermore, 7CN was found to cause a reduction of lymphatic vessels in a murine neovascularization model (Kalin *et al.*, 2009). 7CN was subsequently also identified in a phenotypic *in vitro* screen as an effective inhibitor of lymphangiogenic sprouting (Schulz *et al.*, 2012). More recently, it was demonstrated that human adult dermal microvascular lymphatic endothelial cells express  $A_{2A}$  and  $A_{2B}$  AR, but apparently not  $A_1$  and  $A_3$  ARs (Lenoir *et al.*, 2014). The use of different *in vitro* and *in vivo* models failed however to resolve the role of extracellular adenosine unequivocally. Adenosine was found to inhibit proliferation and migration of lymphatic cells *in vitro*, but to stimulate lymphangiogenesis *in vivo* (Lenoir *et al.*, 2014). Given these discrepancies, further studies to explore the role of adenosine signaling in lymphangiogenesis are warranted. Overall, the exact roles of the four AR subtypes in the development and maintenance of blood and lymphatic vessels remains to be elucidated.

### **Adenosine receptors as therapeutic targets**

The prospect of therapeutically targeting ARs emerged almost 90 years ago when adenosine administration was reported to lower body temperature and contribute to vasodilation (Bennet and Drury, 1931, Drury and Szent-Gyorgyi, 1929). It was believed that vasodilation is caused by the release of adenosine and/or AMP after tissue trauma (Chen et al., 2013). Clinically, the generic drugs adenocard and adenoscan use adenosine as a short-lived, non-selective AR agonist for the treatment of supraventricular tachycardia (Delacretaz, 2006). The therapeutic benefit of interfering with AR signaling is also very powerfully illustrated by the methylxanthines that include caffeine (from coffee beans), theophylline (from tea leaves), and theobromine (from cocoa beans). They are ingested on regularly basis by billions of people worldwide and therefore they are considered the most widely consumed stimulants in the world. The effects of methylxanthines are mediated primarily via blockade of ARs (Snyder et al., 1981). AR action may not only be modulated by agents that directly interact with ARs, but also by compounds that stimulate adenosine release, inhibit the metabolism of extracellular adenosine, or block its cellular uptake (Jacobson and Gao, 2006). Overall, there is growing evidence that therapeutic agents interfering with AR signaling could be beneficial in treating a wide range of conditions, including cerebral and cardiac ischaemic diseases, sleep disorders, immune diseases, inflammatory disorders, and cancer (Jacobson and Gao, 2006, Chen et al., 2013). Numerous selective AR agonists and antagonists have been developed in recent years and several have entered clinical testing (Chen et al., 2013, Jacobson and Muller, 2016). Fig. 13 provides an overview of current disease areas for selective AR ligands. Chen et al. (2013) have reviewed ongoing or recently completed Phase II-III clinical trials targeting ARs.

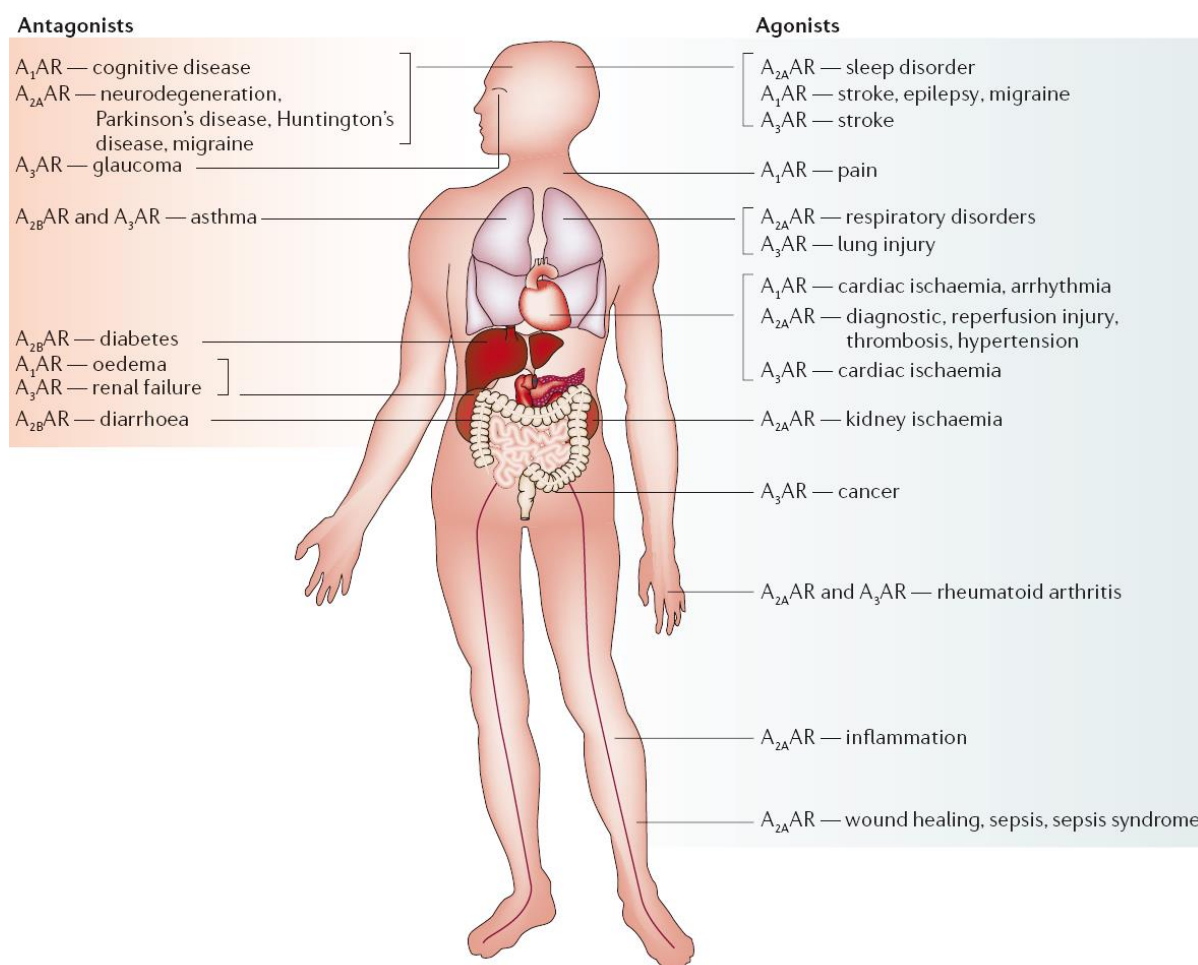


**Figure 13. Proposed disease targets for selective adenosine receptor ligands.** The figure illustrates disease areas that could benefit from AR subtype-specific antagonists (*left*) and agonists (*right*) as therapeutic agents. Figure taken from Jacobson *et al.* (2006).

However, to date only two AR-specific agents targeting A<sub>2A</sub> ARs have gained approval by regulatory medicinal agencies. Regadenoson (CVT-3146; Lexiscan, Astellas Pharma) is a selective agonist of the A<sub>2A</sub> AR. Given its coronary vasodilator activities, it is used as adjunctive pharmacological stress agent for radionuclide myocardial perfusion imaging in patients with suspected coronary artery disease (Ghimire *et al.*, 2013). By contrast, the caffeine analog istradefylline (KW-6002; Kyowa Hakko Kirin) is a selective antagonist of the A<sub>2A</sub> AR. It is approved in Japan as a useful alternative to dopaminergic drugs in the treatment of Parkinson's disease (Lewitt, 2008). Despite the established therapeutic potential of adenosine and agents targeting ARs, the design of effective and safe drugs with validated clinical applications is still a challenge.

For example, a phase III clinical trial to determine the efficacy of the promising A<sub>1</sub> AR-selective antagonist rolofylline in treating patients with acute heart failure had a disappointing outcome (Massie et al., 2010). Increased seizure rates and worsening renal function were among the major side effects of rolofylline. The complexity of adenosine signaling in the human body remains a continuing source for unexpected adverse side effects in clinical applications. ARs are widely distributed throughout the body, with target tissues frequently expressing multiple AR subtypes. Furthermore, the ligand adenosine itself is present ubiquitously. Finally, ARs are involved in or contribute to a wide range of pathophysiological and physiological functions (Fredholm et al., 2005). Despite these many challenges, the potential therapeutic benefits of drugging ARs calls for the development of more sophisticated AR modulators (Massie et al., 2010, Jacobson and Gao, 2006).

### **Hypothesis and Aims**

In a chemical library screen using *Xenopus* embryos, our laboratory had previously identified adenosine receptor (AR) antagonists that acted as inhibitors of blood vascular and lymphatic development (Kalin et al. 2009). In a proof-of-principle study, the adenosine receptor antagonist 7-chloro-4-hydroxy-2-phenyl-1,8-naphthyridine (7CN) was shown to disrupt VEGFA-induced adult neovascularization in mice. These initial results suggested that AR antagonists could act as potent inhibitors of vascular development and angiogenesis. Therefore, the aim of the present thesis was to characterize in detail the effects and specificities of AR antagonists on vascular development using *Xenopus* embryos and mammalian test systems. Towards this end, the following specific aims were formulated:

1. To define the spectrum and subclass specificity of AR antagonists that are effective in disrupting blood and/or lymph vessel development in *Xenopus* embryos;
2. To perform dose-response studies of bioactive AR antagonists in order to establish key pharmacological parameters, *i.e.* EC<sub>50</sub> and LC<sub>50</sub> values, in *Xenopus* embryos;
3. To assess the tissue specificities of AR antagonists *in vivo*;
4. To establish the structure-activity relationship for selected bioactive AR antagonists by changing their chemical structures;
5. To test whether selected AR antagonists affect blood and/or lymph endothelial cells *in vitro*; and
6. To elucidate the mechanisms of action of selected AR antagonists.

**Materials and methods**

### **Obtaining *Xenopus* embryos**

The *Xenopus* studies were conducted under protocols approved by the Regierung von Oberbayern, Munich, Germany (permits 55.2-1-54-2532.6-3-10 and 55.2-1-54-2532.0-95-14). Adult *Xenopus laevis* frogs were obtained from commercial suppliers (Xenopus Express; NASCO) and they were held at temperatures ranging between 18°-22°C. *Xenopus* embryos were obtained by performing *in vitro* fertilization as previously described (Helbling et al., 1998, Brandli and Kirschner, 1995). In brief, testicles were harvested from adult males that were terminally anesthetized with 0.5% tricaine (MS-222; #A5040, Sigma-Aldrich). The isolated testicles were cultured in testis medium [1x MMR, 10% fetal calf serum, 0.01% gentamycin] at 4°C for at least 7 days. 1x MMR refers to Marc's Modified Ringer's Solution: 0.1 M NaCl, 2 mM KCl, 1 mM MgSO<sub>4</sub>, 2 mM CaCl<sub>2</sub>, 5 mM HEPES and pH was adjusted to 7.8. The dorsal lymph sacs of sexually mature female frogs were injected with 600 units of human chorionic gonadotropin (#CG10, Sigma-Aldrich; Ovogest 300 I.E. /ml, Intervet Deutschland GmbH) to induce ovulation and egg laying. Injected females were kept overnight in tap water at 20°C. Typically, egg laying began 14 – 16 hours after hormone injection. Females were gently squeezed and the freshly released eggs were collected in to glass Petri dishes. A sperm-containing solution was generated by cutting a piece of tissue from the testicle and macerated in 1x MMR. To initiate *in vitro* fertilization, the sperm solution was added to the freshly obtained eggs. Subsequently, 0.1 x MMR was added to the fertilized eggs and they were kept at 22°C until the first few cleavages had occurred. Blastula stage embryos were dejellied with 2% cysteine (#7352, Sigma-Aldrich) solution (adjusted with 10 M NaOH to pH 7.8) and washed 3 times with 0.1x MMR to remove cysteine. The dejellied embryos were raised at 22°C. Unfertilized eggs, dead or malformed embryos were regularly removed from the embryo cultures. The embryos were staged according to Nieuwkoop & Faber (Nieuwkoop PD, 1994).

**Pharmacological treatments of *Xenopus* embryos**

Table 7 provides a list of all AR antagonists used in the present study. For each compound, a 10 mM stock solution was prepared in dimethyl sulfoxide (DMSO; #D8418, Sigma-Aldrich) and stored at 4°C. For dose-response studies, the stock solutions were serially diluted to: 5 mM, 2 mM, 1 mM, 0.5 mM, 0.2 mM, 0.1 mM, 0.05 mM, 0.02 mM, and 0.01 mM. Each AR antagonist was tested at final concentrations ranging between 0.01 µM to 100 µM in 0.1x MMR containing 1% DMSO. Compound testing was performed with *Xenopus* embryos at embryonic stage 31 (37 hours post fertilization, hpf). Polystyrene flat-bottom 48-well tissue culture plates (BD Falcon #353078) were used to array 5 embryos per well. Each well contained 1 ml of screening solution (0.1x MMR, AR antagonist dissolved in DMSO). Two negative controls were used for each pharmacological test; one well contained 0.1x MMR only and a second well contained 0.1x MMR plus 1% DMSO. Pharmacological treatments were performed in a humidified incubator at 22°C for the duration of 5 days. Embryo phenotypes were manually scored by visual inspection using a dissecting microscope (SV6; Carl Zeiss). The embryos were scored for morphological defects, primarily edema formation and lethality. Typically, scoring was done once the embryos reached the following stages: 33 (45 hpf), 37-38 (53 hpf), 39 (56 hpf), 41 (76 hpf), 42 (80), 43 (87 hpf), 45 (98 hpf), 46 (110 hpf), and 47 (120 hpf). Fluid evaporation was compensated daily by the addition of water and dead embryos were removed from the cultures. The AR antagonists were considered bioactive when at least 60% of the treated embryos showed a consistent phenotype; edema, morphological defects and/or lethality. AR antagonists were considered inactive, if 30% or less of the treated embryos displayed phenotype at 100 µM, the highest concentration tested. For each compound at least six independent experiments were performed to obtain consistent results and to confirm the observed phenotypes. *Xenopus* embryos were anesthetized with 0.05% tricaine in 0.1x MMR at stage 45 and pictures were taken for documentation. The images were taken using a stereo microscope (M205 FA, Leica Microsystems) equipped with a digital camera. The following pharmacological parameters were established at stage 45: EC<sub>50</sub> (effective concentration, where 50% of the treated embryos present with edema and/or die), LC<sub>50</sub> (lethal concentration, causing lethality in 50% of the treated embryos), and EC<sub>max</sub> (effective concentration, where maximal incidence of edema was observed).

**Table 7. AR antagonists selected for the pharmacological studies**

<b>Compound name (CAS Number)</b>	<b>AR selectivity</b>	<b>Supplier (Catalog number)</b>
1,3-Diethyl-8-phenylxanthine (75922-48-4)	A <sub>1</sub>	Sigma-Aldrich (A003)
1,3-Dimethyl-8-phenylxanthine (961-45-5)	A <sub>1</sub>	Sigma-Aldrich (P2278)
1,3-Dipropyl-8-phenylxanthine (85872-53-3)	A <sub>1</sub>	Tocris Bioscience (0486)
1,3-Dipropyl-8-(p-sulfophenyl) xanthine (89073-57-4)	A <sub>1</sub>	Sigma-Aldrich (A022)
7-Chloro-4-hydroxy-2-phenyl-1,8-naphthyridine ( <i>No CAS number assigned</i> )	A <sub>1</sub>	Angene International Ltd. (AG-I-03578)
7-Methyl-2-phenyl-1,8-naphthyridin-4(1 <i>H</i> )-one ( <i>No CAS number assigned</i> )	A <sub>1</sub>	Angene International Ltd. (AG-I-03577)
7-Chloro-4-hydroxy- [1,8] naphthyridine (286411-21-0)	A <sub>1</sub>	Synchem UG & Co. KG (cdp194fp2vp3)
PSB 36 (524944-72-7)	A <sub>1</sub>	Tocris Bioscience (2019)
SLV 320 (251945-92-3)	A <sub>1</sub>	Tocris Bioscience (3344)
CGS 15943 (104615-18-1)	A <sub>2A</sub>	Sigma-Aldrich (C199)
SCH 442416 (316173-57-6)	A <sub>2A</sub>	Tocris Bioscience (2463)
SCH 58261 (160098-96-4)	A <sub>2A</sub>	Tocris Bioscience (2270)
ZM 241385 (139180-30-6)	A <sub>2A</sub>	Tocris Bioscience (1036)
MRS 1706 (264622-53-9)	A <sub>2B</sub>	Tocris Bioscience (1584)
MRS 1754 (264622-58-4)	A <sub>2B</sub>	Tocris Bioscience (2752)
PSB 1115 (152529-79-8)	A <sub>2B</sub>	Tocris Bioscience (2009)
MRS 3777 hemioxalate (1186195-57-2)	A <sub>3</sub>	Tocris Bioscience (2403)
PSB 11 hydrochloride (453591-58-7)	A <sub>3</sub>	Tocris Bioscience (2012)
VUF 5574 (280570-45-8)	A <sub>3</sub>	Tocris Biosciences (1359)

### Secondary pharmacological testing

Secondary pharmacological tests were performed with bioactive A<sub>1</sub> AR antagonists to investigate if the compounds were interfering with angiogenesis and/or lymphangiogenesis *in vivo*. *Xenopus* embryos at stage 31 (37 hpf) were treated with A<sub>1</sub> AR antagonists at the EC<sub>50</sub> concentrations. The treated embryos were raised to stages 35/36 (50 hpf) or 40-41 (76 hpf). Embryos were fixed with MEMFA fixative (0.1 M MOPS pH 7.4, 2 mM EGTA, 1 mM MgSO<sub>4</sub>, 3.7% formaldehyde) for 2 hours at room temperature (RT) or overnight at 4°C. MEMFA fixative was replaced twice with 100% ethanol and the embryos were kept at -20°C in ethanol for whole mount *in situ* hybridization.

### Whole mount *in situ* hybridizations

Control *Xenopus* embryos and those treated with AR antagonists were stained by whole mount *in situ* hybridization according to the current lab protocol shown in Table 8. It is based on the standard protocol for whole mount *in situ* hybridizations of *Xenopus* embryos (Harland, 1991). The following alterations were introduced. Methanol was replaced with ethanol, digestion of RNase was skipped, and buffers did not contain CHAPS. For blocking and antibody incubation maleic acid buffer (100 mM maleic acid, 150 mM NaCl, pH 7.5) with 2% blocking reagent (#11 096 176 001, Roche Diagnostics;) and 20% sheep serum (S2263, Sigma-Aldrich) was used. Antisense digoxigenin-labeled RNA probes were created by using digoxigenin RNA labeling mix (#11 277 073 910, Roche Diagnostics). The linearized plasmids were purified using PCR purification kit (#28106, Qiagen). Then following transcription reaction was made for digoxigenin-labeled RNA synthesis:

1 µg	Linearized template DNA
2.5 µl	10x reaction buffer
2.5 µl	UTP labeling mix
1 µl	RNA polymerase (SP6/T3/T7)
Up to 25 µl	ddH <sub>2</sub> O

The reaction mix was incubated at 37°C for 4 hours. Subsequently, 1 µl DNase was added for 15 min at 37°C. The reaction was terminated by adding 2 µl 4.9 M LiCl<sub>2</sub> and 62.5 µl 100% ethanol. The solution was mixed and incubated for 1 hour at -20°C. Dig-labeled RNA was pelleted by centrifugation at 13,000 rpm at 30 min at 4°C. Pellet was washed with 70% ethanol and pelleted by centrifugation for 15 min at 13,000 rpm. Finally, Dig-labeled RNA was dissolved

in 20  $\mu$ l 2x saline-sodium citrate (SSC)/50% formamide (FA) and stored at -20°C.

For the detection of digoxigenin-labeled RNA probes sheep anti-digoxigenin Fab fragments conjugated to alkaline phosphatase ((#11 093 274 910, Roche Diagnostics) were used. BM purple (#11 442 074 001, Roche Diagnostics) was used for the color development and embryos were protected from light during color reaction. Embryos were bleached under cold light for 2 hours in bleaching solution (1% hydrogen peroxide, 5% formamide 0.5x SSC) (Helbling et al., 1998). The pictures of stained embryos were taken using a stereo microscope (M205 FA, Leica Microsystems).

**Table 8. Protocol for whole mount *in situ* hybridization of *Xenopus* embryos**

<b>Day 1</b>	<b>Time (min)</b>	<b>Temperature (°C)</b>
100% Ethanol	5	RT
75% Ethanol+ 25% PTW	5	RT
50% Ethanol+ 55% PTW	5	RT
25% Ethanol + 75% PTW	5	RT
PBS-Tween (PTW)	5	RT
PTW	5	RT
PTW	5	RT
PTW	5	RT
10 µg/ml Proteinase K in PTW	15	RT
0.1 M Triethanolamine (TEA)	5	RT
0.1 M TEA	5	RT
TEA + Acetic anhydride	15	RT
PTW	5	RT
PTW	5	RT
Formaldehyde + PTW	20	RT
PTW	5	RT
25% Hybridization buffer (HB)	15	65
50% HB	15	65
75% HB	15	65
100% HB	300	65
HB + Dig-RNA Probe (1 µg/ml)	overnight	65

## Materials and methods

---

<b>Day 2</b>		
HB	15	60
2x SSC	15	60
2x SSC	15	60
2x SSC	15	60
RNase + 2x SSC	30	37
2x SSC	5	RT
2x SSC	5	RT
0.2x SSC	30	60
0.2x SSC	30	60
1x MAB (Maleic acid buffer)	15	RT
1x MAB	15	RT
1x MAB + Blocking reagent (BR)	15	RT
MAB + BR + 20% Sheep serum (SS)	60	RT
MAB + BR + SS+ Digoxigenin antibody (1:2000)	240	RT
1x MAB	15	RT
1x MAB	15	RT
1x MAB	15	RT
1x MAB	o/n	4
<b>Day 3</b>		
1x MAB	15	RT
AP buffer	5	RT
AP buffer	5	RT
BMP purple	-	RT

### **Marker genes for antisense probe synthesis**

To analyze the expression of ARs during embryogenesis, the following cDNAs were used for antisense probe synthesis: *adora1* (GenBank. Acc. No. BC169511), *adora2a* (BC074202), *adora2b* (CX806531), and *adora3* (EL821975). Note that cDNAs for *adora2b* and *adora3* were from *Xenopus tropicalis*. The gene expression patterns for *adora2b* and *adora3* for *Xenopus tropicalis* and *Xenopus laevis* embryos were identical (*not shown*). The plasmids were linearized and antisense RNA transcribed using the appropriate restriction enzymes and RNA polymerases, respectively: *adora1*, NotI/T3; *adora2a*, SalI/T7; *adora2b*, SalI/T7; and *adora3*, SalI/T7. To analyze the organ morphology of compound-treated embryos, the following marker genes were used: *MyoD* (X16106), *SCL/tal1* (AF060151),  *$\alpha$ T3 globin* (X02796.1), *APJ-b* (XL025B17), *VEGFR3* (BM2611245), and *Fxyd* (BU903987). The plasmids were linearized and antisense RNA transcribed using the appropriate restriction enzymes and RNA polymerases, respectively: *MyoD*, Asp 718/T7; *SCL/tal1* Xho/T7;  *$\alpha$ T3 globin* HindIII/T7; *APJ-b*, EcoRI/T7; *VEGFR3* SalI/T7; and *Fxyd*, SalI/T7.

### **Microinjection of morpholino oligonucleotides**

Two translation-blocking antisense morpholino oligonucleotides (MO) targeting the AUG initiation codons, *adora1*-MO (GGATTCCCATGCTGCTTCAGTCCAA) and *adora2a*-MO (ATTTGACACCGTTACCATGGTAATG), were designed and purchased from Gene Tools, Inc (Philomath, Oregon, USA). For knockdown experiments, *Xenopus* embryos at the 2-cell stage were placed into glass Petri dishes containing 1x MMR. Each embryo was injected with 20 ng of *adora1*-MO or *adora2a*-MO (10 ng per blastomere). After MO injection, embryos were transferred to Petri dishes containing fresh 1x MMR and placed into an incubator at 20°C for 3 hours. Afterwards 1x MMR was replaced by 0.1x MMR and embryos were incubated at 20°C until further analysis.

### **Mammalian cell culture**

Human umbilical vein endothelial cells (HUVEC) were purchased from PromoCell GmbH (#C-12203). HUVECs were cultured in Endothelial Cell Growth Medium (ECGM) (#C-22010, PromoCell) according to the manufacturer's instructions in 100-mm tissue culture plates (#430293, Corning). Cells were used for compound treatments at passages 4 and 5.

### **Chemical treatments and immunostaining of cell cultures**

The source of the test compounds is provided with Table 7. Nocodazole (# M1404, Sigma Aldrich) was used as a positive control as it disrupts the microtubule-based cytoskeleton. For chemical treatments, HUVECs ( $2 \times 10^6$  cells in 2 ml ECGM/well) were seeded into six-well plates (#35 3224, BD Falcon) containing glass cover slips (#H-875, Carl Roth). The plates were incubated at 37°C for 3 hours to allow the cells to settle and adhere to the cover slips. Subsequently, A<sub>1</sub> AR antagonists or nocodazole dissolved in DMSO were added to the culture media at the following final concentrations: 1 μM, 3 μM, 10 μM; 0.1% DMSO. The cells were incubated at 37°C for either 2 hours or 16 hours. The cells were washed with phosphate buffered saline (PBS), and fixed with 2% para-formaldehyde (PFA). Fixed cells were washed three times with PBS contained 0.15% Triton X-100 (PBS-Triton). Then blocking solution (PBS with 1% BSA and 0.15% glycine) was added to cells for 10 minutes. The blocking step was repeated 3 times. The mouse anti-α-tubulin monoclonal antibody (1 mg/ml; #A11126, Life Technologies) was diluted in blocking solution to 1 μg/ml, and cells were treated with the antibody solution for 2 hours at room temperature and then overnight at 4°C. Subsequently, the cells were washed with PBS (1x), PBS-Triton (1x), and blocking solution (1x). Secondary anti-mouse IgG conjugated with Alexa Fluor 448 (#A11001, Life Technologies) was diluted (1:200) in blocking solution. Cells were incubated with secondary antibody for one hour at room temperature. Cells were washed with PBS (1x) and PBS-Triton (1x). The washed coverslips containing the stained cells were carefully mounted on microscopy slides with VECTASHIELD antifade mounting medium containing 1.5 μg/ml DAPI (#H-1200, Vectorlabs). Fluorescence imaging was performed using a Zeiss Axiophot microscope with Carl Zeiss AxioCan MRm camera and Axiovision 4.6 Software.

### **FACS analysis of A<sub>1</sub> AR antagonist treated cells**

Fluorescence-activated cell sorting (FACS) was performed with propidium iodide stained HUVECs treated either with A<sub>1</sub> AR antagonists or nocodazole. HUVECs were cultured in ECGM and split in 6 well plates. The plates were incubated overnight at 37°C. The next day, compounds were added to the medium at 0.1 μM, 0.3 μM, 1 μM, 3 μM, and 10 μM in the presence of 0.1% DMSO. The cells were incubated with compounds at 37°C for 48 hours. The medium was removed and the cells were detached from culture wells by addition of 200 μl of trypsin solution (#59427C, Sigma-Aldrich) for 5 minutes at 37°C. 2 ml of ECGM

was added and the released cell suspension was collected in 15-ml conical Falcon tubes. The cells were fixed by addition of 5 ml 95% ethanol at room temperature for 30 minutes. Then cells were centrifuged at 3000 rpm for 5 minutes, ethanol was replaced, and the cells were resuspended in 1 ml of Propidium Iodide (PI) working solution (propidium iodide, 100 ng/ml; RNase-A, 10 µg/ml; NP40, 0.05%). The cells were incubated with PI staining solution at 37°C for 30 minutes. The cells were analyzed for mitotic arrest with a flow cytometer (FCM) from Beckman Coulter (Gallios™ Instrument Fluorochrome). Yellow fluorescence channel containing 575BP/26 filter (range 562-588nm) was used for analysis.

### **Proliferation and sprouting assays**

Proliferation and sprouting experiments using HUVECs and lymphatic endothelial cells (LECs) were performed by our collaborators Dr. Adriana Primorac and Prof. Dr. Michael Detmar (Institute of Pharmaceutical Sciences, ETH Zürich, Switzerland). In brief, HUVECs were purchased from Promocell GmbH. Primary human dermal lymphatic endothelial cells (LEC) were isolated from neonatal human foreskins by immunomagnetic purification as described previously (Nakatsu et al., 2007). Cells were cultured in endothelial basal medium (EBM; Lonza) supplemented with 20% fetal bovine serum (FBS; Invitrogen), antibiotic-antimycotic solution (Invitrogen), 2 mM L-glutamine (Invitrogen), 10 µg/ml hydrocortisone (Sigma-Aldrich) and 25 µg/ml N-6,2'-O-dibutyryladenine 3',5'-cyclicmonophosphate (cAMP; Sigma-Aldrich) for up to 11 passages. Cells were grown on plastic dishes coated with type I collagen (50 µg/ml in PBS; Advanced Biomatrix). All cells were grown in a humidified atmosphere at 37°C and 5% CO<sub>2</sub>.

Cell proliferation assays were performed as follows. Cells ( $1.5 - 3 \times 10^3$ ) were seeded on type I collagen coated 96-well black, clear-bottom plates (Costar 3603, Corning) and incubated with 0.1% DMSO (Sigma-Aldrich) as solvent control, VEGFA (20 ng/ml), A<sub>1</sub> AR antagonists at different concentrations in EBM containing 2% fetal bovine serum. After 2 days of incubation at 37°C, cells were incubated with 4-methylumbelliferylheptanoate (Sigma-Aldrich). The intensity of fluorescence, proportional to the number of viable cells, was measured using a microplate reader (SpectraMax Gemini EM, Molecular Devices). Eight replicates per condition were analyzed. To investigate cell sprouting, cytodex microcarriers were coated with LECs or HUVECs (Schulz et al., 2012). For HUVECs, the microcarriers were coated with fibronectin (10 µg/ml in PBS; Merck Millipore).

Then, the cell-coated microcarriers were embedded in a collagen type I gel and were incubated for 24 hours in 0.1% DMSO, a mixture of VEGFA (40 ng/ml) and basic fibroblast growth factor (bFGF, 40 ng/ml) or different concentrations of test compound. The induced sprouts were imaged at 4x magnification (Molecular Devices ImageXpress Micro HCS microscope MD2, Photometrics CoolSNAP HQ camera; Photometrics). Image analysis was performed using NIH Image J (64-bit) software. The number of sprouts per microcarrier were counted and plotted. Three replicates per condition were performed. For all *in vitro* studies, three independent experiments were performed. Figures show results of one representative experiment. Statistical analyses were performed using one-way ANOVA (Prism 5, Graph Pad).

**Results**

### **Reanalysis of an *in vivo* chemical library screen defines AR-subtype specific antagonists for testing in *Xenopus* embryos**

A two-step *in vivo* chemical library screen was developed in our laboratory to identify small organic molecules that would disrupt blood and/or lymph vessel development in *Xenopus* embryos (Kalin et al., 2009). The primary screening procedure led to the identification of 66 compounds representing different pharmacological classes that either induced edema formation or late lethality in *Xenopus* embryos. Three of the 66 compounds were AR-specific antagonists: 7-Chloro-4-hydroxy-2-phenyl-1,8-naphthyridine (7CN), 1,3-Diethyl-8-phenylxanthine (DEPX); and 9-Chloro-2-(2-furyl) [1,2,4] triazolo [1,5-c] quinazolin-5-amine (CGS 15943). A secondary *in situ* hybridization screen revealed that treatment of *Xenopus* embryos with the A<sub>1</sub> AR-specific antagonists 7CN and DEPX caused vascular defects. This however was not the case in embryos treated with the AR antagonist CGS 15943 (Kalin et al., 2009). These pharmacological findings suggest a role for A<sub>1</sub> ARs in blood and lymph vessel formation in *Xenopus* embryos, which warrants further investigation and characterization.

Given that, adenosine treatment stimulates the formation of new blood vessels in the chick chorioallantoic membrane and in other test systems (see Introduction for details); we first asked whether agonists of ARs were present in the LOPAC chemical library screened by Kalin *et al.* (2009) and whether they had any effect. Table 9 compiles all AR agonists according to their reported AR selectivity. In total 22 AR agonists were present in the LOPAC library. Adenosine and N6-Methyladenosine were non-selective AR agonists, whereas the other 20 agonists are classified as AR-selective agonists. Importantly, treatment of *Xenopus* embryos with any of the 22 AR agonists at a concentration of 20  $\mu$ M neither caused edema formation nor premature lethality. For these reasons, this class of organic compounds were not further investigated in the context of the present thesis.

Table 10 lists the 25 AR antagonists with their reported AR-subtype selectivities that were present in the LOPAC chemical library examined in the study by Kalin *et al.* (2009). Importantly, we noticed that the specificity of CGS 15943 was misrepresented in the manufacturer's information accompanying the LOPAC chemical library. CGS 15943 acts as a potent and selective antagonist for human

A<sub>2A</sub> AR with a K<sub>i</sub> of 1.2 nM (Fredholm et al. 2011; Müller & Jacobsen 2011). It is however only modestly A<sub>2A</sub> AR-selective given that its K<sub>i</sub> for human A<sub>1</sub> AR is 3.5 nM. The K<sub>i</sub> values for A<sub>2B</sub> and A<sub>3</sub> ARs are at least 10-fold higher.

We conclude, in line with the findings of Kalin *et al.* (2009), that *in vivo* testing of 22 agonists and 25 antagonists targeting AR signaling in *Xenopus* embryos resulted in the identification of two A<sub>1</sub> AR antagonists, 7CN and DEPX, that are effective at disrupting blood and lymph vessel formation. To explore the AR-subtype specificity in greater detail, we selected a panel of AR antagonists with high affinity and AR-subtype selectivity (Table 11). For each AR subtype, at least 3 antagonists were chosen for testing alongside of 7CN and DEPX. This panel of compounds will also be employed for *in vivo* dose-response studies, which had not been performed to date.

## Results

**Table 9. AR agonists tested in *Xenopus* embryos by Kalin *et al.* (2009)**

Name	Secondary Name	Cas Number	Molecular weight	Selectivity
Adenosine		58-61-7	267.25	
N6-Methyladenosine	6-Methylaminopurine-9-ribofuranoside	1867-73-8	281.27	
N6-2-Phenylethyladenosine		20125-39-7	371.40	A <sub>1</sub>
N6-Phenyladenosine			343.34	A <sub>1</sub>
R(-)-N6-(2-Phenylisopropyl) adenosine	R (-)-PIA	38594-96-6	385.43	A <sub>1</sub>
(S)-ENBA	PD-126280; ((2S)-N6-[2-endo-Norbornyl] adenosine		361.40	A <sub>1</sub>
N6-Cyclohexyladenosine	CHA	36396-99-3	349.39	A <sub>1</sub>
N6-Cyclopentyladenosine	CPA	41552-82-3	335.37	A <sub>1</sub>
5'-N ethylcarboxamidoadenosine	NECA	35920-39-9	308.30	A <sub>1</sub> / A <sub>2</sub>
2-Chloroadenosine	2-CADO	146-77-0	301.69	A <sub>1</sub> / A <sub>2</sub>
5'-N-Methylcarboxamidoadenosine	MECA	35788-27-3	294.27	A <sub>2</sub> > A <sub>1</sub>
2-Phenylaminoadenosine	CV-1808		358.36	A <sub>2</sub> > A <sub>1</sub>
5'-(NCyclopropyl) carboxamidoade nosine	CPCA	50908-62-8	320.31	A <sub>2</sub>
PD-125944	DPMA	120442-40-2	521.58	A <sub>2</sub>
HE-NECA	2-Hexynyl-5'-ethylcarboxamidoadenosine		388.43	A <sub>2</sub>
Metrifudil	N-[(2-Methylphenyl) methyl]-adenosine		371.40	A <sub>2</sub>
CGS-21680 hydrochloride	2-p-(2-Carboxyethyl) phenethylamino 5'-thylcarboxamidoadenosine	124182-57-6	535.99	A <sub>2A</sub>
N6-2-(4-Aminophenyl) ethyladenosine	APNEA	89705-21-5	386.41	A <sub>3</sub>
AB-MECA	N6-(4-Aminobenzyl)-9-[5-(methylcarbonyl)-beta-Dribofuranosyl] adenine		399.41	A <sub>3</sub>
N6-Benzyl-5'-Nethylcarboxamidoadenosine	N6-Benzyl-NECA		398.42	A <sub>3</sub>
Chloro-IB-MECA	2-Chloro-N6-(3-iodobenzyl)-adenosine-5'-Nmethyluronamide	163042-96-4	544.74	A <sub>3</sub>
1-Deoxy-1-[6-[(3-iodophenyl) methyl] amino]-9H-purin-9-yl]-Nmethyl-beta-Dribofuranuronamide	IB-MECA	152918-18-8	510.29	A <sub>3</sub>

## Results

**Table 10. AR antagonists tested in *Xenopus* embryos by Kalin *et al.* (2009)**

Name	Secondary Name	Cas Number	Molecular weight	Selectivity
Caffeine	1,3,7-Trimethylxanthine	58-08-2	194.19	
1,3-Diethyl-8-phenylxanthine	DEPX	75922-48-4	284.32	A <sub>1</sub>
8-Cyclopentyl-1,3-dipropylxanthine	DPCPX; PD 116,948	102146-07-6	304.40	A <sub>1</sub>
Xanthine amine congener	8-[4-[[[(2- Aminoethyl) amino] carbonyl] met hyl]oxy]phenyl]-1,3- dipropylxanthine		428.50	A <sub>1</sub>
7-Chloro-4-hydroxy-2-phenyl-1,8-naphthyridine	7CN		256.69	A <sub>1</sub>
8-Cyclopentyl-1,3-dimethylxanthine	CPT; 8-Cyclopentyltheophylline	35873-49-5	248.29	A <sub>1</sub>
FSCPX	8-Cyclopentyl-N3-[3-(4-(fluorosulfonyl)benzoyloxy)propyl]-N1-propylxanthine	156547-56-7	506.56	A <sub>1</sub>
1,3-Dimethyl-8-phenylxanthine	8-Phenyltheophylline; DMPX	961-45-5	256.27	A <sub>1</sub>
N6-Cyclopentyl-9-methyladenine	N-0840	109292-91-3	217.28	A <sub>1</sub>
Aminophylline Ethylenediamine	Theophylline ethylenediamine	317-34-0	420.43	A <sub>1</sub> / A <sub>2</sub>
Theophylline	1,3-Dimethylxanthine	58-55-9	179.18	A <sub>2</sub> > A <sub>1</sub>
Theobromine	3,7-Dimethylxanthine	83-67-0	180.17	A <sub>2</sub> > A <sub>1</sub>
1,7-Dimethylxanthine	Paraxanthine	611-59-6	180.17	A <sub>2</sub> > A <sub>1</sub>
3-n-Propylxanthine	Enprofylline	41078-02-8	194.19	A <sub>2</sub> > A <sub>1</sub>
8-(p-Sulfophenyl) theophylline		80206-91-3	336.33	A <sub>2</sub> > A <sub>1</sub>
1,3-Dipropyl-8-psulfophenylxanthine	DPSPX	89073-57-4	392.44	A <sub>2</sub> > A <sub>1</sub>
1,3-Dipropyl-7-methylxanthine		31542-63-9	250.30	A <sub>2</sub>
3,7-Dimethyl-Ipropargylxanthine		14114-46-6	218.22	A <sub>2</sub>
1-Allyl-3,7-dimethyl-8-psulfophenylxanthine		149981-25-9	376.39	A <sub>2</sub>
CGS 15943	9-Chloro-2-(2-furyl) [1,2,4] triazolo[1,5-c] quinazolin -5-amine	104615-18-1	285.69	A <sub>2A</sub> > A <sub>1</sub>
8-(3-Chlorostyryl) caffeine	CSC	147700-11-6	330.78	A <sub>2A</sub>
Alloxazine	Isoalloxazine		214.18	A <sub>2B</sub>
MRS 1754	8- [4-[(4- Cyanophenyl) carbamoylmethyl) oxy]phenyl]-1,3-di(npropyl) xanthine		486.53	A <sub>2B</sub>
VUF 5574	N-(2-methoxyphenyl)-N'-[2-(3-pyridinyl)-4-quinazoliny]-urea		371.40	A <sub>3</sub>
MRS 1523	3-propyl-6-ethyl-5-[(ethylthio)carbonyl]-2-phenyl-4- propyl-3-pyridine carboxylate	212329-37-8	399.56	A <sub>3</sub>

## Results

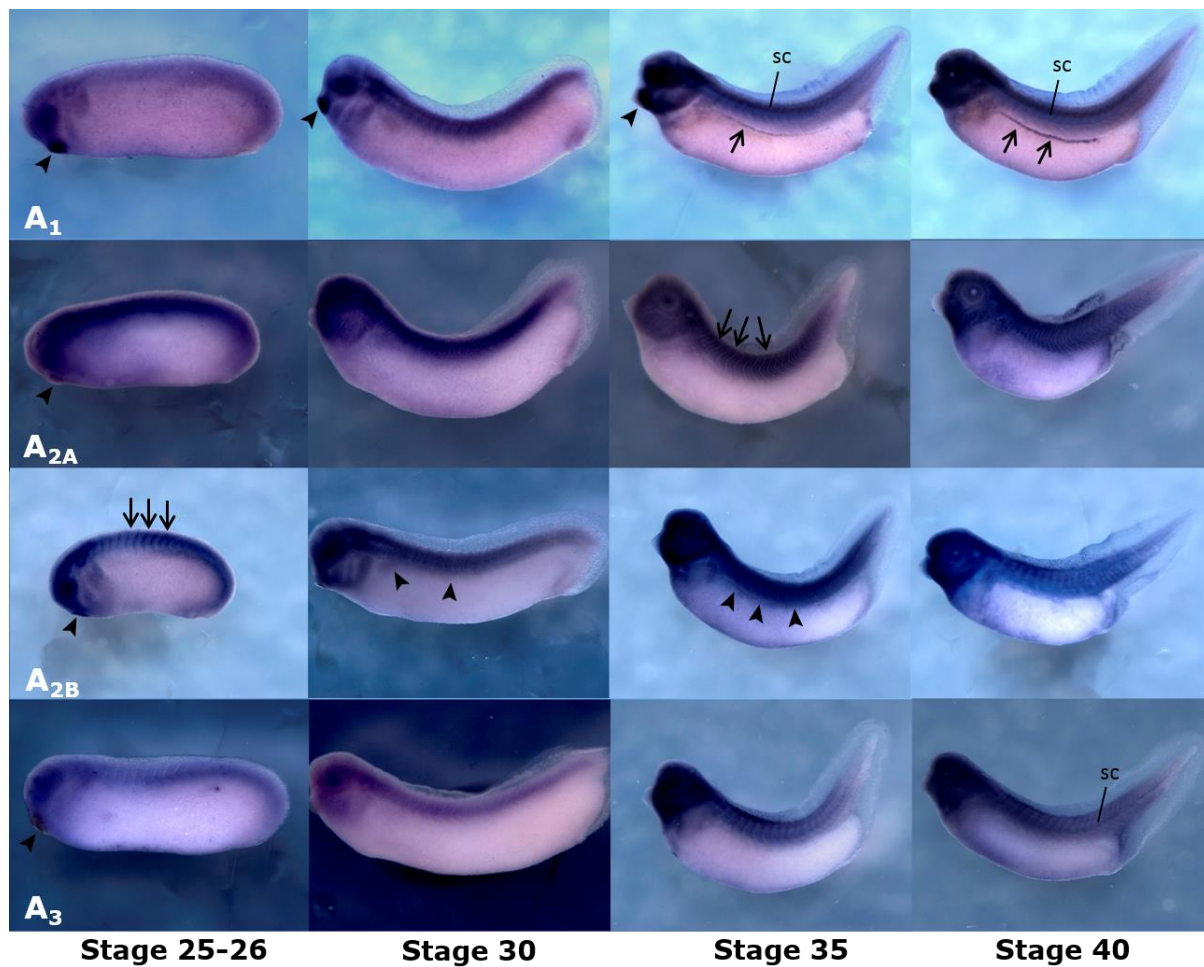
**Table 11. AR-subtype selective antagonists chosen for *in vivo* testing in *Xenopus* embryos**

Compound name	AR selectivity	K <sub>i</sub> Values (nM)				Reference
		A <sub>1</sub>	A <sub>2A</sub>	A <sub>2B</sub>	A <sub>3</sub>	
DEPX	A <sub>1</sub>	44.5 (r)	863 (r)	341	n.a.	(Phelps et al., 2006, Bruns et al., 1987)
7CN	A <sub>1</sub>	0.15 (b) 300	100 (b) 400	n.a.	2100 (b, r)	(Ferrarini et al., 2000, Ferrarini et al., 2004)
PSB 36	A <sub>1</sub>	0.7	980	187	2300	(Fredholm et al., 2011)
SLV 320	A <sub>1</sub>	1	398	3981	200	(Fredholm et al., 2011)
CGS 15943	A <sub>2A</sub>	3.5	1.2	32.4	35	(Fredholm et al., 2011)
SCH 442416	A <sub>2A</sub>	1110	4.1	>10,000	>10,000	(Fredholm et al., 2011)
SCH 58261	A <sub>2A</sub>	725	5	1110	1200	(Fredholm et al., 2011)
ZM 241385	A <sub>2A</sub>	774	1.6	75	743	(Fredholm et al., 2011)
MRS 1706	A <sub>2B</sub>	157	112	1.39	230	(Kalla et al., 2009)
MRS 1754	A <sub>2B</sub>	403	503	1.97	570	(Fredholm et al., 2011)
PSB 1115	A <sub>2B</sub>	>10,000	24,000 (r)	53.4	>10,000	(Fredholm et al., 2011)
MRS 3777	A <sub>3</sub>	>10,000	>10,000	>10,000	47	(Jacobson and Gao, 2006)
PSB 11	A <sub>3</sub>	1640	1280	2100	2.34	(Fredholm et al., 2011)
VUF 5574	A <sub>3</sub>	≤10,000(r)	≤10,000	n.a.	4	(Fredholm et al., 2011)

K<sub>i</sub> values refer to studies with human ARs unless noted. Abbreviations: AR, adenosine receptor; n.a., not available; b, bovine; r, rat.

### **Widespread expression of ARs in *Xenopus* embryos**

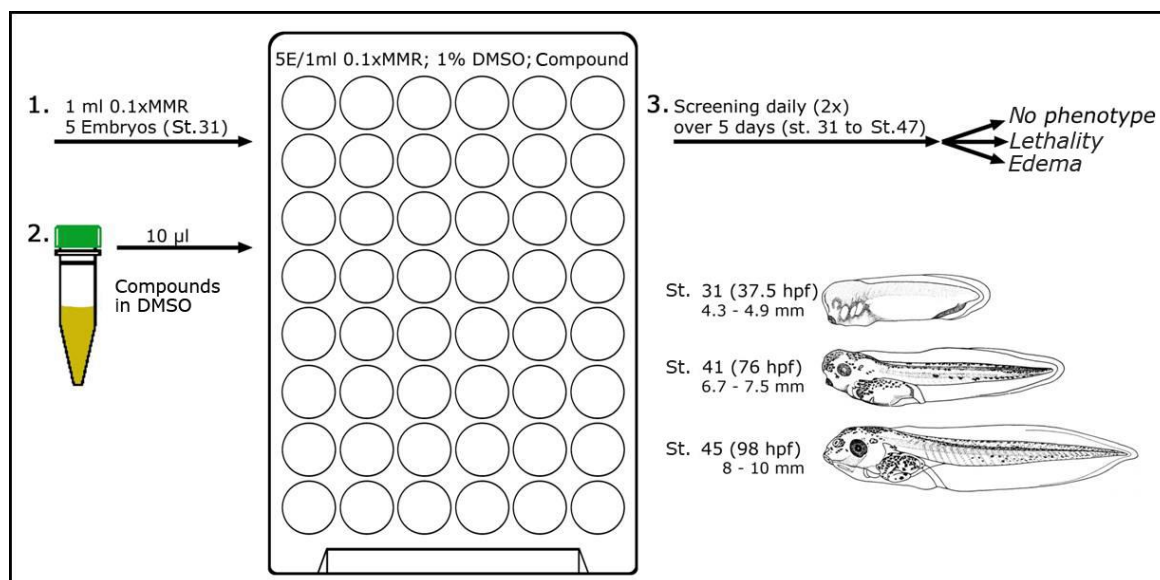
Given the potential role for AR signaling in vascular development and/or function uncovered by our previous chemical library screening strategy, we decided to assess first the expression of ARs in *Xenopus* embryos. The genomes of *Xenopus tropicalis* and *Xenopus laevis* harbor genes for all four AR genes (see [xenbase.org](http://xenbase.org) for details). AR gene expression in *Xenopus* embryos from stage 25 to stage 40 was determined by whole-mount *in situ* hybridization using antisense probes generated from AR cDNAs (Figure 14). All four ARs were expressed in the developing eyes and the central nervous system, particularly throughout the brain and spinal cord. Furthermore, AR subtype specific gene expression domains were observed. For example, A<sub>1</sub> ARs was expressed in the cement gland and pronephric kidney. Pronephric expression was present along the entire nephron. Cement gland expression was also observed for A<sub>3</sub> ARs, but this was confined to stage 25 embryos only. A<sub>2A</sub> and A<sub>2B</sub> ARs were also prominently expressed in somites. Furthermore, A<sub>2B</sub> ARs were widely expressed in the intermediate mesoderm, and moderate A<sub>2B</sub> AR gene expression could be detected in the distal pronephric kidney of stage 40 embryos. The renal expression of ARs in *Xenopus* embryos mirrors remarkably the situation in the adult kidneys of rodents, where A<sub>1</sub> and A<sub>2B</sub> ARs are the primary AR genes with expression in the nephron (Vitzthum et al., 2004). Importantly however, none of the four *Xenopus* ARs were expressed in the developing embryonic blood or lymph vasculature at levels detectable by whole mount *in situ* hybridization.



**Figure 14. Expression of AR genes in *Xenopus* embryos.** AR gene expression was determined by whole mount *in situ* hybridization. Embryos are shown in lateral views. Besides common expression in the brain and eyes, the characteristic expression domains of the different ARs are as follows: A<sub>1</sub> AR, the cement gland (arrowhead), spinal cord (sc), and the pronephric kidney (arrows); A<sub>2A</sub> AR, somites (arrows); A<sub>2B</sub> AR, somites (arrows) and intermediate mesoderm (arrowheads); and A<sub>3</sub> AR, the cement gland (arrowhead) and spinal cord (sc).

### Antagonists with selectivity for A<sub>1</sub> ARs are effective at inducing edema in *Xenopus* embryos

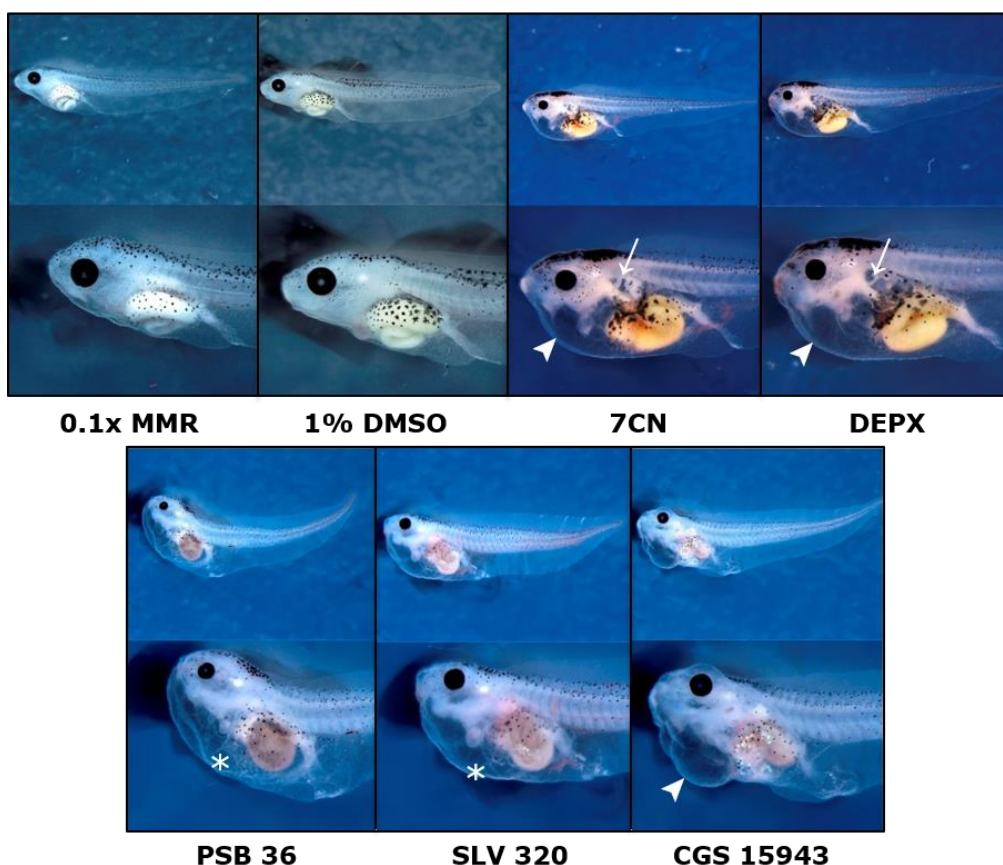
Selected AR antagonists (Table 11) were tested *in vivo* to determine their anti-lymphatic/angiogenic potential by scoring their ability to induce edema in a dose-dependent manner. *Xenopus* embryos at embryonic stage 31 (37 hours post fertilization, hpf), which is prior to the onset of vascular and lymphatic vessel development (Kalin et al., 2009), were arrayed in 48-well dishes and treated with the selected antagonists. Each AR antagonist was tested at final concentrations ranging between 0.01  $\mu$ M to 100  $\mu$ M in the culture media (0.1x MMR; 1% DMSO). Negative controls included embryos treated with 0.1x MMR alone and those with 0.1x MMR plus 1% DMSO alone. Pharmacological treatments were performed for a period of 5 days until embryos reached stage 47 (Fig. 15). The embryonic phenotypes, particularly the appearance of edemas, were scored twice daily by visual inspection using a dissecting microscope. The following pharmacological parameters were established once embryos reached stage 45: EC<sub>50</sub> (effective concentration, where 50% of the treated embryos present with edema and/or die), LC<sub>50</sub> (lethal concentration, causing lethality in 50% of the treated embryos), and EC<sub>max</sub> (effective concentration, where maximal incidence of edema was observed) (see *Material and Methods* for details).



**Figure 15. Procedure to assess the potency of AR antagonists to induce edema formation in *Xenopus* embryos.** The phenotypic screening procedure was performed in 48-well plates with five *Xenopus* embryos (E) per well. The embryos were scored twice daily for the presence of edema or lethality.

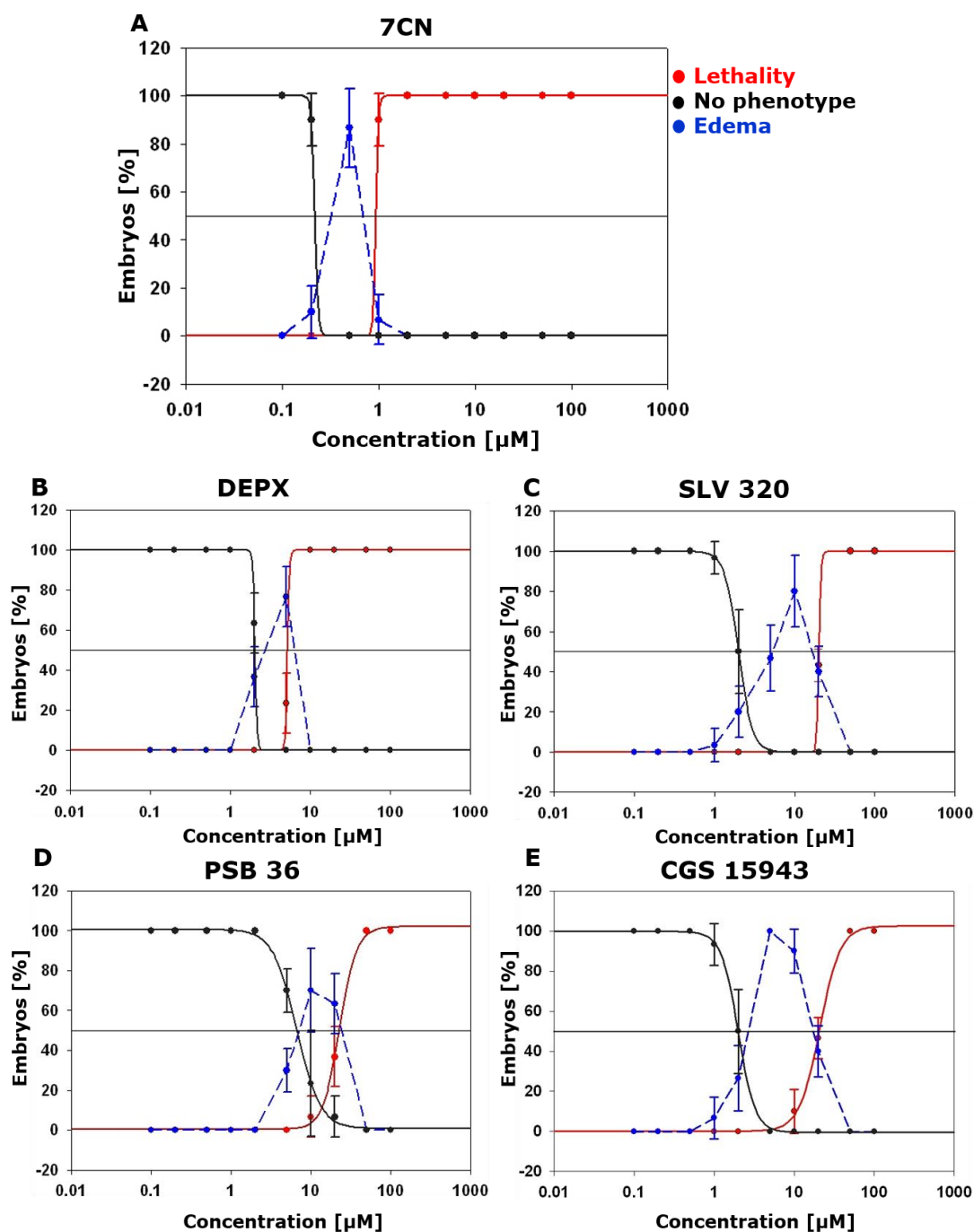
The results obtained from the *in vivo* treatments with subtype-specific AR antagonist were unambiguous. First, none of the antagonists selective for A<sub>2B</sub> and A<sub>3</sub> ARs induced edema or caused lethality even at 100 µM, the highest dose tested (*not shown*). Secondly, CGS 15943 was the only A<sub>2A</sub> AR-selective antagonist that induced edema and embryonic lethality. Finally, all A<sub>1</sub> AR-selective antagonists showed edema and followed by embryonic lethality.

Fig. 16 shows the edema phenotypes observed at stage 45 after treatment with the bioactive AR antagonists. Embryos treated with 7CN and DEPX were characterized by the presence of pericardial and pronephric edema. By contrast, CGS 15943 showed strong pericardial edema without pronephric edema. Finally, PSB 36 and SLV 320 treatments caused the formation of generalized ventral edema.



**Figure 16. Distinct edema phenotypes induced by subtype-specific AR antagonists in *Xenopus* embryos.** The embryos were treated with the indicated AR antagonists at concentrations equivalent to EC<sub>max</sub> (see Table 12) and incubated until stage 45. Control embryos were treated with 0.1x MMR and 0.1x MMR with 1% DMSO. Representative embryos are shown in lateral views with enlargements below depicting head and trunk of the respective embryo. Primary areas of edema formation are marked by arrowheads for pericardial, arrows for pronephric, and asterisks for generalized ventral edema.

The dose-response relationships for the primary phenotypes (edema, lethality) observed in stage 45 embryos treated with bioactive AR antagonists are shown in Fig. 17. At the stage 45 endpoint, the percentage of normal, edema-harboring, and dead embryos were determined. The obtained graphs were used to calculate  $EC_{50}$ ,  $EC_{max}$ , and  $LC_{50}$  values for each AR antagonist tested (Table 12). Furthermore, we defined the therapeutic index (TI) as the ratio of  $LC_{50}$  over  $EC_{50}$ . Our findings demonstrate that the compound concentration ( $EC_{max}$ ) need to induce maximal edema frequency in the embryos was always lower than the one causing half-maximal lethality ( $LC_{50}$ ). The TI values ranged between 2.2 (for DEPX) and 11 (for SLV 320) indicating that SLV 320 was most optimal in that robust edema formation could be induced at concentrations, where no or minimal lethality was observed. With regard to the  $EC_{50}$  values, PSB 36 was the least potent compound with an  $EC_{50}$  value of 6.7  $\mu$ M. By contrast, 7CN was the most potent compound with an  $EC_{50}$  value of 0.3  $\mu$ M. It was therefore the only AR antagonist with edema-inducing efficacy at nanomolar compound concentrations in the media. However, 7CN was also the only AR antagonist with an  $LC_{50}$  value in the high nanomolar range. PSB 36, the least toxic compound, had an  $LC_{50}$  value of 23  $\mu$ M.



**Figure 17. Dose-response relationships of phenotypes induced in *Xenopus* embryos by AR antagonist treatment.** *Xenopus* embryos were treated with the indicated AR antagonists at concentrations ranging from 0.1  $\mu\text{M}$  to 100  $\mu\text{M}$ . The phenotypes (edema, death) were scored once embryos reached stage 45. The black line shows the percentage of normal embryos observed with increasing doses of the AR antagonist. The blue line shows the percentage of embryos with edema. The dose-dependence of embryonic lethality shown with red lines. The graphs shown are compiled from at least six independent experiments. The error bars indicate standard deviations.

**Table 12. Compilation of pharmacological parameters obtained from *Xenopus* embryos after AR antagonist treatment**

Compound	Selectivity	<i>In vivo</i> phenotype	EC <sub>50</sub> [μM]	EC <sub>max</sub> [μM]	LC <sub>50</sub> [μM]	TI
DEPX	A <sub>1</sub>	Edema	2.4	4.9	5.3	2.2
7CN	A <sub>1</sub>	Edema	0.3	0.5	0.9	3
PSB 36	A <sub>1</sub>	Edema	6.7	10	23	3.4
SLV 320	A <sub>1</sub>	Edema	2	10	22	11
CGS	A <sub>2A</sub>	Edema	2	5.1	21	10.5

### Combination treatments with antagonists targeting A<sub>2A</sub>, A<sub>2B</sub> or A<sub>3</sub> ARs were ineffective at inducing edema formation

Pharmacological profiling of subtype-specific AR antagonists indicates that selectivity for A<sub>1</sub> ARs is a requirement for the induction of edema formation in *Xenopus* embryos. We next asked whether edema formation could be achieved by simultaneously inhibiting two AR subtypes *in vivo*. *Xenopus* embryos were treated with all possible combinations of subtype-specific AR antagonists, who by themselves had no edema-inducing potential (Fig. 18; Table 13). Each compound was present at a concentration of 20 μM in the culture media. The embryos were treated with the AR antagonist combinations from stage 31 to stage 45 as in the previous experiments. With one exception, all AR antagonist combinations tested failed to induce edema efficiently in *Xenopus* embryos. Typically, less than 10% of the embryos displayed a phenotype (edema or lethality) and many combinations had no effect at all. Similarly, we found that treatment of embryos with single A<sub>2A</sub> selective antagonists even at a concentration of 40 μM were ineffective at inducing edema at frequencies higher than 15%. By contrast, 80% of the embryos treated with a combination of SCH 442416 and SCH 58261 had a phenotype: 45% manifested with edema, and 35% had died (Table 13). However, concentrations of at least 20 μM of each antagonist were required to elicit these phenotypes, whereas A<sub>1</sub> selective AR antagonists were alone effective at lower concentrations. Overall, the combination experiments indicate that co-inhibition of any two A<sub>2A</sub>, A<sub>2B</sub> or A<sub>3</sub> AR is not sufficient to cause edema formation in *Xenopus* embryos.

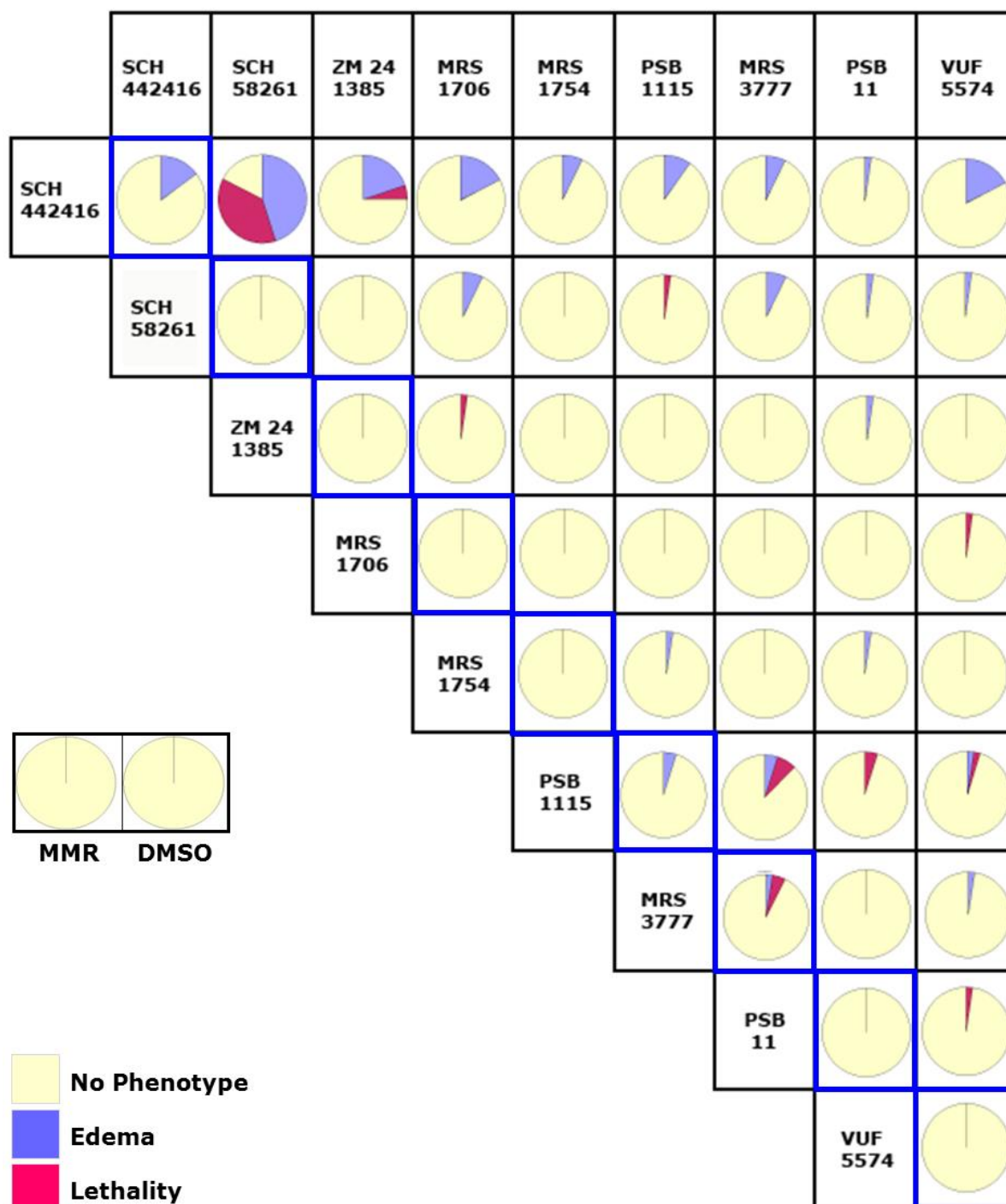


**Figure 18. Summary of the phenotypes observed after treatment of *Xenopus* embryos with AR antagonist combinations.** The matrix shows all tested compound combinations. The pie charts visualize the relative frequencies of the observed main phenotypes (normal, edema, lethality). MMR and DMSO denote negative control experiments, where embryos were treated with the culture medium 0.1x MMR and 0.1x MMR containing 1% DMSO. The pie charts were generated from the primary data shown in Table 13.

**Table 13. Frequencies of phenotypes observed in *Xenopus* embryos treated with AR antagonist combinations**

AR antagonist	Normal [%]	Edema [%]	Lethality [%]
SCH 442416 + SCH 442416	85	15	0
SCH 442416 + SCH 58261	20	45	35
SCH 442416 + ZM 241385	75	20	5
SCH 442416 + MRS 1706	85	15	0
SCH 442416 + MRS 1754	85	5	0
SCH 442416 + PSB 1115	90	10	0
SCH 442416 + MRS 3777	95	5	0
SCH 442416 + PSB 11	98	2	0
SCH 442416 + VUF 5574	85	15	0
SCH 58261 + SCH 58261	100	0	0
SCH 58261 + ZM 241385	100	0	0
SCH 58261 + MRS 1706	90	10	0
SCH 58261 + MRS 1754	100	0	0
SCH 58261 + PSB 1115	98	0	2
SCH 58261 + MRS 3777	90	10	0
SCH 58261 + PSB 11	98	2	0
SCH 58261 + VUF 5574	98	2	0
ZM 241385 + ZM 241385	100	0	0
ZM 241385 + MRS 1706	98	0	2
ZM 241385 + MRS 1754	100	0	0
ZM 241385 + PSB 1115	100	0	0
ZM 241385 + MRS 3777	100	0	0
ZM 241385 + PSB 11	98	2	0
ZM 241385 + VUF 5574	100	0	0
MRS 1706 + MRS 1706	100	0	0
MRS 1706 + MRS 1754	100	0	0
MRS 1706 + PSB 1115	100	0	0
MRS 1706 + MRS 3777	100	0	0
MRS 1706 + PSB 11	100	0	0
MRS 1706 + VUF 5574	98	0	2
MRS 1754 + MRS 1754	100	0	0
MRS 1754 + PSB 1115	98	2	0
MRS 1754 + MRS 3777	100	0	0
MRS 1754 + PSB 11	98	2	0
MRS 1754 + VUF 5574	100	0	0
PSB 1115 + PSB 1115	95	5	0
PSB 1115 + MRS 3777	85	5	10
PSB 1115 + PSB 11	95	0	5
PSB 1115 + VUF 5574	98	2	2
MRS 3777 + MRS 3777	93	2	5
MRS 3777 + PSB 11	100	0	0
MRS 3777 + VUF 5574	98	2	0
PSB 11 + PSB 11	100	0	0
PSB 11 + VUF 5574	98	0	2
VUF 5574 + VUF 5574	100	0	0

Note: The final concentration of each compound in the culture media was 20  $\mu$ M. The results listed per compound combination were compiled from 6 independent experiments with a total of 60 embryos. No abnormalities were observed when embryos were cultured in 0.1x MMR or 0.1x MMR with 1% DMSO.

### **AR antagonists affecting blood and lymph vessel morphogenesis**

Four A<sub>1</sub> AR antagonists and the A<sub>2A</sub> AR-selective CGS 15943 antagonist were found to be capable of inducing edema in *Xenopus* embryos (Table 12). The appearance of edema in compound-treated embryos may be attributed to dysfunction of the cardiovascular system, the lymphatics, and/or the kidneys. Therefore, compound-treated embryos were analyzed by whole mount *in situ* hybridization for any alterations in tissue and organ morphology using organ-specific molecular markers. The embryos were treated with the AR antagonists at concentrations equivalent to previously established EC<sub>50</sub> values (Table 12). The embryos were raised to stages 35/36 (50 hpf) for the analysis of blood vessels and pronephric kidneys, and to stage 40-41 (76 hpf) for the lymphatics, respectively.

A comparison of blood vessel development revealed nicely established vascular structures with vitelline vein networks and sprouting intersomitic vessels (ISVs) in embryos raised under control conditions (0.1x MMR; 0.1x MMR with 1% DMSO) (Fig. 19). By contrast, vascular abnormalities were evident in DEPX- and 7CN-treated embryos (Fig. 19). VVN formation and ISV sprouting was impaired, particularly in 7CN-treated embryos. These findings are consistent with those reported by us previously (Kalin et al., 2009). Surprisingly, the blood vascular system appeared largely unaffected in embryos treated with PSB 36, SLV 320, and CGS 15943 (Fig. 19). Abnormal blood vessel morphogenesis is therefore unlikely to be the underlying defect causing edema formation in the embryos treated with this set of compounds.

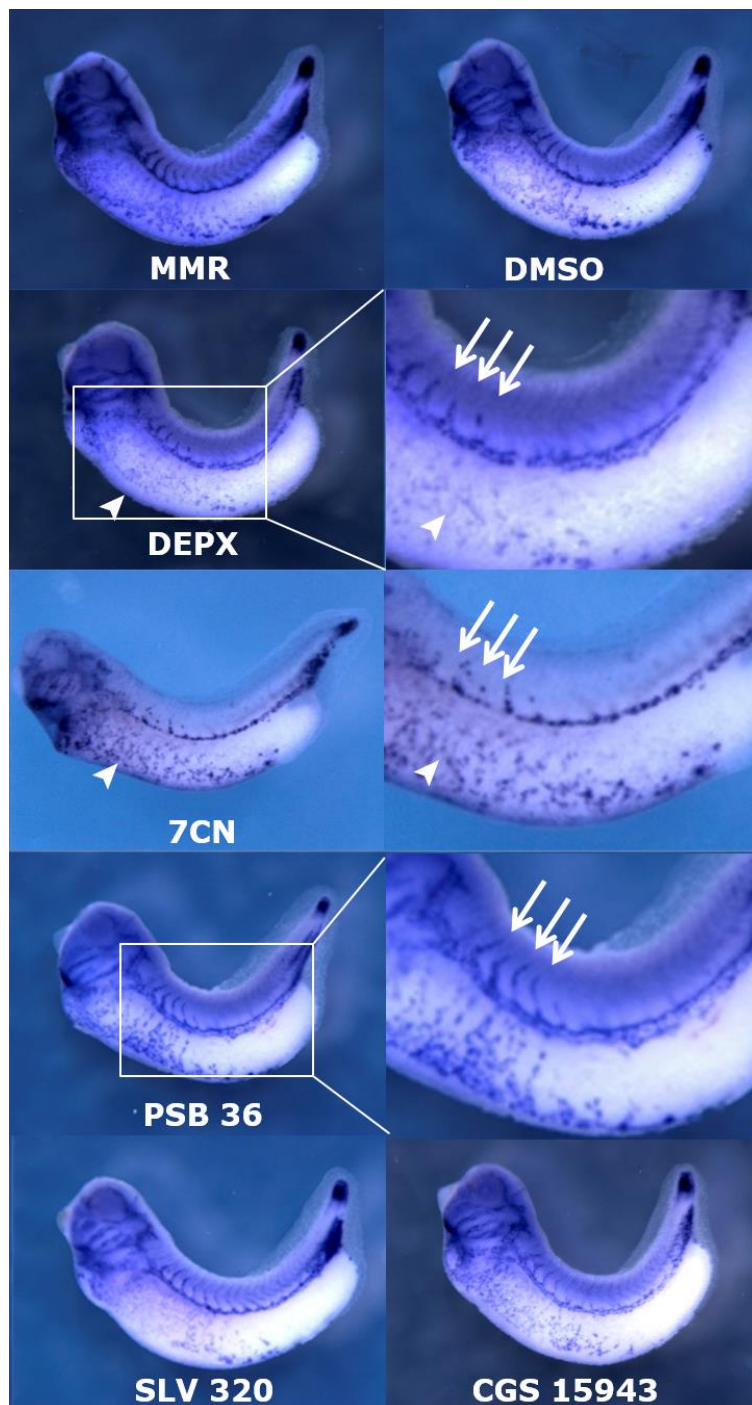


**Figure 19. AR antagonists interfering with blood vessel morphogenesis.** Embryos were treated with the indicated AR antagonists at concentrations equivalent to the EC<sub>50</sub> values (see Table 12) and raised until they reached stage 35/36. Subsequently, the embryos were fixed and the expression of the blood vessel marker *aplnr* (*msr*, *apj-b*) was determined by whole mount *in situ* hybridization. Arrowheads and arrows indicate disrupted VVN networks and impaired ISV sprouting, respectively.

### **DEPX and 7CN treatments disrupt lymph vessel morphogenesis**

To determine possible defects in lymphatic vessel development, compound-treated embryos were raised to stages 40 and 41, when they were subjected to whole mount *in situ* hybridization to visualize the expression of lymphatic marker *vegfr3* (Kalin et al., 2009). At these stages the lymphatic system includes the bilateral anterior lymph hearts (ALH), posterior lymph vessels (PLVs), and the anterior lymph sacs (ALS). Besides lymphatic endothelia, *vegfr3* is also expressed in the VVNs (Fig. 20).

The embryos treated with DEPX and 7CN showed large-scale deficiencies of their lymphatic systems (Fig. 20). The ALHs were devoid of afferent lymph vessels, the ALSs appear to be underdeveloped, and the VVNs were disorganized. Patches of *vegfr3*-expressing cell clusters suggest the presence of endothelial cells, which failed to assemble into vessel and capillary networks. The absence of VVNs is consistent with previous results (compare with Fig. 19). Embryos treated with the other AR antagonists did not show overtly abnormal lymphatic structures (Fig. 20). For example, ALHs, ALSs, and VVNs were well established and comparable to control embryos. Taken together, DEPX and 7CN disrupted both blood and lymph vessel morphogenesis, whereas the edema-inducing activities of PSB 36, SLV 320 and CGS 15943 cannot be attributed to defects in the morphogenesis of these vessel systems.

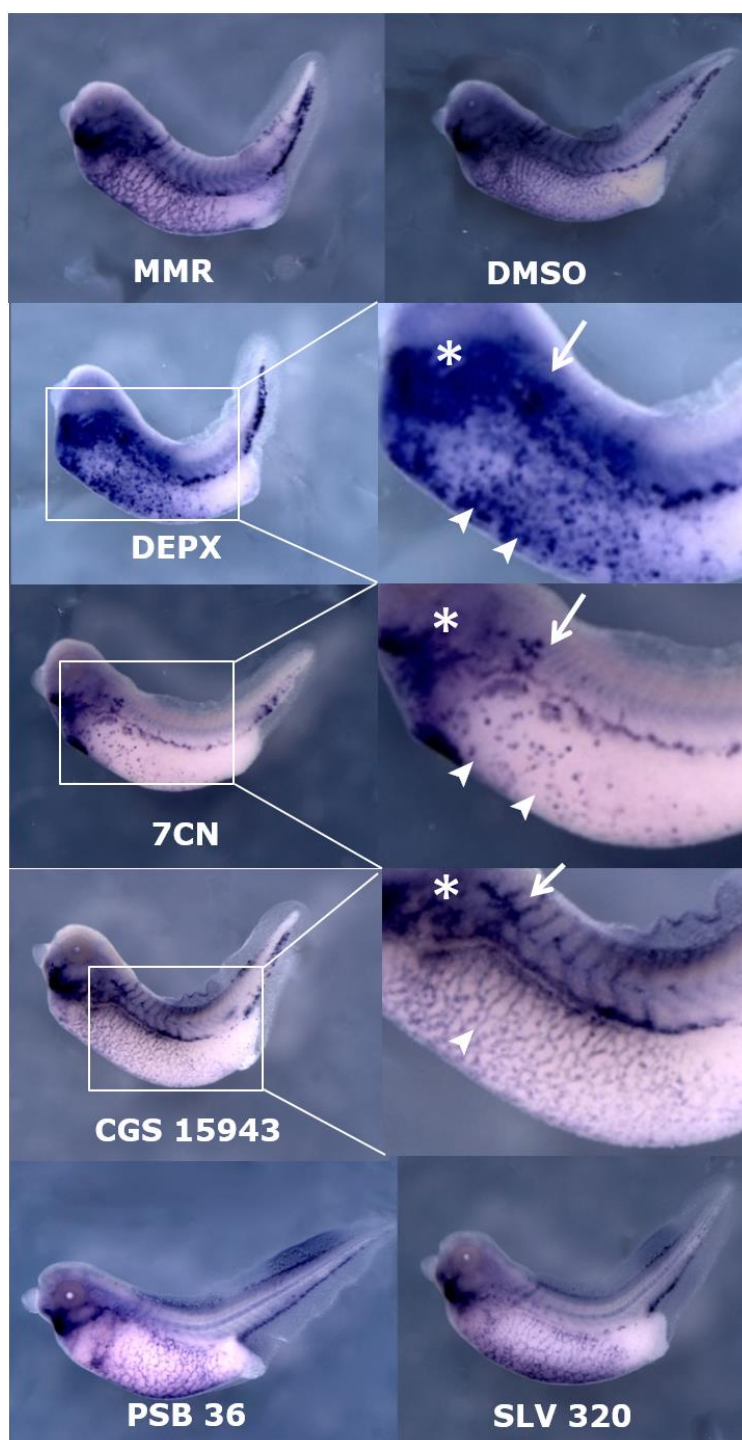


**Figure 20. AR antagonists interfering with lymph vessel morphogenesis.** Embryos were treated with the indicated AR antagonists at concentrations equivalent to the EC<sub>50</sub> values (see Table 12) and raised until they reached stage 40/41. Subsequently, the embryos were fixed and the expression of the lymph vessel marker *vegfr3* was determined by whole mount *in situ* hybridization. Abnormalities in lymphatics feeding to the ALH (arrows), underdeveloped ALSs (asterisks) and disrupted VVNs (arrowheads) are indicated. Note that VVNs are normal in PSB 36, SLV 320 and CGS 15943 treated embryos.

### Normal pronephric kidney morphogenesis in embryos treated with AR subtype-selective antagonists

The pronephros marker *fxyd 2* ( $\gamma$  subunit of  $\text{Na}^+ \text{K}^+$  ATPase) was used to assess possible defects in pronephric kidney morphogenesis in AR antagonists-treated embryos at stage 35/36. At this stage the pronephric nephron is comprised of four main segments (proximal tubule, intermediate tubule, distal tubule, and connecting tubule) expressing *fxyd2* (Raciti et al., 2008). The morphologies of the pronephric kidneys of control and compound-treated embryos are shown in Fig. 21. The pronephric kidneys of compound-treated embryos were comparable to controls, and no defects in nephron segment development were apparent. Edema formation in 7CN- and DEPX-treated embryos may therefore be attributed to arrested or disrupted blood and lymph vessel development, without affecting pronephric kidney development. With regard to PSB 36, SLV 320, and CGS 15943, the morphogenesis of pronephric kidneys and blood and lymphatic vessels appears to be normal suggesting the other mechanisms cause edema formation in embryos treated with these compounds. Of all the AR antagonists tested by us to date in *Xenopus* embryos, only 7CN and DEPX were able to disrupt vascular and lymphatic vessel development.

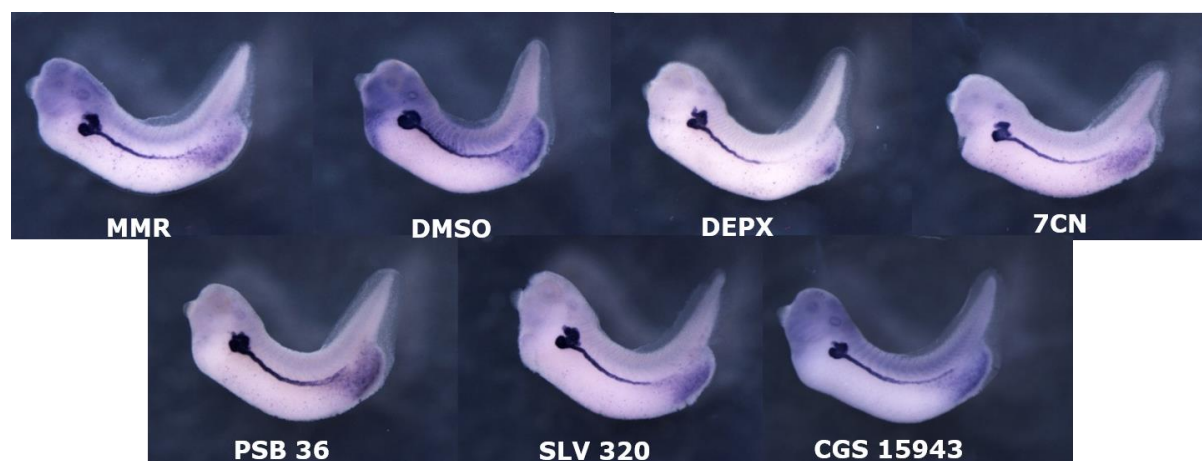


**Figure 21. AR antagonist treatments do not affect pronephric kidney development.** Embryos were treated with the indicated AR antagonists at concentrations equivalent to the  $\text{EC}_{50}$  values (see Table 12) and raised until they reached stage 35/36. Subsequently, whole mount *in situ* hybridization was performed to visualize expression of the pronephric marker *fxyd2*. Compound-treated embryos retain normal pronephric kidneys, which were comparable in morphology to control embryos (0.1x MMR; 0.1x MMR with 1% DMSO).

### **7CN and DEPX specific antagonists did not affect hematopoiesis, erythrocyte dispersal and muscle differentiation**

Next, we asked whether treatment of 7CN and DEPX interfered with the development of other organ systems in *Xenopus* embryos. Whole mount *in situ* hybridizations were performed on compound-treated stage 40 embryos to visualize the expression of hemoglobin  $\alpha$ T3 subunit (*hba3*,  *$\alpha$ T3 globin*) for erythrocytes, *tal1* (*scl*) for hemangioblasts, and *myod1* (*myoD*) for myoblasts (Fig. 22).

Unlike mammalian erythrocytes, erythrocytes in *Xenopus* are nucleated and therefore they can be traced by visualizing globin gene expression (Kelley et al., 1994). Stage 40 embryos have a functional cardiovascular system with circulating erythrocytes present in blood vessels, including PCVs, ISVs and VVNs (Fig. 22A,B). By contrast, erythrocyte dispersal was strongly reduced or blocked in compound-treated embryos (Fig. 22C,D). The erythrocytes were largely confined to the ventral blood islands indicating that specification and differentiation of erythrocytes is not affected by 7CN or DEPX treatment. As these compounds disrupt VVNs formation (Fig. 19), the erythrocytes remain trapped in the ventral blood islands and are unable to circulate.

The transcription factor *tal1* (*scl*) is initially expressed in the ventral blood island and the dorsal lateral plate (DLP), where it is crucial for the development of hemangioblasts in *Xenopus* embryos (Ciau-Uitz et al., 2013). The hemangioblasts of the DLP migrate to the midline, where they coalesce to form the dorsal aorta and, subsequently will give rise to the hemogenic endothelium and hematopoietic stem cells (Ciau-Uitz et al., 2013, Ciau-Uitz et al., 2000). As expected, the *tal1*-expressing hemangioblasts of stage 40 embryos are found in the ventral blood islands and in blood vessels of the DLP (Fig. 22 E,F). In compound-treated embryos, *tal1*-expressing hemangioblasts are confined to the ventral blood islands, where they appear to be more abundant than in control embryos (Fig. 22G,H). No *tal1*-expressing hemangioblasts were detected in the DLP. This suggests that 7CN and DEPX interfere with the formation or differentiation of hemangioblasts in the DLP, where they would normally contribute to blood vessels and adult HSCs.

In stage 40 embryos, the myoblast marker *myod1* is expressed primarily in the somites and in migrating myoblasts, which will contribute to the hypaxial muscles of the abdomen (Maczkowiak et al., 2010). We observed that compound treatment of *Xenopus* embryos did not interfere with *myod1* expression and

clusters of migrating myoblasts were present in normal numbers (Fig. 22I-L). Therefore, myogenesis is not affected by DEPX or 7CN treatment. Overall, the effects of DEPX and 7CN treatment in *Xenopus* embryos appear not to be of pleiotropic nature, disrupting the morphogenesis of multiple tissues or organs. Rather, the effects appear to be limited to interfering with blood and lymph vessel formation.

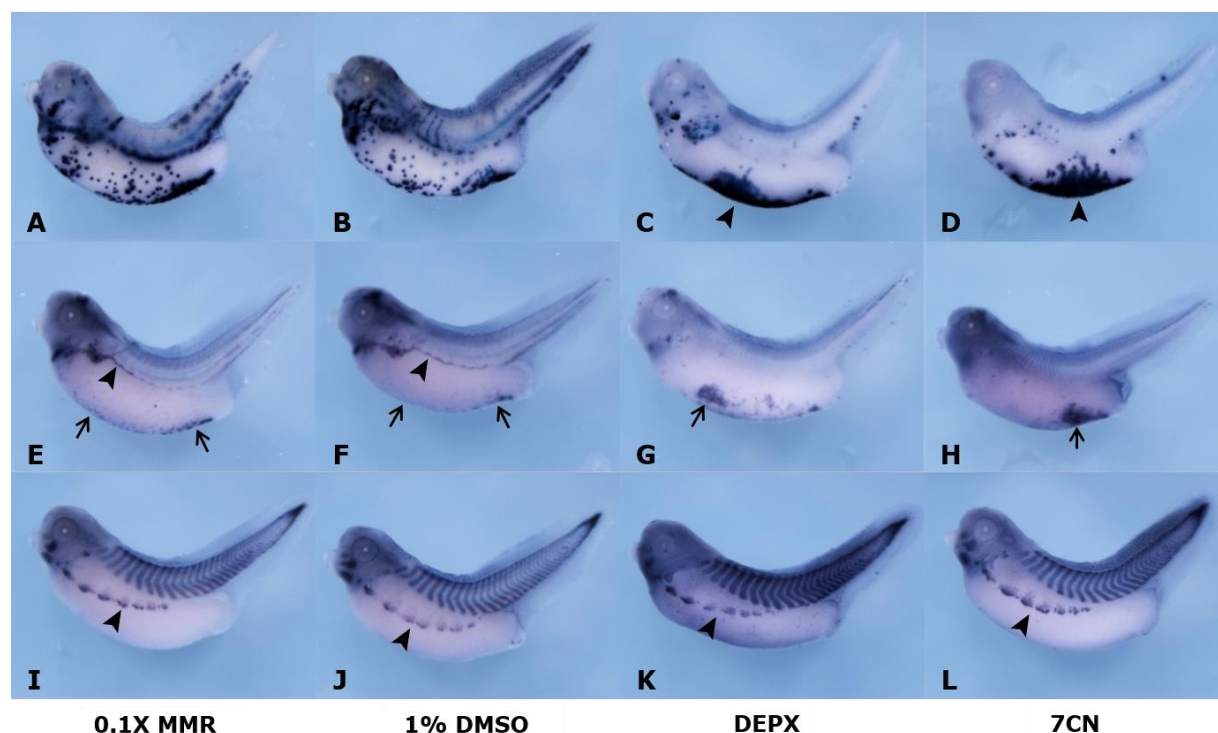


**Figure 22. Effects of DEPX and 7CN treatments on erythropoiesis, hemangiopoiesis, and myogenesis in *Xenopus* embryos.** Embryos were treated with the DEPX and 7CN from stages 31 to 40. Whole mount *in situ* hybridizations were performed to detect the expression of marker genes for erythrocytes (*hba3/αT3 globin*; a-d), hemangioblasts (*tal1/scl*; e-h), and myoblasts (*myod1*; i-l). (a-d) Erythrocytes remain largely confined to the ventral blood islands (arrowheads) in compound-treated embryos. (e-h) Hemangioblasts expressing *tal1* present in ventral blood islands (arrows), but absent from the DLP regions (arrowheads). (i-l) Expression of *myod1* in the somites and migrating myoblasts (arrowheads) is not affected by DEPX or 7CN treatment.

### **Effects of DEPX and 7CN on endothelial cell proliferation and sprouting *in vitro***

The AR antagonists DEPX and 7CN were found to specifically disrupt blood and lymphatic vessel development in *Xenopus* embryos. We therefore asked whether these compounds are also active in mammals and whether they exert their effects directly or indirectly on blood vascular and lymphatic endothelial cells. Furthermore, we wondered whether they interfere with endothelial cell proliferation and/or sprouting. To address these points, experiments in cell cultures using human umbilical vein endothelial cells (HUVECs) and lymphatic endothelial cells (LECs) were carried out by our collaborator Dr. Adriana Promorac in the laboratory of Prof. Dr. Michael Detmar (Institute of Pharmaceutical Sciences, ETH Zurich, Zurich, Switzerland).

Cell proliferation assays were performed by treating endothelial cells with the compounds in a dose-dependent manner. The compound concentrations tested ranged from 0.1 to 10  $\mu\text{M}$  in presence of 0.1% DMSO. The cells were treated with VEGFA to enhance cell proliferation and compound treatments were carried out for 48 hours. The control compound SU 4312, a VEGFR antagonist, served as a potent inhibitor of endothelial cell proliferation. DEPX appears to suppress in a dose-dependent manner VEGFA-dependent cell proliferation to control levels, but this effect was not statistically significant (Fig. 23). This was the case for HUVECs as well as for LECs. By contrast, 7CN inhibited HUVEC and LEC proliferation stronger and brought down cell proliferation below the control levels in a statistically significant manner. A 10  $\mu\text{M}$ , proliferation was reduced to levels comparable with those obtained in the presence of 10  $\mu\text{M}$  SU 4312. The half-maximal inhibitory concentration ( $\text{IC}_{50}$ ) for 7CN were 2.09  $\mu\text{M}$  and 2.42  $\mu\text{M}$  for HUVECs and LECs, respectively.

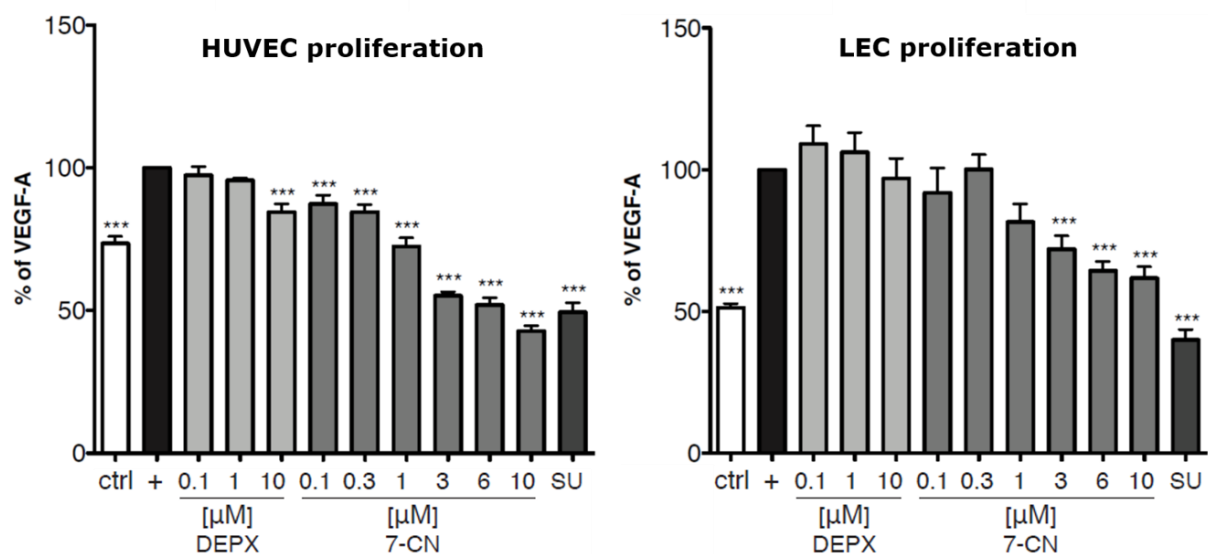


**Figure 23. Effects of DEPX and 7CN on endothelial cell proliferation.** The compounds were tested *in vitro* on LEC and HUVEC cultures at the concentrations indicated. SU 4312 concentration was 10  $\mu$ M. After 48 hours, live cells were stained with 4-methylumbelliferyl heptanoate (4-MUH) and fluorescence intensities were measured. Data is expressed as mean values  $\pm$  standard error of mean (SEM) with  $n=8$ . Results are representative for 3 independent experiments. \*  $p<0.05$ , \*\*  $p<0.01$ , \*\*\*  $p<0.001$ .

Microcarrier beads coated with endothelial cells were used to assess the effects of DEPX and 7CN on sprouting (Fig. 24). The process was induced *in vitro* by treating HUVECs with basic fibroblast growth factor (bFGF) and VEGFA for 48 hours. For LECs, sprouting was initiated with bFGF, VEGFA, and sphingosine-1-phosphate (S1P). The concentrations of DEPX and 7CN ranged from 0.1 to 10  $\mu$ M in presence of 0.1% DMSO. The control compound SU 4312 inhibited LEC and HUVEC sprouting with  $IC_{50}$  values of 1.55  $\mu$ M and 2.27  $\mu$ M, respectively (Fig. 23, *data not shown*). DEPX treatment had marginal effects on sprout formation by LECs (Fig. 24C, D, G), and for HUVEC sprouting, there were not significant effects (Fig. 24J, K, N). 7CN however was a potent inhibitory of both LEC and HUVEC sprouting with  $IC_{50}$  values of 0.20  $\mu$ M and 0.37  $\mu$ M, respectively (Fig. 24).

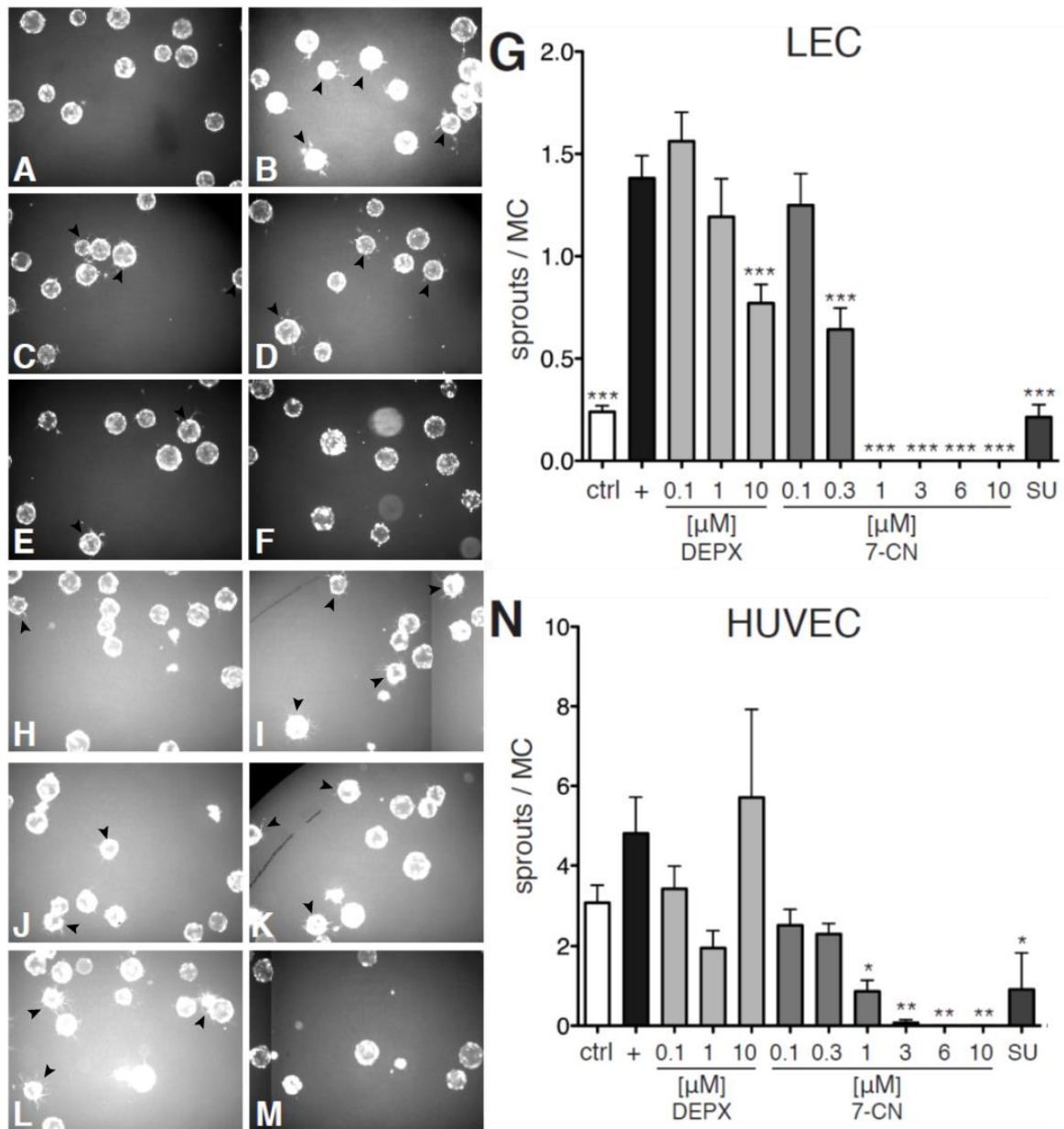


**Figure 24. Effects of DEPX and 7CN on endothelial cell sprouting.** (A-F) Images of collagen gel-embedded microcarriers coated with LEC after treatment with 0.1% DMSO (A), VEGFA/bFGF/S1P (B), 0.1  $\mu\text{M}$  or 10  $\mu\text{M}$  DEPX (C, D), and 0.1  $\mu\text{M}$  or 10  $\mu\text{M}$  7CN (E, F). (G) Results of the LEC sprouting experiments. (H-M) Images of collagen gel-embedded microcarriers coated with HUVEC after treatment with 0.1% DMSO (H), VEGFA/bFGF (I), 0.1  $\mu\text{M}$  or 10  $\mu\text{M}$  DEPX (J, K), and 0.1  $\mu\text{M}$  or 10  $\mu\text{M}$  7CN (L, M). (N) Results of the HUVEC sprouting experiments. Examples of endothelial sprouting are indicated with arrowheads. SU 4312 concentration was 10  $\mu\text{M}$ . The data are shown as mean values  $\pm$  SEM, n=3. Results are representative for 3 independent experiments. \*p < 0.05, \*\*p < 0.01, \*\*\* p<0.001.

In summary, the *in vitro* experiments with HUVECs and LECs indicate that 7CN was a strong inhibitor of endothelial cell proliferation and sprouting, whereas the effects of DEPX were at best marginal.

### Structure-activity relationship studies

Structure-activity relationship (SAR) studies were carried out to determine the relationship between the chemical structures of our two lead compounds, DEPX and 7CN, and their biological activity, i.e. their ability to induce edema and disrupt blood and lymph vessel development. Database searches were performed to identify commercially available derivatives of DEPX and 7CN, which would be then tested *in vivo* for bioactivity in *Xenopus* embryos.

#### The *in vivo* activity of DEPX is influenced by side chain length

Three derivatives of DEPX (1,3-Diethyl-8-phenylxanthine) were identified, which were commercially available: 1,3-Dimethyl-8-phenylxanthine (DMPX); 1,3-Dipropyl-8-phenylxanthine (DPPX); and 1,3-Dipropyl-8-(p-sulfophenyl) xanthine (DPSPX). The chemical structures of the selected compounds in comparison to DEPX are shown in Fig. 25. DMPX contains methyl groups in place of the ethyl groups at positions 1 and 3 of the xanthine moiety. In DPPX, the side chains are extended to propyl groups. Finally, DPSPX is essentially identical to DPPX, but its phenyl ring is sulfonated. DMPX and DPPX are useful as we can determine whether the length of the 1,3 substitutes (methyl, ethyl and propyl) of 8-phenylxanthine influence compound activity *in vivo*. With DPSPX, we could assess whether sulfonation of the phenol group provides a benefit. The selected DEPX derivatives have been shown in the past to act as antagonists of AR signaling (Table 14). On the basis of the available data, DEPX and its derivatives appear to preferentially target A<sub>1</sub> ARs, with DMPX having the highest affinity.

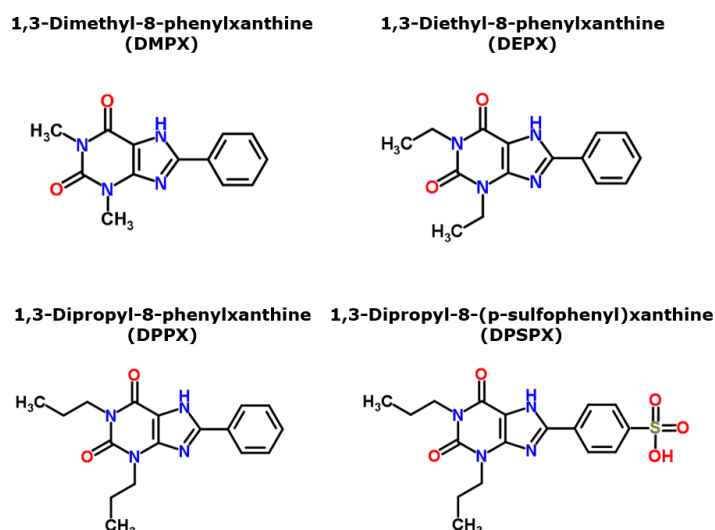


**Figure 25. Selected derivatives of DEPX.** The chemical structures of DMPX, DEPX, DPPX, and DPSPX were downloaded from ChemSpider (chemspider.com)

**Table 14. DEPX derivatives and their AR subtype selectivities**

Compound name	K <sub>i</sub> Values (nM)				Reference
	A <sub>1</sub>	A <sub>2A</sub>	A <sub>2B</sub>	A <sub>3</sub>	
DEPX	44.5 (r)	863 (r)	341	n.a.	(Phelps et al., 2006, Bruns et al., 1987)
DMPX	1.2 (b)	n.a.	n.a.	n.a.	(Bruns et al., 1983)
DPPX	10 (r)	190 (r)	18.9	n.a.	(Yan and Muller, 2004)
DPSPX	210 (r)	1400 (r)	250	183	(Yan and Muller, 2004)

K<sub>i</sub> values refer to studies with human ARs unless noted otherwise. Abbreviations: n.a., not available; b, bovine; r, rat.

Dose-response studies with DMPX, DPPX, and DPSPX were performed *in vivo* to assess their ability to induce edema in *Xenopus* embryos and to establish pharmacological parameters. Fig. 26 compares the dose-response profile of DEPX with those obtained for the DEPX derivatives for the standard 5-day treatment assay. Neither DMPX nor DPSPX had significant effects on *Xenopus* embryos. At none of the concentrations tested did they induce edema formation and limited lethality was observed at 100 μM, the highest compound concentration tested. By contrast, DPPX was essentially indistinguishable from DEPX with regard to its ability to induce edema and cause lethality. Consequently, the pharmacological values (EC<sub>50</sub>, EC<sub>max</sub>, LC<sub>50</sub>, TI) for DPPX were very similar to those of DEPX (Table 15).

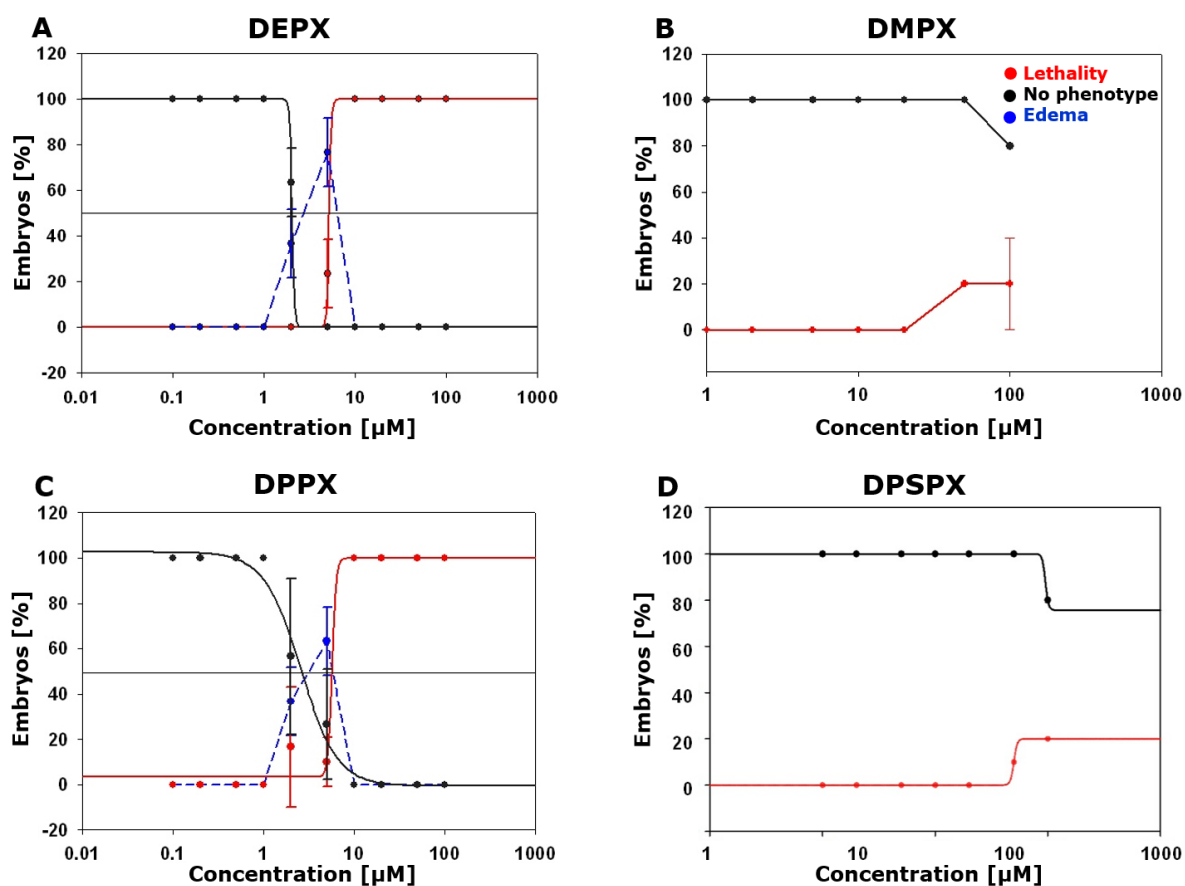


**Figure 26. Dose-response relations of phenotypes induced by AR antagonists in *Xenopus* embryos.** *Xenopus* embryos were treated with DMPX, DPPX, and DPSPX at concentrations ranging from 0.1  $\mu\text{M}$  to 100  $\mu\text{M}$ . Embryos were scored at stage 45 for phenotypes (edema, death). The black line shows the percentage of normal embryos, blue line shows the percentage of edema observed with increasing doses of the AR antagonist. Dose-dependency for embryonic lethality is shown with red lines. The graphs shown are compiled from at least six independent experiments. The error bars indicate standard deviations. Panel A was taken from Fig. 17 and is shown for comparative purposes.

**Table 15. Pharmacological values obtained from *Xenopus* embryos after treatment with DEPX derivatives**

Compound	<i>In vivo</i> phenotype	EC <sub>50</sub> [ $\mu\text{M}$ ]	EC <sub>max</sub> [ $\mu\text{M}$ ]	LD <sub>50</sub> [ $\mu\text{M}$ ]	TI
DMPX	-	n.a.	n.a.	n.a.	n.a.
DEPX	Edema	2.4	4.9	5.3	2.2
DPPX	Edema	2.7	4.8	5.7	2.1
DPXS	-	n.a.	n.a.	n.a.	n.a.

Abbreviations: n.a., not available.

Interestingly, DPPX shared with DEPX a similar pattern of edema induction that was characterized by the appearance of pericardial and pronephric fluid accumulations (Fig. 27). The shared anatomy of edema formation provides further evidence that DPPX acts *in vivo* similarly to DEPX.

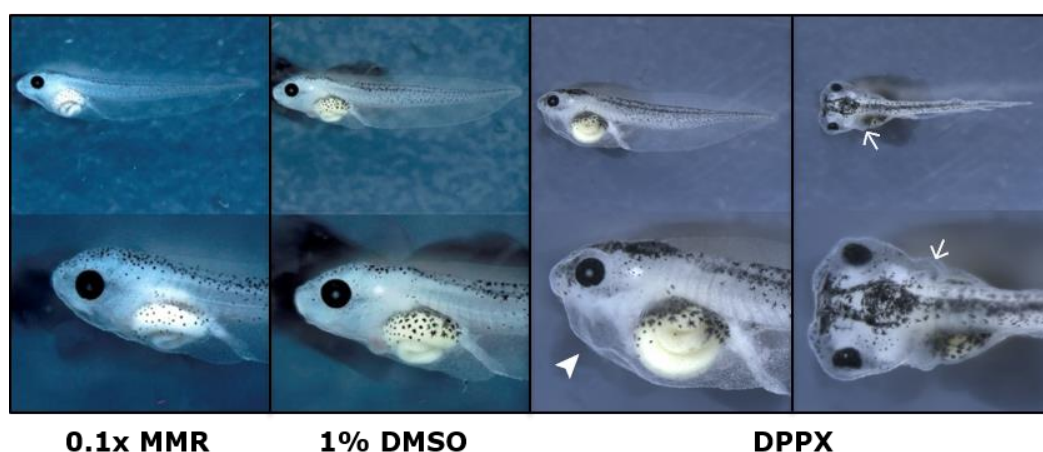


**Figure 27. Edema phenotypes induced by DPPX in *Xenopus* embryos.** The embryos were treated with DPPX at concentrations equivalent to  $EC_{50}$  (see Table 15) and incubated until stage 45. Control embryos were treated with 0.1x MMR and 0.1x MMR with 1% DMSO. Representative embryos are shown in lateral and dorsal views with enlargements below depicting head and trunk of the respective embryo. Primary areas of edema formation are marked by arrowheads for pericardial, arrows for pronephric kidney edema.

Since DPPX was found to be a potent inducer of edema in *Xenopus* embryos, we assessed by whole mount *in situ* hybridization whether compound treatment affected blood and lymph vessel development (Fig. 28). The abnormalities with blood vessels and the lymphatics in DPPX-treated embryos were very reminiscent of those seen with DEPX (compare Figs. 19 & 20 with Fig. 28).

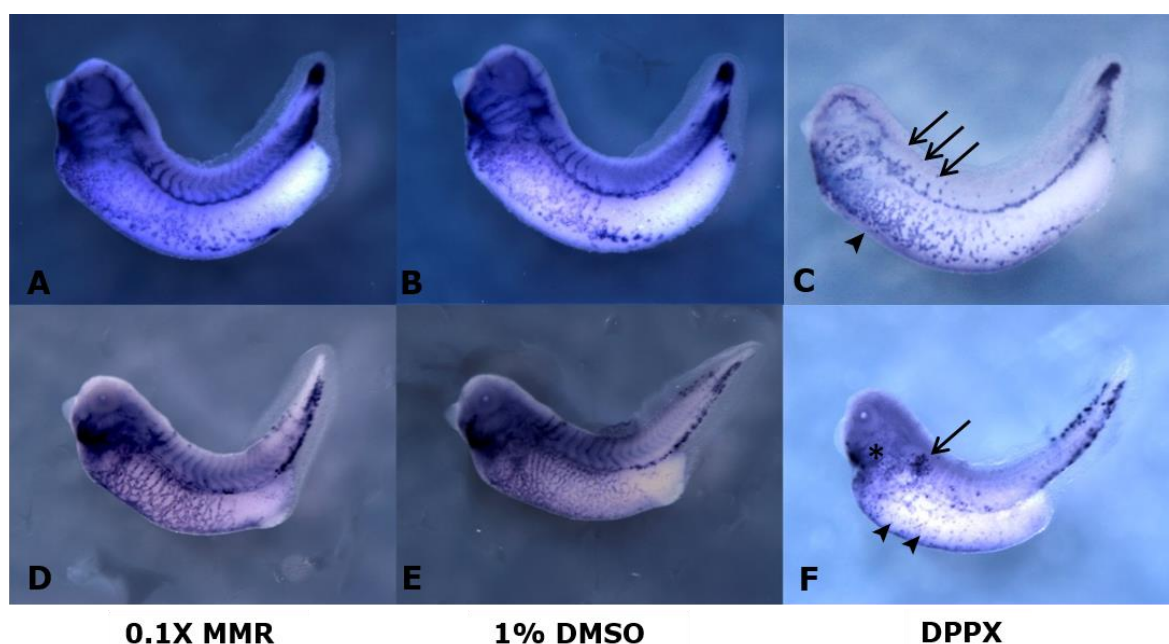


**Figure 28. DPPX disrupts vascular development in developing embryos.** Embryos were treated with the DPPX and expression of the blood vessel marker *aplnr* and the lymph vessel marker *vegfr 3* were determined by whole mount *in situ* hybridization. (C) Disrupted VVNs and impaired ISVs sprouting are indicated by arrowheads and arrows, respectively. (F) Impaired ALHs, ALSs and disrupted VVNs are indicated by arrow, asterisks and arrowheads, respectively.

DPPX-treated embryos were also stained for expression of *fxyd2*, *hba3*, *tal1* and *myod1* by performing whole mount *in situ* hybridization (Fig. 29). As with DEPX, the distribution of hemangioblasts and erythrocytes was altered as a consequence of the vascular defects caused by compound treatment (Fig. 29A-F). DPPX treatment had no apparent effect on the morphology and development of pronephric kidney (Fig. 29G-H). Furthermore, we observed that DPPX did not interfere with myogenesis and myoblast migration (Fig. 29J-L). In summary, DEPX and its derivative DPPX are indistinguishable in their bioactivities in *Xenopus* embryos suggesting that they interact with the same molecular targets.

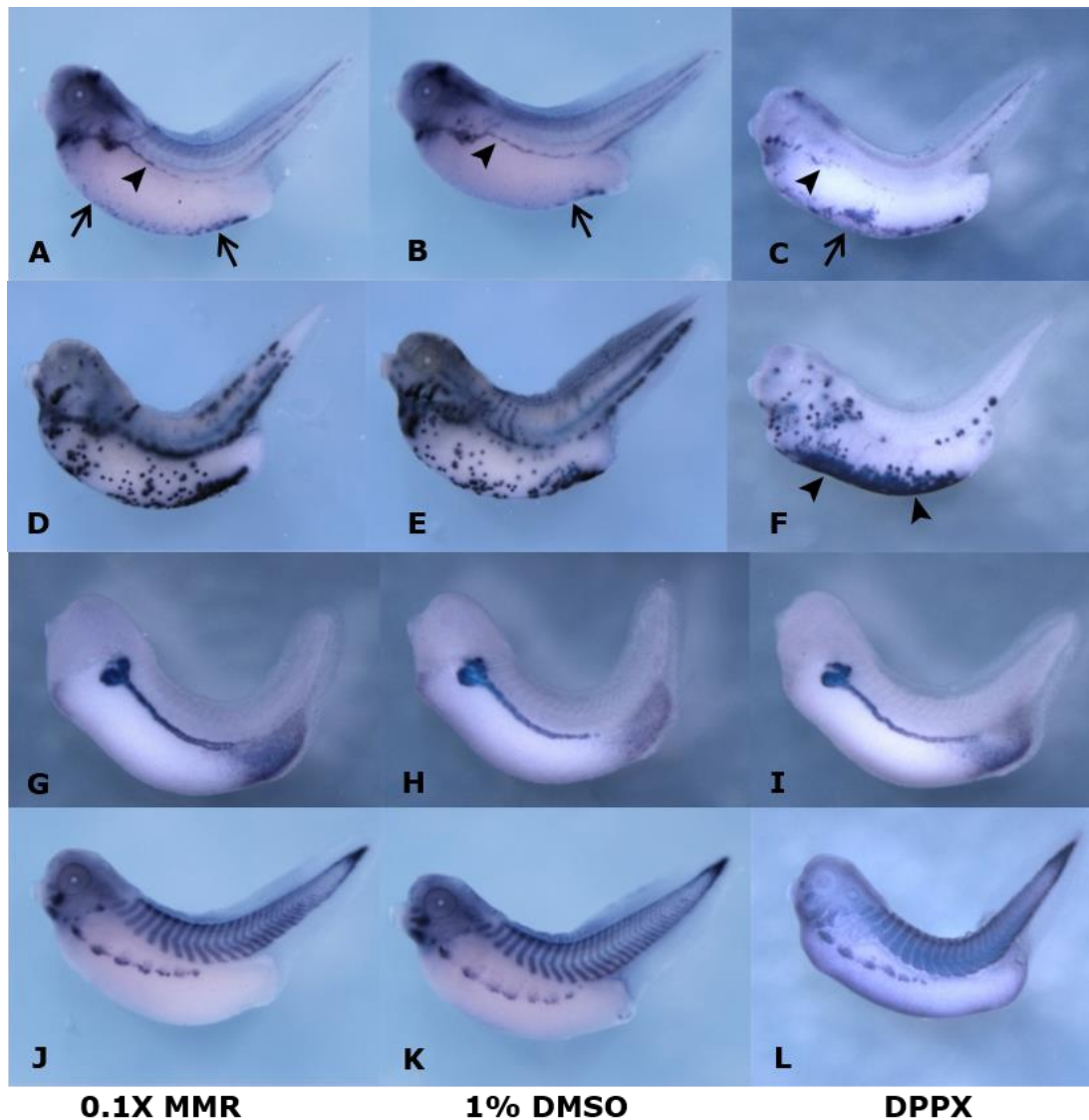


**Figure 29. Effects of DPPX on selected tissues and organs of *Xenopus* embryos.** Embryos were treated with DPPX and the expression of hemangioblasts marker *tal1* (A-C), erythrocyte marker *hba3* (D-F), pronephros marker *fxyd2* (G-I) and myoblast marker *myod1* (J-L) were determined by whole mount *in situ* hybridization. (A-C) DPPX did not affect the production of hemangioblasts and they were present in ventral blood island (arrows) and DLP region (arrowheads). (D-F) Erythrocytes were normally generated in ventral blood island (arrowheads) of DPPX-treated embryos but did not disperse due to the absence of VVNs. DPPX did not interfere with the morphology and development of pronephric kidney (G-I) and neither with the differentiation and migration of myoblasts (J-L).

### Endothelial cell proliferation is not affected by DEPX derivatives

As for DEPX (Fig. 23), possible effects of DPPX, DMSP and DPSPX treatments on human vascular and lymphatic endothelial cell proliferation were assessed (Fig. 30). Each compound was tested at three concentrations: 0.1  $\mu\text{M}$ , 1  $\mu\text{M}$ , and 10  $\mu\text{M}$ . However, under most of the conditions tested no effect of the compounds on HUVECs or LECs proliferation was observed. DPPX, at the highest concentration tested, moderately inhibited VEGFA-induced proliferation of HUVECs and LECs, which is reminiscent of DEPX.

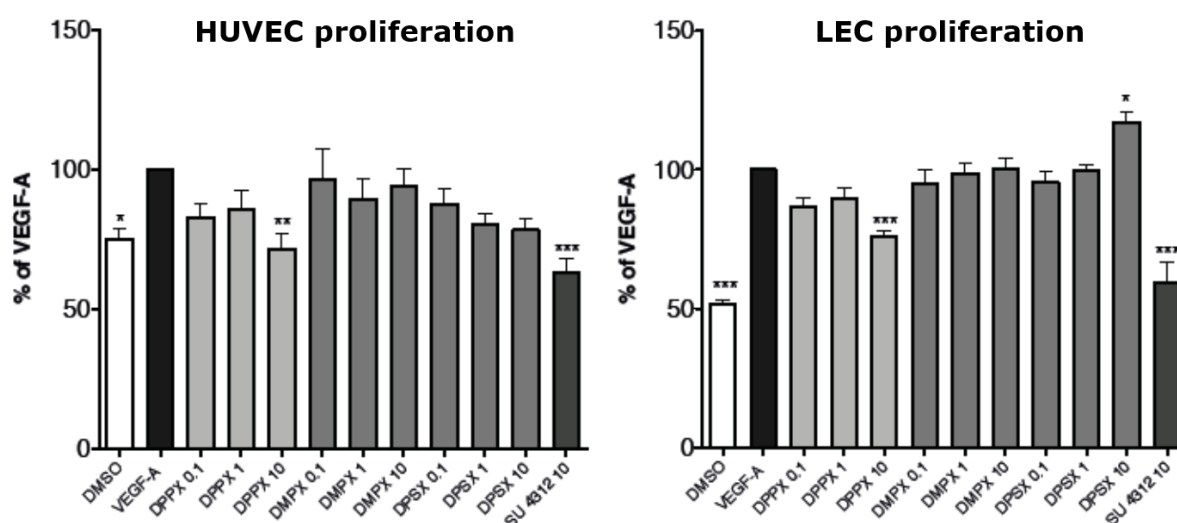


**Figure 30. DEPX derivatives did not affect endothelial cell proliferation.** The compounds were tested *in vitro* on HUVEC and LEC cultures at the concentrations indicated. SU 4312 concentration was 10  $\mu\text{M}$ . After 48 hours, live cells were stained with 4-methylumbelliferyl heptanoate (4-MUH) and fluorescence intensities were measured. Data is expressed as mean values  $\pm$  standard error of mean (SEM) with  $n=8$ . Results are representative of four or five independent experiments for LECs and HUVECs, respectively. \*  $p<0.05$ , \*\*  $p<0.01$ , \*\*\*  $p<0.001$ .

### The *in vivo* activity of 7CN requires the presence of a phenyl ring

Two commercially available compounds structurally related to 7CN (7-chloro-4-hydroxy-2-phenyl-1, 8-naphthyridine) were identified: 7-Methyl-2-phenyl-1, 8-naphthyridin-4(1*H*)-one (7MN), and 7-Chloro-4-hydroxy- [1, 8] naphthyridin (7CH). The chemical structures of 7CN derivatives are shown in Fig 31. 7CH lacks the phenyl group present in 7CN. In 7MN, the chloro group of 7CN is replaced by a methyl group. 7MN and 7CH are therefore useful to determine the functional significance of the chloro and phenyl moieties in 7CN, respectively. Based on available data, selected derivatives appear to preferentially target the A<sub>1</sub> ARs (Table 16).

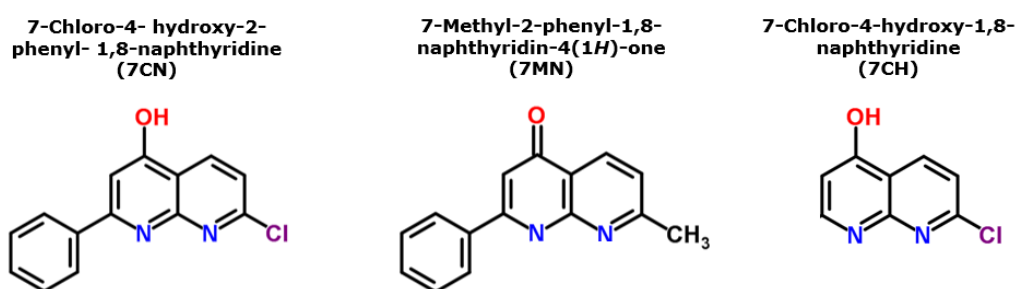


**Figure 31. Compound structurally related to 7CN.** The chemical structures of 7CN, 7MN, and 7CH shown were downloaded from ChemSpider (chemspider.com).

**Table 16. 7CN derivatives and their AR subtype selectivities**

Compound name	K <sub>i</sub> Values (nM)				Reference
	A <sub>1</sub>	A <sub>2A</sub>	A <sub>2B</sub>	A <sub>3</sub>	
7CN	0.15 (b)	100 (b)	n.a.	2100 (b,r)	(Ferrarini et al., 2000)
7MN	5.3 (b)	460 (b)	n.a.	8800 (b,r)	(Ferrarini et al., 2000)
7CH	n.a.	n.a.	n.a.	n.a.	

K<sub>i</sub> values refer to studies with human ARs unless noted otherwise. Abbreviations: n.a., not available; b, bovine; r, rat.

*Xenopus* embryos were treated with 7MN and 7CH to assess their potential to induce edema in dose-dependent manner. The compounds were tested from a concentrations ranging from 0.1 μM to 100 μM concentrations. 7CH did not show any effect on *Xenopus* embryos even at 100 μM, the highest concentration tested (*data not shown*). Neither edema nor lethalties were observed, which suggest that phenyl ring is essential for the edema-inducing activity of 7CN. By

contrast, 7MN induced edema and led to lethality at submicromolar concentrations (Fig. 32, Table 17). The obtained pharmacological parameters were very similar to 7CN, but 7MN had a lower LC<sub>50</sub> and TI values.

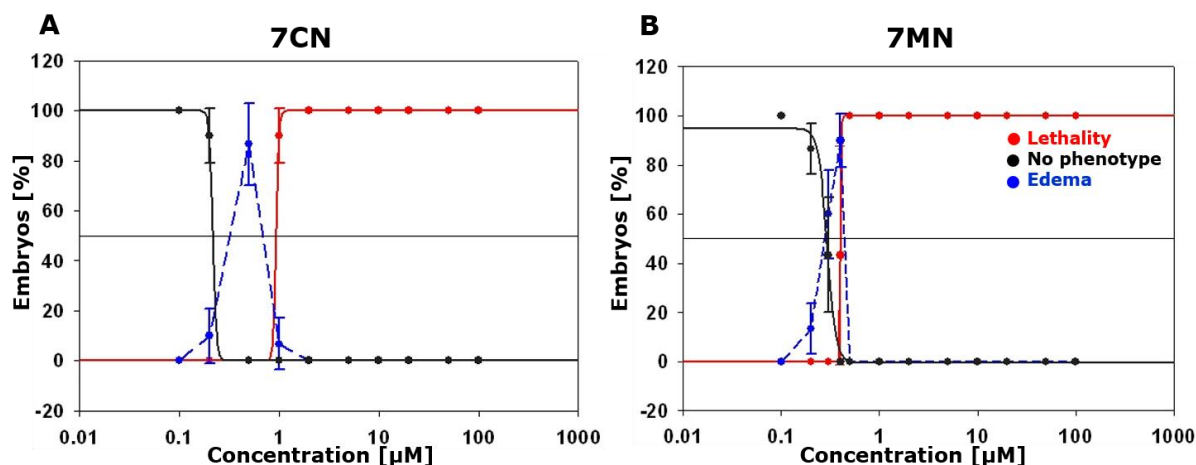


**Figure 32. Dose-response relationship of phenotypes induced by 7MN.** *Xenopus* embryos were treated with 7MN and pharmacological values were established as described before. Embryos were phenotypically analyzed at stage 45 and normal (black), edema formation (blue), and lethality (red) was scored. The graphs shown are compiled from at least six independent experiments ( $n = 10$ ). The error bars indicate standard deviations. Panel A with 7CN was taken from Fig. 17 and is shown for comparative purposes.

**Table 17. Pharmacological values of 7CN derivatives obtained from the treatment of *Xenopus* embryos**

Compound	<i>In vivo</i> Phenotype	EC <sub>50</sub> [µM]	EC <sub>max</sub> [µM]	LC <sub>50</sub> [µM]	TI
7CN	Edema	0.3	0.5	0.9	3
7MN	Edema	0.3	0.38	0.4	1.3
7CH	None	n.a.	n.a.	n.a.	n.a.

Abbreviations: n.a., not available.

As previously observed with DEPX and DPPX, we noted that the pattern of edema induction seen after 7MN treatment was essentially identical to the one observed with 7CN (Fig. 33; compare with Fig. 16). This is consistent with the notion that the two compounds act on the same pathway(s).

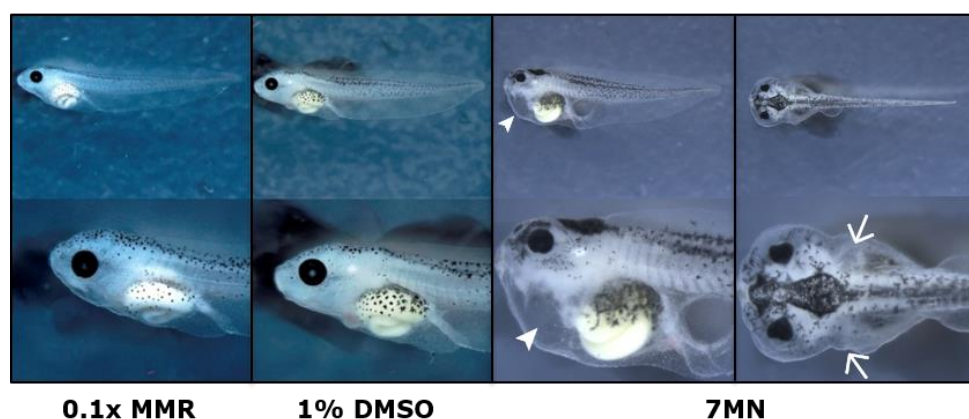


**Figure 33. Edema phenotypes induced by 7MN in *Xenopus* embryos.** The embryos were treated with 7MN at concentrations equivalent to  $EC_{50}$  (see Table 17) and incubated until stage 45. Control embryos were treated with 0.1x MMR and 0.1x MMR with 1% DMSO. Representative embryos are shown in lateral and dorsal views with enlargements below depicting head and trunk of the respective embryo. Primary areas of edema formation are marked by arrowheads for pericardial, and arrows for pronephric kidney edema.

As 7MN was found to be a potent inducer of edema in *Xenopus* embryos, we assessed by whole mount *in situ* hybridization whether compound treatment affected vascular development (Fig. 34). Blood vessel and lymphatic defects were extensive in 7MN-treated embryos and they were comparable with those observed after 7CN treatment (compare Figs. 19 & 20 with Fig. 34).

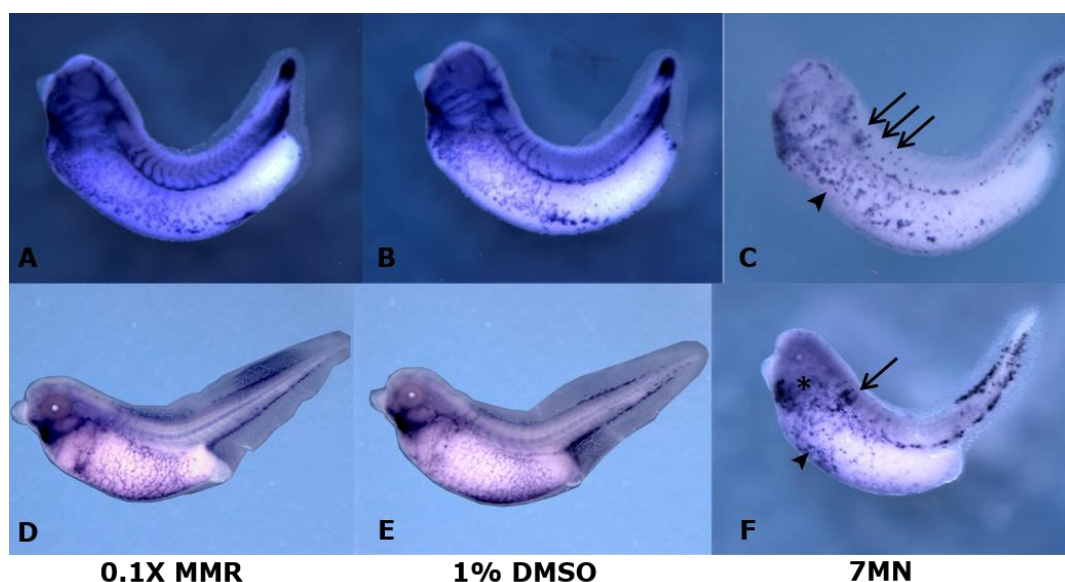


**Figure 34. 7MN interfered with vasculature development in *Xenopus* embryos.** 7MN-treated embryos analyzed for possible defects in blood and lymphatic vessel development. (A-C) Arrowheads and arrows indicate (C) disrupted VVNs and impaired ISVs sprouting, respectively. (D-F) Impaired ALH, abnormal ALSs, and disrupted VVNs are indicated by arrows, asterisks, and arrowheads, respectively.

7MN-treated embryos were also stained for expression of *fxyd2*, *hba3*, *tal1* and *myod1* by performing whole mount *in situ* hybridization (Fig. 35). The distribution of hemangioblasts and erythrocytes was affected as a result of the vascular defects caused by 7MN-treatment (Fig. 35A-F). 7MN treatment did however not alter pronephric kidney morphology (Fig. 35 G-H), myogenesis, and myoblast migration (Fig. 35J-L). Overall, 7MN and 7CN were comparable in their ability to induce edema and to interfere with vascular development in *Xenopus* embryos. The substitution of the methyl group in the naphthyridine moiety for chloride was beneficial as this correlated with less toxicity for 7CN compared to 7MN.

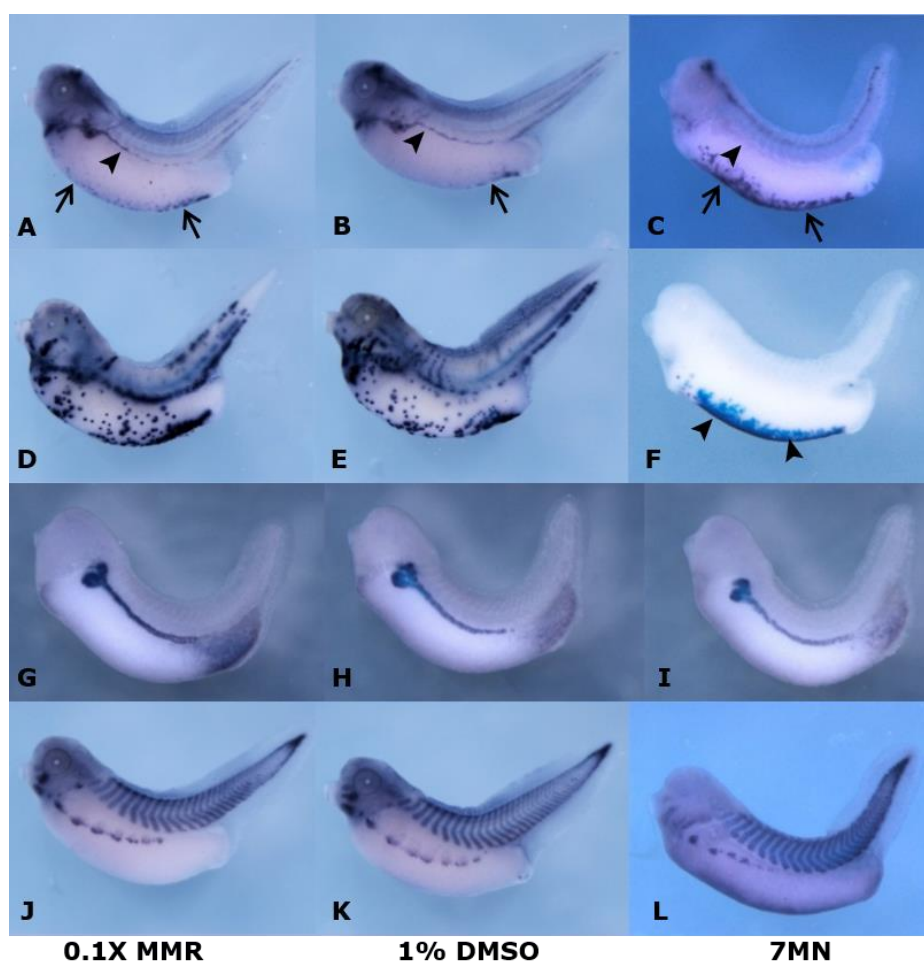


**Figure 35. Effects of 7MN treatment on selected organs in *Xenopus* embryos.** 7MN-treated embryos were fixed and the expression of hemangioblast (*tal1*; A-C), erythrocyte (*hba3*; D-F), pronephric kidney (*fxyd2*; G-I) and myoblasts (*myod1*; J-L) markers were determined by whole mount *in situ* hybridization. (A-C) 7MN treatment showed abundance of hemangioblasts in ventral blood island (arrows) but hemangioblasts were not present in DLP region (arrowheads). (D-F) Erythrocytes were restricted to ventral blood island (arrowheads) of 7MN-treated embryos. Morphology and development of pronephric kidney (G-I) and differentiation and migration of myoblasts (J-L) were not affected by treatment with 7MN.

### 7MN inhibits endothelial cell proliferation and sprouting

The similarities in bioactivities between of 7CN and 7MN observed in *Xenopus* embryos extended also to human endothelial cell cultures. Cell proliferation and sprouting assays were performed with HUVEC and LEC treated with 7MN. Fig. 36 shows the effect of 7MN on HUVECs and LECs proliferation, respectively. 7MN significantly inhibited VEGFA-induced proliferation of HUVECs at concentrations as low as 0.3  $\mu\text{M}$ . For LEC proliferation, 7MN concentrations as low as 1  $\mu\text{M}$  were sufficient.

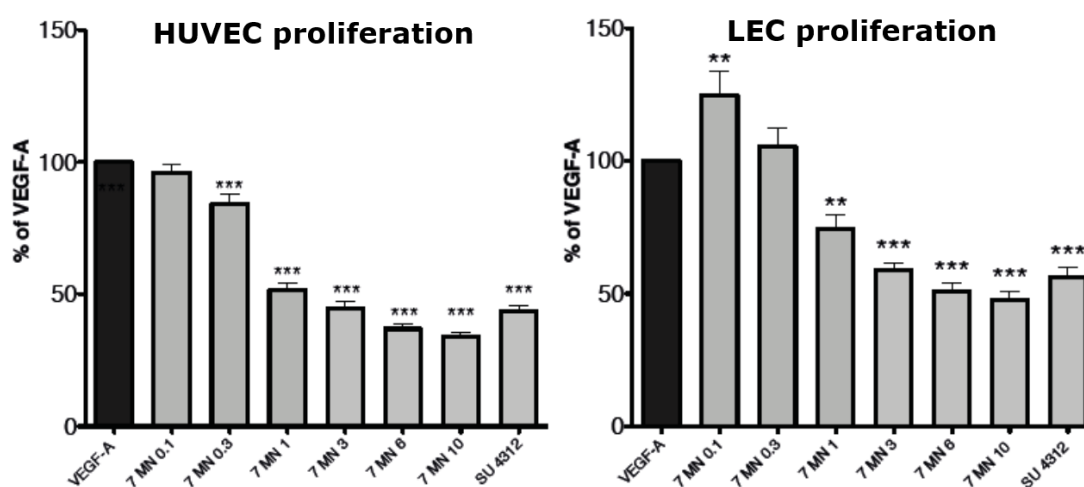


**Figure 36. Human endothelial cell proliferation is inhibited by 7MN.** 7MN was tested *in vitro* for 48 hours on LEC and HUVEC cultures, respectively, at the concentrations indicated. SU 4312 concentration was 10  $\mu\text{M}$ . Cell proliferation was assessed by fluorescent dye labeling and photospectrometric quantitation. The data is expressed as mean values  $\pm$  standard error of mean (SEM) with  $n=8$ . Results are representative for 3 independent experiments. \*\*  $p<0.01$ , \*\*\*  $p<0.001$ .

Cell sprouting assays using microcarriers coated with HUVECs and LECs, respectively, demonstrated that 7MN was as potent as 7CN (Fig. 37). Minimal effective concentrations of 7MN for inhibition of sprout formation were 0.3  $\mu\text{M}$  for HUVECs and 0.1  $\mu\text{M}$  for LECs, respectively. These findings mirror the situation observed with 7CN (see Fig. 24).

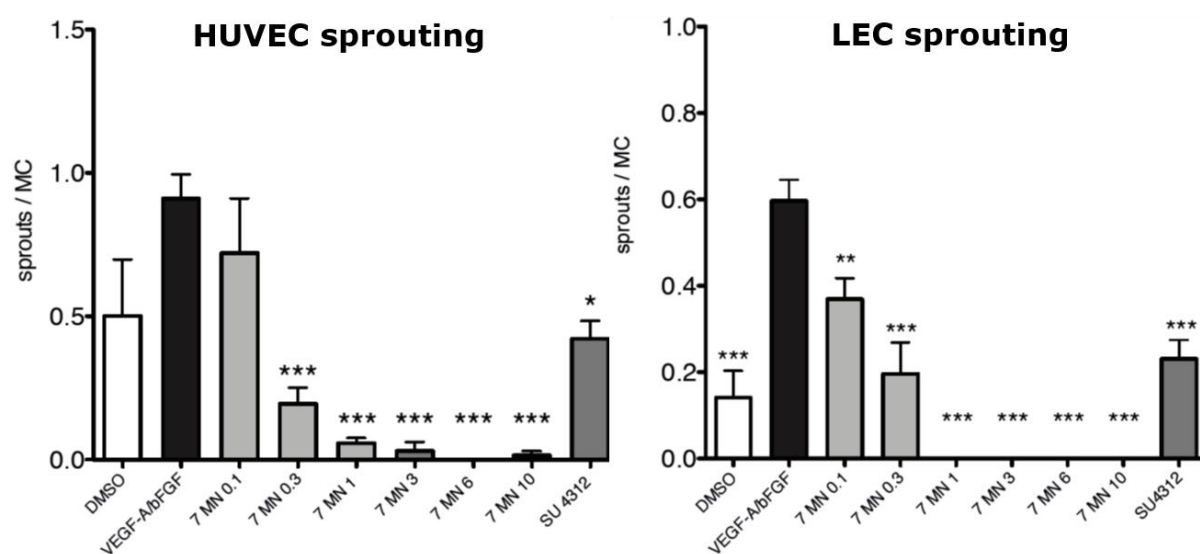


**Figure 37. 7MN inhibited on endothelial sprout formation.** Sprouting of collagen gel-embedded microcarriers coated with HUVECs or LECs was induced by VEGFA/bFGF or VEGFA/bFGF/S1P, respectively. 7MN concentration tested ranged from 0.1 to 10  $\mu$ M. SU 4312 concentration was 10  $\mu$ M. The data are shown as mean values  $\pm$  SEM, n=3. Results are representative of 3 and 4 independent experiments for HUVECs and LECs, respectively. \*p < 0.05, \*\*p < 0.01, \*\*\* p<0.001.

**7MN and 7CN cause mitotic arrest *in vitro***

Our *in vivo* and *in vitro* studies demonstrated that 7MN and 7CN, but not DEPX, inhibited proliferation of blood vascular and lymphatic endothelial cells. We next wanted to understand how these compounds interfere with the cell division cycle. Therefore, we employed fluorescence-activated cell sorting (FACS) of propidium iodide (PI) stained cells after compound treatment to assess their DNA content. The experiments were performed with HUVECs and they were treated with 7MN, 7CN, and DEPX for 48 hours prior to FACS analysis. Nocodazole was used as a positive control as it arrests the cell cycle in M-phase (Cooper, 2003). HUVECs were treated with compound concentrations ranging from 0.1 to 10  $\mu$ M in presence of 0.1% DMSO. The results of the flow cytometric analysis are shown in Figure 38. On the basis of DNA content, three distinct cell populations were identified; 2N (cells with diploid DNA content), 4N (tetraploid cells) and >4N (polyploid cells); and their relative abundancies were quantitated. The histograms of the FACS analysis of HUVECs after treatment with 1  $\mu$ M of the test compounds are shown to illustrate the profound changes observed (Fig. 38A). In the DMSO control, 68% of the cells had DNA content of 2N and 25% were of 4N. As expected, nocodazole-treated cells were arrested in mitosis with increased DNA content: 2% (4N) and 95% (>4N). The DNA content of DEPX treated cells was indistinguishable from controls with 67% (2N) and 27% (4N). For 7CN and 7MN, the numbers were 58% (4N) and 40% (>4N) and 7% (4N) and 90% (>4N), respectively. This indicates that both compounds induce mitotic arrest, but 7MN was moderately more potent than 7CN. The observed effects were dose-dependent as shown in Figure 38B. Two peaks in the histogram of 7MN and nocodazole represent 8N and 16N DNA contents. At concentrations of 3  $\mu$ M and higher, typically 95-98% of the nocodazole-, 7MN- and 7CN-treated cells failed to progress in the cell cycle and they were arrested with DNA contents >4N. 7MN and 7CN were therefore comparable with nocodazole in their ability to arrest the cell cycle.

## Results

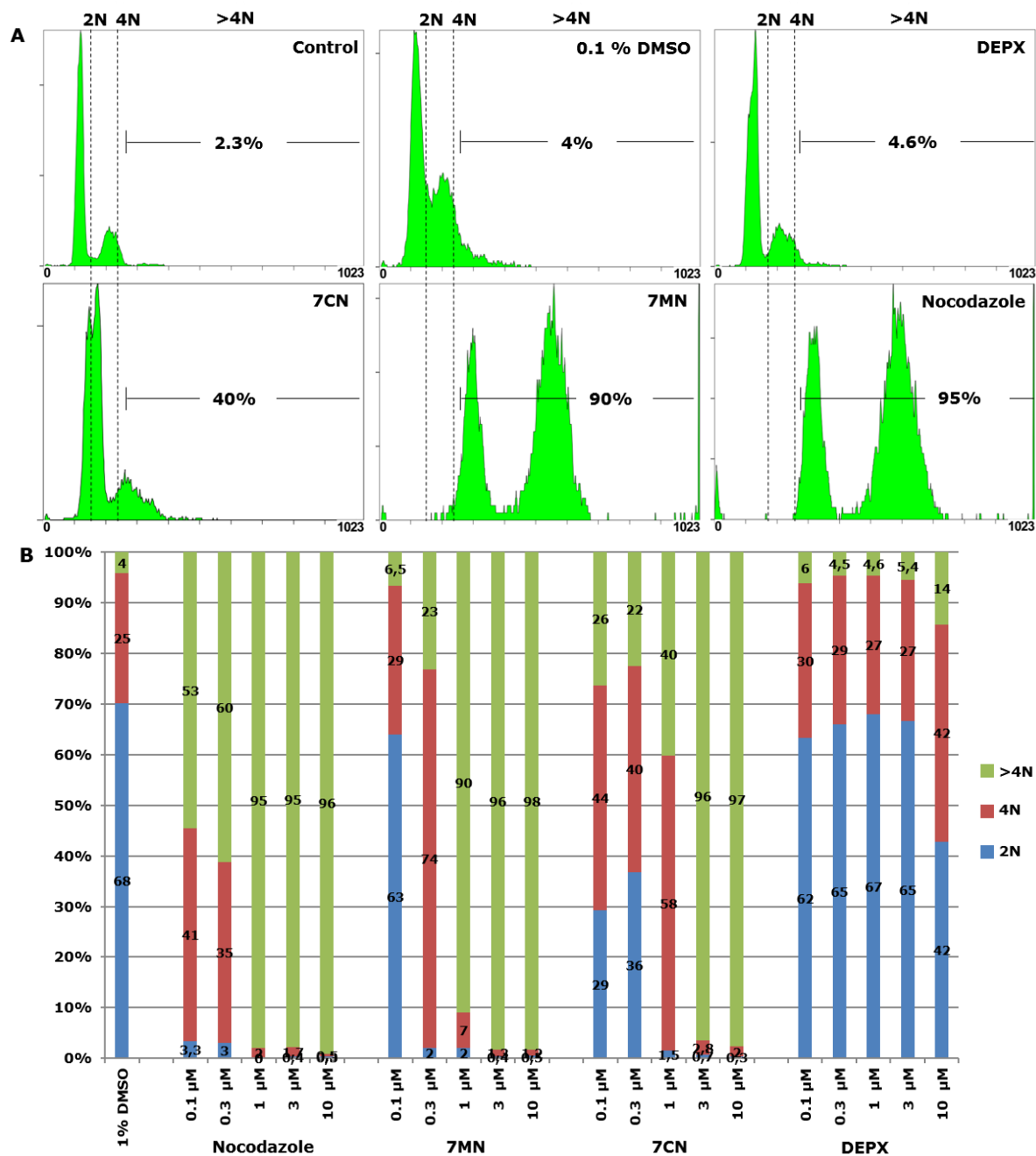


**Figure 38. 7MN and 7CN induce mitotic arrest with increased DNA content.** HUVECs were treated for 48 hours with the indicated compounds and the DNA contents were measured by FACS. (A) FACS analysis of HUVECs treated with test compounds at a concentration of 1  $\mu\text{M}$ . The histograms of control HUVEC cultures (media, media plus 1% DMSO) and those of compound-treated HUVECs are shown. The regions consisting of cells with diploid (2N), tetraploid (4N) and polyploid (>4N) DNA contents are indicated. (B) Dose response studies to assess compound-induced mitotic arrest in HUVECs. FACS analysis was performed to quantify the percentage of endothelial cells undergoing mitotic arrest. The percentage of cells with DNA contents of 2N, 4N and >4N, respectively are indicated. The data shown is compiled from three independent experiments.

### **7MN and 7CN disrupt the microtubular cytoskeleton**

Nocodazole arrests cell cycle progression by interfering with the polymerization of microtubules. The cells enter mitosis but cannot form metaphase spindles because the microtubules cannot polymerize, causing cells to arrest in prometaphase. Given that 7MN and 7CN cause mitotic arrest, we asked whether they also interfere with the polymerization of microtubules. Cultures of HUVECs were therefore treated with the compounds for 2 or 16 hours. Three concentrations (1, 3 and 10  $\mu\text{M}$ ) were tested. Cells were fixed and stained by immunofluorescence for the presence of microtubules. Figures 39 and 40 show examples of the stained cells after incubation for 2 and 16 hours, respectively. After the 2-hour treatments, the microtubular cytoskeleton of the cells treated with nocodazole was disrupted at all concentrations tested (Fig. 39). The cell shapes were rounded and there was a pronounced presence of lamellipodia. A similar picture was seen with 7MN. However, at the lowest concentration (1  $\mu\text{M}$ ), cells containing an intact microtubular network were occasionally seen. This was even more pronounced in cells treated with 1  $\mu\text{M}$  7CN, where many cells appeared to be normal. Incubation of cells for 16 hours with the compounds did not change this general picture (Figure 40). However, multinucleated cells were now apparent as more cells became arrested in M phase after duplicating their DNA. In summary, both 7MN and 7CN induced disassembly of the microtubular network similar to nocodazole.

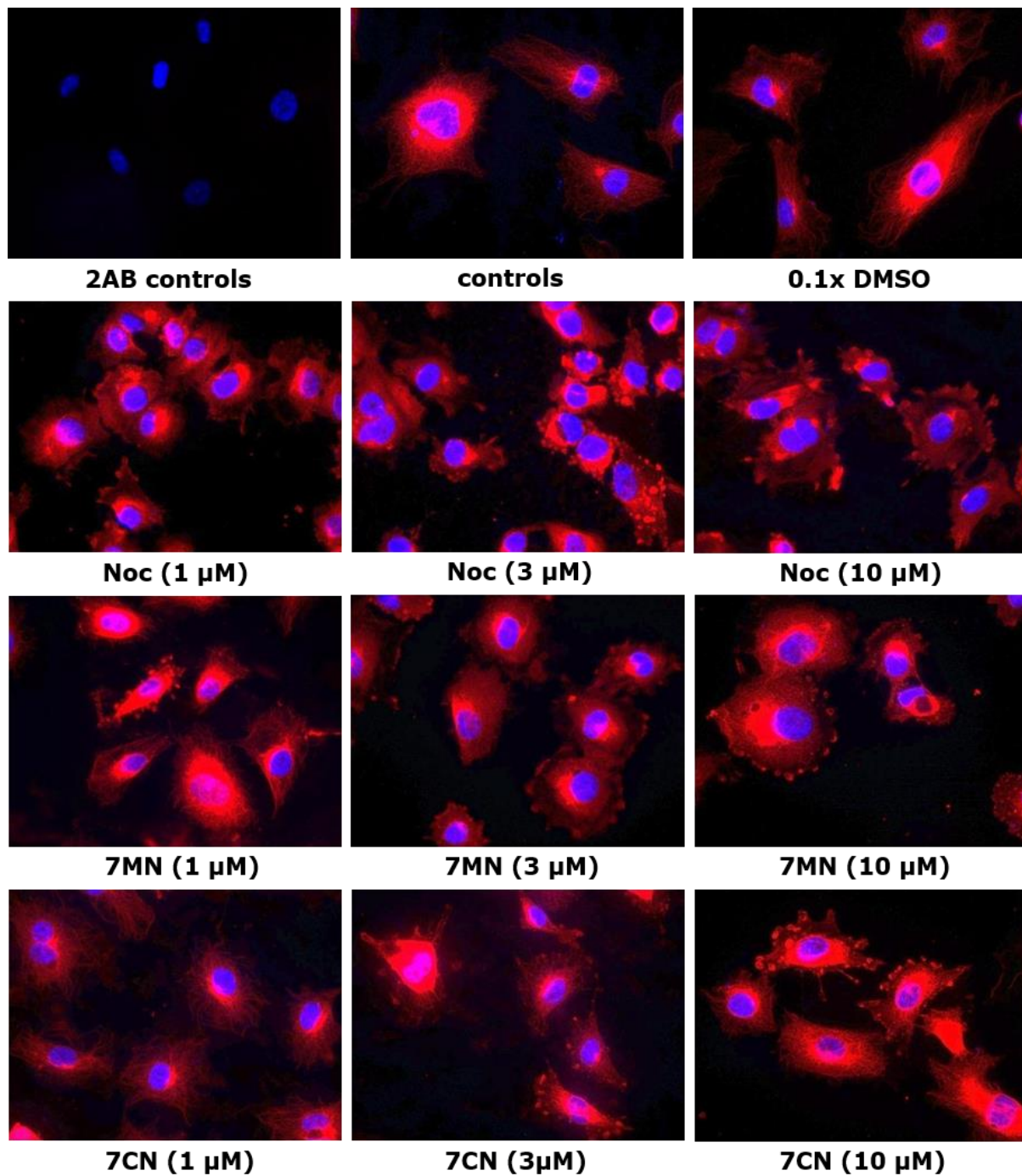


**Figure 39. Effects on the microtubular cytoskeleton of HUVECs after a 2-hour treatment with 7MN and 7CN.** HUVECs were treated for two hours with media containing either 0.1% DMSO alone or supplemented with 1  $\mu\text{M}$ , 3  $\mu\text{M}$  or 10  $\mu\text{M}$  nocodazole (Noc), 7MN, or 7CN. The cells were fixed and stained with a monoclonal anti- $\alpha$ -tubulin antibody to visualize the microtubules. Nuclei were counterstained with DAPI. Immunofluorescence images are shown with the microtubules stained red and the nuclei in blue.

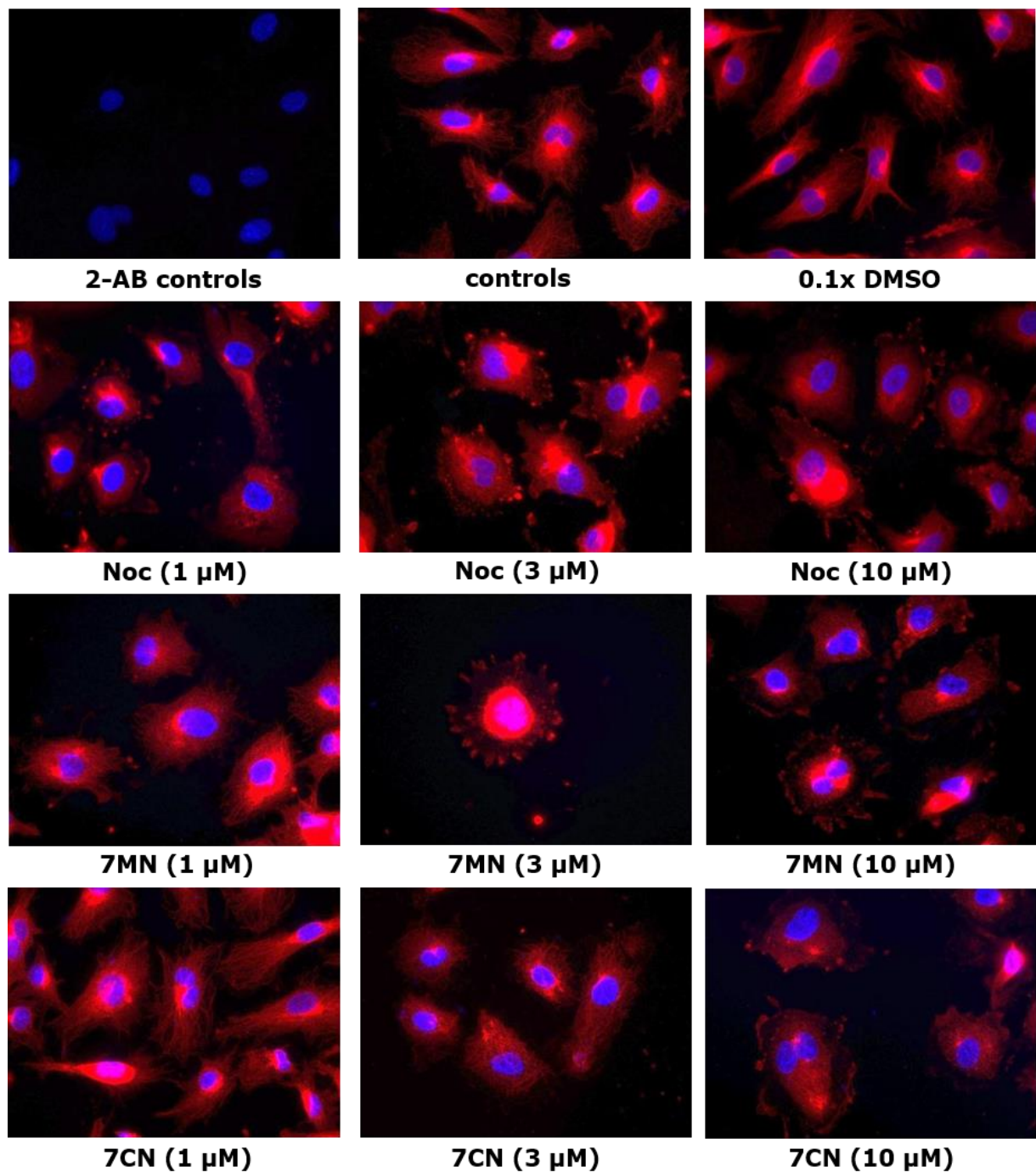


**Figure 40. Effects on the microtubular cytoskeleton of HUVECs after a 16-hour treatment with 7MN and 7CN.** HUVECs were treated for 16 hours with media containing either 0.1% DMSO alone or supplemented with 1  $\mu\text{M}$ , 3  $\mu\text{M}$  or 10  $\mu\text{M}$  nocodazole (Noc), 7MN, or 7CN. The cells were fixed and stained with a monoclonal anti- $\alpha$ -tubulin antibody to visualize the microtubules. Nuclei were counterstained with DAPI. Immunofluorescence images are shown with the microtubules stained red and the nuclei in blue.

**Discussion**

***In vivo* identification of vascular disruptive agents**

The formation of new blood and lymph vessel is a hallmark of many pathological conditions, such as in cancer and inflammation. In cancer, tumor growth relies on attracting the growth of new blood vessel that supply with the tumor with oxygen and nutrients. The upregulation of angiogenesis and lymphangiogenesis triggers disease progression. Carcinoma cells disperse via blood and lymphatic vessel and they survive and grow at distant organs, where they cause metastases. Pathological angiogenesis and lymphangiogenesis have therefore become attractive targets for tumor therapy (Weis and Cheresh, 2011, Chung et al., 2010). The notion is that vascular disruption agents would destabilize the vasculature feeding the tumor, cause hypoxia and drive the cancer cells to necrosis (Cesca et al., 2013). The effectiveness of this approach in cancer therapy has been demonstrated by avastin (bevacizumab), a recombinant humanized monoclonal antibody that blocks angiogenesis by inhibiting VEGFA (Greillier et al., 2016, Shih and Lindley, 2006). Avastin was the first angiogenesis inhibitor to be approved for use in combination with chemotherapy to treat metastatic colon cancer. The widespread clinical application of angiogenesis inhibitors has however uncovered that tumors are able to resist treatment by activating VEGF-independent mechanisms to promote angiogenesis. This makes it necessary to develop alternative strategies to disrupt vessel growth. To address this need, our laboratory had developed an *in vivo* drug screening strategy using *Xenopus* embryos to identify small organic molecules that interfere with vessel formation or function (Kalin et al., 2009). Using edema formation as a highly predictive pathophysiological readout, 32 compounds were identified as vascular disruptive agents, which also included antagonists of AR signaling. In the present thesis, we carried out extensive pharmacological studies to explore the specificity, efficacy, and structural determinants of a broad range of AR antagonists as a potential inhibitors of angiogenesis and lymphangiogenesis in *Xenopus* embryos and mammalian endothelial cell cultures. We found that only two compounds, 7CN and DEPX, and derivatives thereof were effective as vascular disruptive agents. Furthermore, our *in vitro* studies indicated that 7CN acts by disrupting the microtubular cytoskeleton to cause mitotic arrest.

***Xenopus* embryos as a powerful model to identify the vascular disruptive agents *in vivo***

Chemical genetic screens to identify biochemical pathways regulating a biological process, such as vascular development, require three basic components (Lokey, 2003). The first component is a chemical library of small organic molecules with established pharmacologies; which can include agonists and antagonists targeting specific receptors, kinases and other downstream signaling mediators. The second component is a meaningful biological assay system, which will be used to screen the chemical library for compounds with the desired bioactivity. Cell cultures, organ cultures, or whole animals, typically embryos or larvae, may serve as test systems. Once bioactive hits have been identified, the final step requires the identification and validation of the biological target(s) modulated by the active compounds.

Any chemical library screen will fail, if the biological test system is inadequate to start with. *In vitro* cell culture systems have been widely used by the pharmaceutical industry for compound screening. More recently, the development of induced pluripotent stem cell technology has opened up the possibility of using patient-derived primary cells to develop patient-specific cell lines (Robinton and Daley, 2012). In general, *in vitro* cell cultures are easy to establish in multi-well plates; and thus they can be used in high-throughput chemical screening strategies aimed at evaluating ten thousands of chemical agents for specific bioactivities. *In vitro* cell cultures represent highly simplified tissue states in a well-controlled, but artificial environment. This poses a number of limitations. Typically, these cultures consist of a single cell type, which does not reflect the complexity of an entire organ. Furthermore, the cell's behavior and organization *in vitro* can be very different from the *in vivo* situation, where different cells of an organ are interacting and communicating with each other. Drug candidates emerging from screens carried out with *in vitro* culture may therefore not show the same effects when tested *in vivo*. Furthermore, adverse side effects of a positive hit, such as toxicities, may not manifest in cell culture assays but can become a serious problem later.

Drug screening using more complex biological systems, such whole animals, may offer an attractive alternative (Astashkina et al., 2012). *In vivo* systems have the advantage that the cells to be targeted by a specific drug are present in the correct tissue and organ context and the cellular interactions contributing to the pathophysiology of disease manifestation are preserved. Furthermore,

drug metabolism is only fully possible in animal models. These conditions are difficult to reproduce with *in vitro* systems. Finally, the recent development of sophisticated gene knockdown or knockout techniques, including CRISPR-Cas, enable now the tailoring of precise animal disease models for drug discovery and development (Liu et al., 2016, Schmitt et al., 2014).

Different animal models have been used during the last fifteen years for whole organism-based drug screening, such as *Caenorhabditis elegans*, *Drosophila*, zebrafish and *Xenopus* (Pandey and Nichols, 2011, Liu et al., 2016, Schmitt et al., 2014). *C. elegans* and *Drosophila* are good model systems to address the genetics of basic signaling pathways, but they have their limitations when it comes to complex human disease processes. Drug delivery is also a problem as drugs do not easily penetrate into *C. elegans* and *Drosophila* larvae. Furthermore compound dosing is difficult due to variations in body size and the amount of ingested compound differ among organisms (Pandey and Nichols, 2011). Zebrafish and *Xenopus* are the only vertebrate models, which are small enough to offer the benefit of performing high-throughput compound screening (Wheeler and Brandli, 2009, Schmitt et al., 2014). They have simple husbandry requirements, are easy to handle in the laboratory, and they generate large number of embryos. Importantly, the embryos and subsequent larvae are small enough to grow in multiwell plates, where they can be treated with thousands of compounds.

From an evolutionary point of view, amphibians are evolutionary closer to humans than fish. This will transcend into more shared similarities at the genomic, histological and physiological levels. This favors the use of *Xenopus* over zebrafish. After hormone stimulation, *Xenopus* frogs will lay thousands of eggs, which can be fertilized *in vitro*. The embryos can be raised in a simple salt solution at room temperature. Test compounds can be added in bathing medium from which they are easily absorbed through skin of the embryos and tadpoles (Wheeler and Brandli, 2009, Schmitt et al., 2014). In a proof-of-principle study, our lab had developed successfully a high-throughput drug screening method to identify anti-angiogenic and/or anti-lymphangiogenic compounds using *Xenopus* embryos (Kalin et al., 2009). Furthermore, one of the identified compounds, 7CN, was shown to suppress VEGFA-induced adult neovascularization in mice. Taken together these studies validate the use of *Xenopus* embryos for *in vivo* drug discovery purposes.

**AR agonists fail to induce edema in *Xenopus* embryos**

Several studies have indicated in the past that AR agonists promote angiogenesis (Hasko et al., 2008, Auchampach, 2007). For example, topical application of A<sub>2A</sub> AR agonists increases the rate of wound healing, in part, by stimulating in angiogenesis in the skin using direct and indirect mechanisms (Montesinos et al., 1997). The proliferation of microvascular endothelial cells occurs either directly by stimulation of endothelial ARs, e.g. A<sub>2A</sub> and A<sub>2B</sub>, or indirectly via stimulation of autocrine production of VEGF, a potent angiogenic factor. In the chick chorioallantoic membrane model, treatment with the A<sub>1</sub> AR agonist N<sup>6</sup>-cyclopentyladenosine (CPA) increases the blood vessel number by 40% (Clark et al., 2007). Finally, the adenosine analog 5'-N-ethylcarboxamidoadenosine (NECA), a well-known A<sub>1</sub> AR and A<sub>2</sub> AR agonist, increases blood vessel formation by stimulating VEGF release (Ryzhov et al., 2007). This raises the question whether AR agonists would interfere with blood vessel development in *Xenopus* embryos and induce edema? 22 different AR agonists, including CPA and NECA, were present in the LOPAC library, which was screened *in vivo* to identify edema-inducing compounds (Kalin et al., 2009). At a final concentration of 20 µM, none of the 22 AR agonists induced edema phenotypes nor did they cause obvious changes in the morphology of *Xenopus* embryos. This is surprising as the collection of AR agonists was diverse by including subtype-specific AR agonists as well as those targeting multiple ARs. Currently, it is unclear whether AR agonist treatment had any effect on vascular development or function in *Xenopus* embryos. Such effects may first become visible after treatment with higher compound concentrations. This may however also increase the possibility of unspecific effects of compound treatment. Despite the absence of obvious macroscopic phenotypes, we cannot exclude the possibility that AR agonists stimulate endothelial cell proliferation in an orderly manner without disrupting normal vascular functions. Future studies will have to address these issues in greater detail and may possibly reveal subtle vascular effects of AR agonists in *Xenopus* embryos.

**Pharmacological inhibition of A<sub>2A</sub>, A<sub>2B</sub> or A<sub>3</sub> AR signaling does not affect vascular development**

A two-step screening protocol of the LOPAC library, which was performed previously in our laboratory led to the identification of two AR antagonists, 7CN and DEPX, with anti-angiogenic and anti-lymphangiogenic activities (Kalin et al., 2009). The chemical treatments were performed by bathing *Xenopus* embryos in media containing single compounds at a final concentration of 20  $\mu$ M. These findings suggested role for AR signaling in regulating vascular and lymphatic vessel development, which was explored in greater detail in the present study. AR subtype-specific antagonists for all four ARs were selected and tested for their ability to induce dose-dependently edema in *Xenopus* embryos. The findings were clear cut. All A<sub>1</sub> AR-specific antagonists plus the A<sub>2A</sub> selective AR antagonist CGS 15943 were found to cause edema formation. Despite its ability to induce edema with an EC<sub>50</sub> of 2  $\mu$ M, CGS 15943 did not interfere with blood or lymph vessel development in *Xenopus* embryos. In general, antagonists specific for the AR subtype A<sub>2A</sub>, A<sub>2B</sub>, and A<sub>3</sub> did not show any discernable effects on *Xenopus* embryos, even at 100  $\mu$ M, the highest concentration tested. These findings were surprising given that our *in situ* hybridization analysis demonstrated broad and tissue-specific expression of all four AR genes in *Xenopus* embryos. Given the widespread and partially overlapping expression of AR genes, we reasoned that the lack of visible phenotypes may be due to functional redundancies. However, even combination treatments with two A<sub>2A</sub>, A<sub>2B</sub>, and A<sub>3</sub> AR antagonists did not result in significant edema formation in *Xenopus* embryos for any two combinations tested. Collectively, this indicates that pharmacological inhibition of A<sub>2A</sub>, A<sub>2B</sub> and A<sub>3</sub> AR signaling is not sufficient to disrupt embryonic vascular development or function in *Xenopus*. Furthermore, knockdown of A<sub>2A</sub> AR gene function using a translation-blocking MO failed to have any effect on *Xenopus* embryogenesis. Blood and lymph vessel development occurred unaffected (*data not shown*). Similarly, mice homozygous for a targeted mutation of the A<sub>2A</sub> AR gene are born viable and fertile suggesting that vascular development was unaffected (Ledent et al., 1997). In zebrafish embryos, A<sub>2B</sub> ARs are predominantly expressed in the vasculature within the aorta-gonad-mesonephros region and the caudal hematopoietic tissue (Boehmler et al., 2009, Jing et al., 2015). Knockdown of A<sub>2B</sub> ARs interfered with hematopoietic stem development, but did not affect general development of the embryos. Specifically, mutant embryos had normal heart beating and vascular circulation. Furthermore, vascular differentiation was unaffected and intersomitic

vessels were observed. Interestingly, treatment of zebrafish embryos with the AR antagonist CGS 15943 decreased hematopoietic stem cell emergence without altering vascular development and blood circulation (Jing et al., 2015). In summary, the pharmacological experiments in zebrafish and *Xenopus* demonstrate clearly that CGS 15943 treatment has no effect on vascular development in vertebrate embryos. The reasons why CGS 15943 causes edema in *Xenopus* but not in zebrafish embryos remain unknown. Finally, there is currently no genetic evidence suggesting a role for A<sub>3</sub> AR signaling in the vasculature. According to the Zebrafish Model Organism Database (zfin.org), the zebrafish genome is devoid of A<sub>3</sub> AR genes. Furthermore, A<sub>3</sub> AR-deficient mice are phenotypically indistinguishable from wild-type mice (Salvatore et al., 2000). We conclude that genetic and pharmacological experiments in zebrafish, *Xenopus* and mouse fail to support an essential function for A<sub>2A</sub>, A<sub>2B</sub>, or A<sub>3</sub> ARs in vascular development.

#### **A<sub>1</sub> AR antagonists induce edema *in vivo***

Out of the 14 AR antagonists tested, all four with reported selectivity for A<sub>1</sub> ARs, namely 7CN, DEPX, PSB 36 and SLV 320, were found to induce in a dose-dependent manner edema in *Xenopus* embryos. We therefore were able to confirm the edema-inducing activity of 7CN and DEPX previously reported by our laboratory (Kalin et al., 2009). The efficacy of these compounds was however unknown. On the basis of extensive *in vivo* dose-response studies, we report here the establishment of four pharmacological parameters, EC<sub>50</sub>, EC<sub>max</sub>, LC<sub>50</sub> and TI (Table 18). Irrespective of the pharmacological parameter considered, 7CN was most potent by inducing edema and lethality at submicromolar compound concentrations. 7CN was followed by DEPX, which was effective in the low micromolar range. PSB 36 and SLV 320 were very similar and they were the least potent compounds with activities typically above 10 μM. Except for SLV 320 with a TI value of 11, the TI values were very similar (2.1 to 3.4) for the other A<sub>1</sub> AR antagonists tested. The K<sub>i</sub> values for A<sub>1</sub> ARs shown in Table 18 were taken from the literature and they range between 0.12 and 5 μM. On this basis, PSB 36 and 7CN are the most potent A<sub>1</sub> AR inhibitors followed by SLV 320 and then DEPX. Whereas 7CN was also the most potent edema-inducing compound, this was not the case for PSB 36, which was the least potent one *in vivo*. For a number of reasons, these conclusions have however to be taken with some caution. The K<sub>i</sub> values of the tested compounds for *Xenopus* A<sub>1</sub> ARs are currently unknown and the mammalian K<sub>i</sub> values were not established identically. For

example, the cells used for the displacement studies were not uniform with regard to the species and/or tissue origin. Furthermore, it is not clear whether the test cells express A<sub>1</sub> AR only, or they express other ARs. Furthermore, different biochemical assays were used to establish the K<sub>i</sub> values in the different studies. It is therefore not surprising that widely different K<sub>i</sub> values have been reported for a given antagonist depending on whether human, bovine or rat A<sub>1</sub> ARs were used (see Table 11). Ideally, the K<sub>i</sub> values for a given AR antagonist were to be established using a competition assay, where the radiolabeled A<sub>1</sub> AR antagonist would be displaced by increasing amounts of the unlabeled antagonist. Furthermore, these displacement experiments would have to be carried out using four different cell lines expressing solely one *Xenopus* AR subtype at a time, but at comparable expression levels. Using the outlined approach, one could establish unequivocally the K<sub>i</sub> values for each antagonist and its AR-subtype specificity. This was clearly out of scope for the present project.

**Table 18. Comparison between K<sub>i</sub> values and selected pharmacological parameters of A<sub>1</sub> AR antagonists**

Compound	K <sub>i</sub> A <sub>1</sub> (nM)	EC <sub>50</sub> (μM)	EC <sub>max</sub> (μM)	LC <sub>50</sub> (μM)	TI
<b>7CN</b>	0.15 (b)	0.3	0.5	0.9	3
<b>7MN</b>	5.3 (b)	0.3	0.38	0.4	1.3
<b>DEPX</b>	44 (r)	2.4	4.9	5.3	2.2
<b>DPPX</b>	10 (r)	2.7	4.8	5.7	2.1
<b>PSB 36</b>	0.12	6.7	10	23	3.4
<b>SLV 320</b>	1	2	10	22	11

The K<sub>i</sub> values were taken from the published literature (see Table 11 for references). They refer to bovine (b), rat (r) or human A<sub>1</sub> ARs. The other parameters refer to *Xenopus* embryos and were established in the present thesis (see Table 12, 14 and 16).

**Only a subset of A<sub>1</sub> AR antagonists affect blood and lymph vessel development *in vivo***

Whereas all four AR antagonists with reported selectivity for A<sub>1</sub> AR were found to induce edema, only 7CN and DEPX were effective in interfering with vascular development. Thus, PSB 36 and SLV 320 must cause edema via some other mechanism. Despite the robust A<sub>1</sub> AR expression in the developing pronephric kidney, we did not observe any renal morphogenesis defects in compound-treated embryos. At present, we however cannot rule out the possibility that edema formation by A<sub>1</sub> AR antagonist results from interfering with vital pronephric kidney functions. This raises the question, whether the four antagonists indeed share *in vivo* A<sub>1</sub> ARs as their primary target? Several pieces of evidence argue that this is probably not the case. First, we observed differences in the patterns of edema that were induced after compound treatment. Embryos treated with PSB 36 and SLV 320 developed ventral edema. By contrast, 7CN and DEPX treatment resulted in a more complex pattern of edema formation with fluid accumulation manifesting in close proximity to the developing heart, pronephric kidneys, and the blood island; described here as pericardial, pronephric and ventral edema. These phenotypic differences strongly suggest that the test compounds act at the molecular level differently *in vivo*. In fact, we had previously reported that compound treatment can cause different types of edema and that compounds targeting the same pathway share the same anatomical pattern of edema formation in *Xenopus* embryos (Kalin et al., 2009). In addition, there were differences in the timing of edema induction. Embryos treated with 7CN and DEPX develop edema early, starting at stages 37/38, whereas edema were first detected from stage 42 onwards in PSB 36- and SLV 320-treated embryos. The phenotypic differences seen *in vivo* between the two subsets of A<sub>1</sub> AR antagonists (7CN, DEPX; PSB 36, SLV 320) are therefore indicative that, besides A<sub>1</sub> ARs, they may have additional, subset-specific targets or, alternatively, they may engage completely different molecular targets. Given this, we asked whether A<sub>1</sub> ARs are at all the relevant *in vivo* targets of the four A<sub>1</sub> AR antagonists studied here? As mentioned earlier, we were unable to demonstrate any significant A<sub>1</sub> AR expression in the developing blood and lymphatic vasculature. Furthermore, knockdown of A<sub>1</sub> AR gene function using a translation-blocking MO did not impair *Xenopus* embryogenesis, failed to induce edema, and had no effects on vascular morphogenesis or function (*data not shown*). This is consistent with findings in the mouse, where the loss of A<sub>1</sub> AR gene function does not cause any apparent

phenotype and homozygous mutants are viable and fertile. Furthermore, homeostasis as well as cardiovascular and renal functions of the mutant animals are indistinguishable from controls (Sun et al., 2001). Collectively, these findings strongly suggest that neither the edema phenotypes seen with all A<sub>1</sub> AR antagonists tested here nor the vascular phenotypes observed after 7CN and DEPX treatment of *Xenopus* embryos can be attributed to the inhibition of A<sub>1</sub> ARs only. It is therefore likely that the different edema phenotypes observed after treatment of *Xenopus* embryos with A<sub>1</sub> AR antagonists have to be attributed to the complex and presently poorly understood polypharmacologies of the compounds used.

### **Structure-activity relationship studies reveal critical molecular determinants for bioactivity *in vivo***

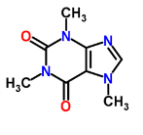
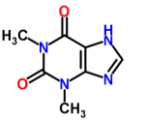
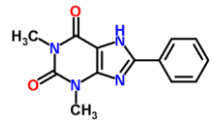
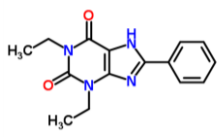
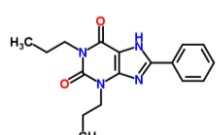
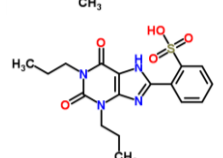
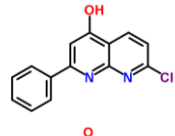
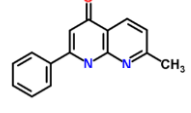
The assessment of AR antagonists in *Xenopus* embryos has led to the identification of two compounds, 7CN and DEPX, that harbor the desired anti-angiogenic activities *in vivo*. Structurally, these two lead compounds have little in common (Table 19). Similar to caffeine, DEPX is based on a methylxanthine scaffold, but carries also a phenyl group. By contrast, 7CN is a naphthyridine derivative, with no structural resemblance to the natural AR ligands adenosine and caffeine. As DEPX, it carries a phenyl group substitution. Structure-activity relationship (SAR) studies were carried out to determine the relationship between key chemical structure determinants and the biological activity of the two lead compounds. The SAR studies were presently limited to commercially available derivatives of DEPX and 7CN, respectively (Table 19). The compounds were tested in a dose-dependent manner in *Xenopus* embryos.

Three derivatives of DEPX, DMPX, DPPX and DPSPX, were tested. Interestingly, *in vitro* studies have shown that all compounds have affinities to ARs ranging from low to high nanomolar concentrations (see Table 14). The AR subtype selectivity has to date not been completely resolved for all four compounds, but the reported K<sub>i</sub> values are typically lowest for A<sub>1</sub> ARs. DMPX and DPSPX were previously shown to be inactive at 20 μM in *Xenopus* embryos (Kalin et al., 2009). These observations were here confirmed for both compounds with test concentrations up 100 μM. These findings were rather surprising, particularly for DMPX, which is the DEPX derivative with the highest reported affinity for A<sub>1</sub> ARs. By contrast, *in vivo* testing demonstrated that DPPX was as potent as DEPX at inducing edema in *Xenopus* embryos and it also disrupted vascular development. Furthermore, DPPX and DEPX share similar anatomical patterns of edema

induction, which suggests that they interfere via the same molecular target(s) *in vivo*. The functional equivalence is further demonstrated by nearly identical TI values. Structurally, DMPX, DEPX and DPPX differ only in the length of the 1,3 substitutions of the phenylxanthine core structure. Given that DMPX was inactive *in vivo*, we can conclude that the ethyl or propyl moieties are essential for bioactivity. This conclusion is further supported by the fact that embryos treated with caffeine (1,3,7-trimethylxanthine) do not develop edema (Kalin et al., 2009)(see also Table 10). The presence of the phenyl group is also essential for bioactivity of DEPX and DPPX. Theophylline, one of the primary liver metabolites of caffeine, is also known as 1,3-Dimethylxanthine. Thus, it lacks the phenyl substitution found in DEPX and DPPX. While not explicitly tested in the present study, it had previously been shown that theophylline does not induce edema in *Xenopus* embryos (Kalin et al., 2009) (see also Table 10). Finally, sulfonation of the phenyl moiety abrogates the *in vivo* activity of DPPX as demonstrated by the treatment of embryos with DPSPX.

Regarding 7CN, two derivatives, 7MN and 7CH, were also tested *in vivo*. 7MN carries a 7-methyl substitution in place of the chloro substitution found in 7CN. With a  $K_i$  value of 5.3 nM, it has more than 30-fold less affinity for  $A_1$  ARs than 7CN (Ferrarini et al., 2000) (see also Table 16). We found however that this substitution had no negative influence on the ability to induce edema. Furthermore, the pattern of edema formation and the vascular defects in *Xenopus* embryos were as with 7CN. If anything, 7MN was more toxic than 7CN resulting in a less favorable TI value. 7CH turned out to be devoid of any edema inducing activity demonstrating that the presence of a phenyl moiety is indispensable for bioactivity. We conclude that both DEPX and 7CN require phenyl substitutions to the core scaffolds for full *in vivo* activity, i.e. the ability to induce edema.

**Table 19. Chemical properties of 7CN, DEPX, and their derivatives**

Structure	Name	Molecular weight	XlogP
	Adenosine	267.24	-1.1
	Caffeine	194.19	-0.1
	Theophylline	180.16	-0.17
	1,3-Dimethyl-8-phenylxanthine (DMPX)	256.26	2.2
	1,3-Diethyl-8-phenylxanthine (DEPX)	284.31	2.9
	1,3-Dipropyl-8-phenylxanthine (DPPX)	312.37	4.0
	1,3-Dipropyl-8-(p-sulfonyl)xanthine (DPSPX)	392.43	3.1
	7-Chloro-4-hydroxy-2-phenyl-1,8-naphthyridine (7CN)	256.68	3.4
	7-Methyl-2-phenyl-1,8-naphthyridin-4(1H)-one (7MN)	236.37	3.61
	7-Chloro-4-hydroxy-[1,8] naphthyridine (7CH)	180.59	1.8

The chemical structures, molecular weights and the computer-predicted logP (XlogP) values of 7CN, DEPX, and their derivatives were taken from the ChemSpider ([chemspider.com](http://chemspider.com)) and PubChem ([pubchem.ncbi.nlm.nih.gov](http://pubchem.ncbi.nlm.nih.gov)) databases.

**Physicochemical properties and *in vivo* bioactivities of AR antagonists**

The central aim of SAR studies is to reveal possible connections between the chemical structure of a compound with its physicochemical properties (water solubility, molecular weight, etc.) and its biological activities, such efficacy, toxicity, and lethality (Lushington et al., 2013, Ritchie, 2001). Besides the known compounds 7CN and DEPX, two novel ones, 7MN and DPPX, emerged as additional compounds with largely similar *in vivo* properties as their parent compounds. All four compounds have been developed as AR antagonists with  $K_i$  values for  $A_1$  ARs ranging between 0.15 (for 7CN) and 44 nM (DEPX). By contrast, the differences in the  $EC_{50}$  and  $LC_{50}$  values obtained *in vivo* for the four compounds were less pronounced, typically not more than 10 fold. This indicates that there is no direct correlation between the reported *in vitro* affinities for  $A_1$  ARs and the observed bioactivities of the test compounds in *Xenopus* embryos. We conclude that the anti-angiogenic activities of 7CN and DEPX cannot be solely attributed to the inhibition of  $A_1$  AR signaling *in vivo*.

The  $A_1$  AR antagonists PSB 36 and SLV 320 induced edema, but had no anti-angiogenic activity. Whereas the  $A_1$  AR antagonists DMPX and DPSPX had no edema-inducing activity at all. Interestingly, PSB 36, SLV 320 and DMPX are considered to be potent  $A_1$  AR antagonists with  $K_i$  values of 1 nM or less. Nevertheless, they have *in vivo* no antiangiogenic activity. The lack of bioactivity may be attributed to reduced absorption or penetration of these compounds into *Xenopus* embryos. Studies in zebrafish indicate that the logarithm of the partition ratio between octanol and water ( $\log P$ ) of a compound correlates well with a compound's membrane permeability (Sachidanandan et al., 2008, Milan et al., 2003). Compounds with  $\log P$  values higher than +1 were well absorbed and active (Wheeler and Brandli, 2009). As shown in Table 19, the computer-predicted  $\log P$  values, XlogP, were for the 7CN and DEPX derivatives in the range of 1.8 to 4.0. Furthermore, PSB 36 and SLV 320 had XlogP values of 4 and 3.3, respectively. Thus, all these compounds are expected to penetrate aquatic larvae including *Xenopus* embryos. By contrast, the lack of bioactivity of caffeine and theophylline in *Xenopus* embryos could, at least in part, be attributed to poor penetration given that they have XlogP values below +1. With regard to compound size, active compounds exhibited no bias at least up to molecular weights of 700 Da. None of the tested compounds exceeded this empirical threshold (Table 19). At present, we cannot exclude the possibility that some compounds might have become inactive due to rapid metabolism and biotransformation in the embryo.

**Endothelial cells are direct targets of 7CN and 7MN**

The described anti-angiogenic effects of a subset of A<sub>1</sub> AR antagonists in *Xenopus* embryos raises the question whether these compounds have similar activities on mammalian endothelia, which is a prerequisite if they were to be developed as drug candidates for clinical testing. Primary human blood and lymphatic endothelial cell cultures were employed to assess the effects of compound treatment on cell proliferation and sprouting ability. It was previously demonstrated that 7CN blocks cell proliferation and tube formation of both blood and lymphatic endothelia *in vitro*. Furthermore, 7CN interferes with VEGFA-induced neovascularization in adult mice (Kalin et al., 2009). Here we found that 7CN as well as 7MN inhibited both the proliferation and sprouting of endothelial cells *in vitro*. Both compounds blocked proliferation of human blood and lymphatic endothelial cells at concentrations in the low  $\mu\text{M}$  range. To inhibit sprouting, compound concentrations as low as 0.1  $\mu\text{M}$  were sufficient. Interestingly, edema formation and disruption of vascular development in *Xenopus* embryos was achieved at comparable compound concentrations. Taken together, 7CN and 7MN interfered with endothelial cell functions *in vitro* as well as *in vivo*; and this occurred across vertebrate species ranging from *Xenopus* to humans. Furthermore, the *in vitro* experiments indicate that the molecular targets of 7CN and 7MN causing the arrest of cell proliferation and sprouting are present in blood and lymphatic endothelial cells.

**DEPX and DPPX exert their anti-angiogenic activities via an indirect mechanism**

Besides 7CN and 7MN, we have also demonstrated that DEPX and DPPX act as edema-inducing, anti-angiogenic compounds in *Xenopus* embryos. However, they had, at best, marginal *in vitro* effects on the proliferation of human blood and lymphatic endothelial cells. Furthermore, DEPX did not interfere with *in vitro* sprouting irrespective of the vascular cell type tested. Taken together, the *Xenopus* experiments demonstrate unequivocally that DEPX and DPPX have anti-angiogenic activities *in vivo*, but these compounds appear to be inactive when tested *in vitro* using human endothelial cell cultures. At present, we cannot exclude the possibility that the vascular targets of DEPX and DPPX in *Xenopus* embryos are either not present in the mammalian vasculature or they lack sufficient conservation. This would imply that the anti-angiogenic effects of DEPX and DPPX are species-specific and limited to *Xenopus* or other amphibians. If this were indeed the case, this would of course disqualify DEPX and DPPX for

further pre-clinical development. Alternatively, the anti-angiogenic activities observed in *Xenopus* embryos but not *in vitro* using human endothelial cell cultures may indicate a requirement for metabolic transformation of DEPX and DPPX in the liver. To our knowledge, there are no reports in the literature describing the metabolism of DEPX or DPPX in vertebrate organisms. Future *in vivo* studies using either mice or rats will therefore be necessary to address the issues of species-specific bioactivities and liver metabolism of DEPX and DPPX. Finally, our findings could be consistent with a model, where the anti-angiogenic activities of DEPX and DPPX observed *in vivo* are of indirect nature, not involving endothelial targets.

A model of paracrine stimulation of angiogenesis has been described by Clark *et al.* (2007), where adenosine-mediated activation of A<sub>1</sub> ARs on human mononuclear cells (macrophages, monocytes) promotes release of VEGFA, a potent stimulator of angiogenesis. Treatment of the cells with the A<sub>1</sub> AR selective antagonists WRC-0571 or CPX blocked the A<sub>1</sub> AR-mediated release of VEGFA. These findings are consistent with the hypothesis that A<sub>1</sub> ARs modulate angiogenesis through an indirect mechanism involving stimulation of inflammatory cells (Clark *et al.*, 2007). It should be however noted that CPX treatment has no effect on *Xenopus* embryogenesis (Kalin *et al.*, 2009)(see also Table 10). Nevertheless, it is conceivable that DEPX and DPPX treatment of *Xenopus* embryos disrupts paracrine proangiogenic signaling mechanisms. For example, VEGFA is highly expressed in the developing somites, where it appears to act as a proangiogenic factor for intersomitic vessel growth in *Xenopus* embryos (Kalin *et al.*, 2007). Here we have demonstrated that somites express predominantly A<sub>2A</sub> and A<sub>2B</sub> ARs indicating that somites are responsive to extracellular adenosine. Whether DEPX or DPPX treatments have any effects on somitic VEGFA expression in *Xenopus* embryos is currently not known. Taken together, it is most likely that DEPX and DPPX elicit their vascular disruptive activities *in vivo* via an indirect mechanism, for example by inhibiting the release of pro-angiogenic factors from non-endothelial cells.

**7CN and 7MN inhibit endothelial cell proliferation and sprouting by destabilization of the microtubular cytoskeleton**

Our findings with primary endothelial cell cultures demonstrate that 7CN and 7MN exert their activities by directly targeting endothelial cells. Both compounds showed strong anti-proliferative effects on HUVEC and LEC cultures. FACS analysis revealed that the compound-treated cells were arrested in pro-metaphase with tetraploid (4N) and/or polyploid (>4N) DNA contents. As expected, DEPX treatment did not cause any cell cycle arrest and the DNA content of the treated cells was 2N as with controls. These findings are consistent with the proposed indirect mechanism of action for DEPX (and DPPX) on endothelial cells *in vivo*. Disruption of microtubule assembly or disassembly both inhibits mitosis and induces excess DNA replication (Kavallaris, 2010). Indeed, we found that 7CN and 7MN were able to destabilize the microtubular cytoskeleton. Disruption of the cytoplasmic microtubules was rapid, detectable already two hours after compound addition to the media, and the effect was dose-dependent. Disassembly of the microtubular cytoskeleton was similar to the effects seen after treatment with nocodazole, a widely used agent to interfere with microtubule polymerization (Vasquez et al., 1997). Nocodazole-treated cells do enter mitosis but cannot form metaphase spindles because the microtubules are no longer able to polymerize. Microtubules are composed of tubulin molecules, which are heterodimers, composed of  $\alpha\beta$  subunits. Both  $\alpha$  and  $\beta$  subunits exist as numerous isotypes differing in amino acid sequence and encoded by different genes. High-resolution crystal structures have revealed that nocodazole binds to a site located deep in the  $\beta$  subunit of unassembled tubulin (Kavallaris, 2010, Zhou and Giannakakou, 2005). This binding site is known as the colchicine-binding site (CBS) that can be occupied by a set of structurally diverse inhibitors of microtubule polymerization, which includes colchicine, nocodazole, and plinabulin. Nocodazole binding prevents microtubule formation either by restricting the subdomain movements that are essential for structural transformation or by steric interference with the  $\alpha$  subunit of tubulin (Barbier et al., 2010, Ravelli et al., 2004). Besides the CBS, most microtubule-disrupting agents in development will target one of four other distinct binding sites on  $\beta$ -tubulin; namely the laulimalide, vinca alkaloid, taxane, or maytansine binding sites (Wang et al., 2016, Prota et al., 2014). At present, we do not know whether the observed microtubule-destabilizing activity of 7CN and 7MN is mediated by binding to tubulin or occurs via an indirect mechanism. 7CN and 7MN share no structural resemblance with, nocodazole, colchicine or any of the

other compounds defining the five distinct binding sites on  $\beta$ -tubulin targeted by microtubule-destabilizing agents (*data not shown*). This fact does however not exclude the possibility that 7CN and 7MN directly bind to tubulin. This issue needs to be addressed in future studies. Alternatively, the two compounds could act on microtubules via an indirect mechanism. The stability of microtubules is regulated by proteins, which interact with the microtubular lattice, known as microtubule-associated proteins (MAPs). Many different MAPs, such as MAP1, MAP2, MAP4, and tau, have been identified in recent years and they can carry out a wide range of functions, which includes both stabilization and destabilization of microtubules (Janke and Bulinski, 2011). The activity of MAPs is regulated via phosphorylation, for example by the microtubule-affinity-regulating kinase (MARK). Phosphorylation typically causes detachment of MAPs and followed by destabilization of microtubules (Drewes et al., 1997, Akhmanova and Steinmetz, 2015). Besides MAPs, many other proteins can interfere with microtubule function. For example, katanin is a microtubule-severing heterodimeric protein with an intrinsic ATPase activity (Nakamura, 2015, Sharp and Ross, 2012). Taken together, assembly and disassembly of microtubules is governed via a complex system of regulation involving many different proteins, whose activities are in part controlled by phosphorylation or other posttranslational mechanisms. Which aspect of this elaborate regulatory machine becomes altered after treatment with 7CN or 7MN is still a big mystery. The identification of the relevant intracellular targets of 7CN and 7MN should therefore be pursued with high priority.

### **Tissue and cell-type selectivities of the active compounds**

The assessment of AR antagonists in *Xenopus* embryos has led to the identification of four compounds, 7CN, 7MN, DEPX and DPPX that harbor the desired anti-angiogenic activities *in vivo*. Our findings demonstrate that all four compounds disrupted blood as well as lymph vessel formation in embryos up to about embryonic stage 40 (2.5 days post fertilization), the last stage investigated. We also asked whether these compounds affect the development or morphogenesis of other embryonic tissues. Specifically, pronephric kidney morphogenesis, hemangioblast specification, erythrocyte differentiation, and the formation of migratory myoblasts were investigated and none of these processes appeared to be impaired by compound treatment. While the list of tissues and organs assessed is not exhaustive, it appears that compound treatment of embryos between stage 29/30 and stage 40 selectively interferes with functions

of blood and lymphatic endothelia. Furthermore, general cytotoxicity of the compounds can be excluded. On the basis of *in vitro* experiments with primary human endothelia cells, we found that 7CN and 7MN blocked cell proliferation by destabilizing microtubules to cause mitotic arrest. By contrast, DEPX and DPPX were essentially inactive *in vitro*, which suggests that both compounds exert their effects on the developing vasculature of *Xenopus* embryos via an indirect mechanism. The molecular nature of this mechanism, and whether it requires other embryonic cell types is presently unknown. We also formally cannot exclude the possibility that the molecular targets of DEPX and DPPX are not conserved between *Xenopus* and human endothelial cells. If this were the case, this would explain why DEPX and DPPX treatment does not show any significant effect on human endothelial cell but has profound effects in *Xenopus* embryos. Irrespective of which scenario turns out to be correct, the potential of DEPX and DPPX as drug candidates for therapeutic applications in patients is strongly diminished given the lack of compound activities in primary human endothelial cell cultures.

Whereas 7MN remains poorly studied, several pieces of evidence indicate that the antiangiogenic and anti-proliferative effects of 7CN reported here are not entirely selective for endothelial cells. High-throughput screens of the LOPAC chemical library for compounds with inhibitory activities towards mammalian tumor cells *in vitro* led to the identification of 7CN as an active compound. This included mouse mammary tumor cell lines, where the IC<sub>50</sub> values were between 3-4  $\mu$ M (Evers et al., 2010). Similarly, 7CN was cytotoxic for human breast cancer cell lines LM2 and MDA-MB-231 (Desmet et al., 2013). Finally, 7CN was active in a screen for compounds that induce excess DNA replication in both the human colorectal cancer cell line SW480 and in the human breast epithelial cell MCF10A with EC<sub>50</sub> values ranging between 2-7  $\mu$ M (Zhu et al., 2011). 9 of 15 active compounds emerging from the screen, such as taxol, colchicine and nocodazole, are known to affect microtubule dynamics. This implies that 7CN has probably a similar destabilizing activity on microtubules, which is a hypothesis that was now confirmed in the present study. Collectively, these studies demonstrate that 7CN acts antimitotic in the low micromolar range on several mammalian cell lines derived from different cancer types.

The fact that 7CN (and 7MN) treatment selectively disrupts blood and lymph vessel development without apparent effects on other tissues and organs of the *Xenopus* embryo appear to be surprising at first glance. The *in vivo* activities of 7CN were however also confirmed in the mouse (Kalin et al., 2009). With regard to *Xenopus* embryos, these findings may indicate that endothelial cells are the primary cells undergoing rapid cell proliferation between embryonic stages 29/30 to 40, when compound treatment occurred. This hypothesis needs to be addressed in future studies. Importantly, 7CN was unique as none of the other AR antagonists present in the LOPAC library scored positive in the *in vitro* screens targeting cancer cells (Desmet et al., 2013, Zhu et al., 2011, Evers et al., 2010). This provides further circumstantial evidence supporting the notion that the antiangiogenic and anti-proliferative activities of 7CN (and 7MN) are not related to the known effects on AR signaling.

## Conclusions

The central aim of the present thesis project was to explore whether AR antagonists could be used as pharmacological agents to selectively disrupt blood and lymph vessel formation in *Xenopus* embryos. The project was inspired by the previous findings that 7CN and DEPX, two known A<sub>1</sub> AR selective antagonists, caused edema formation and disrupted vascular development in *Xenopus* embryos (Kalin et al., 2009). In the present thesis, testing of a comprehensive panel of 14 AR subtype-selective antagonists demonstrated that only two compounds, 7CN and DEPX, were able to induce edema and interfere with vascular development in *Xenopus* embryos. We established that these two compounds exert their activities at concentrations in the high nanomolar to low micromolar range. The calculated therapeutic indices were between 2 to 3 indicating a narrow therapeutic window. Structure-activity relationship studies identified first structural determinants important for the observed activities of 7CN and DEPX, respectively. *In vitro* studies with human endothelial cell cultures suggest that 7CN and DEPX act via different mechanisms *in vivo*. 7CN acts directly on endothelial cells to block cell proliferation and sprouting, whereas DEPX appears to act indirectly without any significant effects on endothelial cells in culture. Whether DEPX needs to be metabolized *in vivo* to exert its antiangiogenic function or whether it targets specific cells exerting pro-angiogenic activities remains to be determined. In *Xenopus* embryos, the activity of 7CN (and its derivative 7MN) appear to be selective for endothelia of the blood and lymph vasculature. However, it appears that also tumor cells respond to 7CN treatment. Several pieces of experimental evidence suggest that the antiangiogenic activities of 7CN cannot be solely attributed to its known biochemical activity as an A<sub>1</sub> AR selective antagonist. No other AR antagonist had comparable activities in *Xenopus*. Furthermore, we found no significant A<sub>1</sub> AR gene expression in the vascular systems of *Xenopus* embryos. Finally, knockdown of A<sub>1</sub> AR gene function did not result in edema formation or abnormal vascular development. Overall, this suggests that the inhibition of A<sub>1</sub> AR signaling by 7CN does not sufficiently explain the observed endothelial phenotypes. In fact, *in vitro* studies indicate that 7CN treatment of endothelial cells has a profound impact on the cytoskeleton, where it appears to interfere with the dynamics of microtubules. We conclude that our studies have identified 7CN and DEPX as unique compounds with potent anti-angiogenic activities *in vivo*. They act via distinct, at present poorly understood mechanisms, to exert their effects on endothelial cell functions.

## Outlook

The present work demonstrated clearly that the treatment of *Xenopus* embryos with the AR antagonists 7CN and DEPX interferes with blood and lymph vessel formation in a dose-dependent manner. We also identified derivatives of 7CN and DEPX that have similar bioactivity *in vivo*. Finally, we showed that 7CN acts by destabilizing microtubules of endothelial cells resulting in mitotic arrest, and excess DNA replication. The potential of these compounds as future vascular disruptive agents for clinical applications remain intact. The physicochemical properties of 7CN and DEPX comply with Lipinski's Rule of Five, an empirical measure of druglikeness and potential of a drug candidate to become an orally active drug in humans (Lipinski, 2004). Importantly, both compounds have molecular masses less than 500 daltons and logP value not greater than 5. Drug-plasma protein binding is an important major determinant of drug distribution and elimination. High affinity of a drug for human serum albumin (HAS), while diminish the free drug concentration available to the site of action. In a high-throughput screen of the LOPAC chemical library, neither 7CN nor DEPX were identified as compounds with high capability of HSA binding (McCallum et al., 2014). Furthermore, an analysis of the LOPAC library for compounds capable of inducing cardiotoxicity associated with the inhibition of the human ether-a-go-go-related gene (hERG) channel failed to highlight cardiotoxic potentials for 7CN or DEPX (Titus et al., 2009). Taken together, 7CN and DEPX have drug-like properties warranting further development and they can be considered lead compounds suitable to enter the lead optimization phase of preclinical drug development.

Lead optimization will require the synthesis of an array of derivatives by medicinal chemists with the aim of identifying variants with improved efficacy, higher target affinity, and reduced toxicity profiles. For example, it would be desirable to develop an improved version of 7CN, with an EC<sub>50</sub> value in the low nanomolar range, while preserving or raising the current LC<sub>50</sub> value well above 1 μM. This would improve the therapeutic index significantly. Having access to the crystal structure of the drug target can facilitate lead optimization. As discussed extensively in the introduction, several crystal structures for the A<sub>2A</sub> AR have been determined at high resolution and in the presence of key agonists and antagonists. In the present case, this structural information is however of limited utility. First, 7CN and DEPX have significantly higher affinities for A<sub>1</sub> than A<sub>2A</sub> ARs (see Table 11). Secondly, the work presented here provides compelling evidence

that the observed activities of 7CN and DEPX imply other targets than ARs only. We cannot exclude that they are the result of polypharmacology. As a first test of this hypothesis, it will be important to perform compound-treatment experiments with A<sub>1</sub> AR knockdown embryos. If our hypothesis is correct, these embryos should develop edema and have vascular defects. Subsequently, it will be important to identify the nature of the targets that are responsible for the antiangiogenic effects of 7CN and DEPX in *Xenopus* embryos. We suspect that 7CN and DEPX interact with different targets, as they exert their antiangiogenic activities via two distinct mechanisms. Target identification for DEPX will help in understanding how this compound acts antiangiogenic without directly targeting endothelial cells.

The two-step *in vivo* screening strategy described by Kalin *et al.* (2009) that led to the identification of 7CN and DEPX as antiangiogenic compounds used edema formation as a relevant pathophysiological read out of compound-inflicted defects in blood and lymphatic vessel formation or function. In a second step, compound validation relied on whole mount *in situ* hybridization to identify those edema-inducing compounds capable of disrupting vascular development. While this strategy was highly successful, it does not address the issue of endothelial cell selectivity, which is one of the desirable features of a vascular disruptive agent. In fact, as discussed above 7CN not only acts antiproliferative for different primary human endothelial cells, but also has similar activities towards mammalian tumor cell lines. We would therefore propose to modify the screening strategy of Kalin *et al.* (2009) by a third step. This third step would screen all positive hits with antiangiogenic activity *in vivo* across a panel of human endothelial, selected non-endothelial and tumor cell lines to identify those that are truly selective for human endothelial cells. This third step would also eliminate that compounds whose antiangiogenic activities are specific to *Xenopus*. This third step relies fully on *in vitro* cell cultures and thus has also disadvantages. For example, DEPX would not score as a positive hit, since it acts *in vivo* via an indirect mechanism. Overall, however we believe that the proposed third screening step would provide sufficient stringency to further prioritize compounds for lead optimization.

We would like to end by stressing the importance of whole animal drug screening to identify promising drug candidates. This is nicely illustrated by the discovery of DEPX and the characterization of its activities in the present study. DEPX and subsequently its derivative DPPX were shown to interfere selectively

with vascular development of *Xenopus* embryos. These compounds would not have been identified in chemical library screens performed with *in vitro* cultures of endothelial cells. They do not seem to require direct targeting of the vasculature in order to exert their antiangiogenic effects *in vivo*. In fact, a recently described phenotype-based *in vitro* screening assay designed to identify inhibitors of lymphangiogenesis present in the LOPAC chemical library was successful in identifying 7CN, but failed to detect DEPX (Schulz et al., 2012). Conventional cell culture screening systems typically do not adequately reproduce metabolic compound modifications or liver-based biotransformation processes that may be essential for the compound activity *in vivo*. We are therefore confident that phenotypic drug discovery in small vertebrate organisms, such as *Xenopus* or zebrafish larvae provide a much need alternative to conventional approaches of drug discovery.

### Bibliography

- ADAIR, T. H. 2005. Growth regulation of the vascular system: an emerging role for adenosine. *Am J Physiol Regul Integr Comp Physiol*, 289, R283-R296.
- AKHMANOVA, A. & STEINMETZ, M. O. 2015. Control of microtubule organization and dynamics: two ends in the limelight. *Nat Rev Mol Cell Biol*, 16, 711-26.
- AMAKYE, D., JAGANI, Z. & DORSCH, M. 2013. Unraveling the therapeutic potential of the Hedgehog pathway in cancer. *Nat Med*, 19, 1410-22.
- ARDURA, J. A. & FRIEDMAN, P. A. 2011. Regulation of G protein-coupled receptor function by Na<sup>+</sup>/H<sup>+</sup> exchange regulatory factors. *Pharmacol Rev*, 63, 882-900.
- ASTASHKINA, A., MANN, B. & GRAINGER, D. W. 2012. A critical evaluation of in vitro cell culture models for high-throughput drug screening and toxicity. *Pharmacol Ther*, 134, 82-106.
- AUCHAMPACH, J. A. 2007. Adenosine receptors and angiogenesis. *Circ Res*, 101, 1075-7.
- BALLARIN, M., FREDHOLM, B. B., AMBROSIO, S. & MAHY, N. 1991. Extracellular levels of adenosine and its metabolites in the striatum of awake rats: inhibition of uptake and metabolism. *Acta Physiol Scand*, 142, 97-103.
- BARBIER, P., DORLEANS, A., DEVRED, F., SANZ, L., ALLEGRO, D., ALFONSO, C., KNOSSOW, M., PEYROT, V. & ANDREU, J. M. 2010. Stathmin and interfacial microtubule inhibitors recognize a naturally curved conformation of tubulin dimers. *J Biol Chem*, 285, 31672-81.
- BELIKOFF, B. G., HATFIELD, S., GEORGIEV, P., OHTA, A., LUKASHEV, D., BURAS, J. A., REMICK, D. G. & SITKOVSKY, M. 2011. A2B adenosine receptor blockade enhances macrophage-mediated bacterial phagocytosis and improves polymicrobial sepsis survival in mice. *J Immunol*, 186, 2444-53.
- BENNET, D. W. & DRURY, A. N. 1931. Further observations relating to the physiological activity of adenine compounds. *J Physiol*, 72, 288-320.
- BOEHMLER, W., PETKO, J., WOLL, M., FREY, C., THISSE, B., THISSE, C., CANFIELD, V. A. & LEVENSON, R. 2009. Identification of zebrafish A2 adenosine receptors and expression in developing embryos. *Gene Expr Patterns*, 9, 144-51.
- BOREA, P. A., GESSI, S., MERIGHI, S. & VARANI, K. 2016. Adenosine as a Multi-Signalling Guardian Angel in Human Diseases: When, Where and How Does it Exert its Protective Effects? *Trends Pharmacol Sci*, 37, 419-34.
- BRANDLI, A. W. & KIRSCHNER, M. W. 1995. Molecular cloning of tyrosine kinases in the early *Xenopus* embryo: identification of Eck-related genes expressed in cranial neural crest cells of the second (hyoid) arch. *Dev Dyn*, 203, 119-40.

## Bibliography

---

- BRUNS, R. F., DALY, J. W. & SNYDER, S. H. 1983. Adenosine receptor binding: structure-activity analysis generates extremely potent xanthine antagonists. *Proc Natl Acad Sci U S A*, 80, 2077-80.
- BRUNS, R. F., FERGUS, J. H., BADGER, E. W., BRISTOL, J. A., SANTAY, L. A., HARTMAN, J. D., HAYS, S. J. & HUANG, C. C. 1987. Binding of the A1-selective adenosine antagonist 8-cyclopentyl-1,3-dipropylxanthine to rat brain membranes. *Naunyn Schmiedebergs Arch Pharmacol*, 335, 59-63.
- CARMELIET, P. 2003. Angiogenesis in health and disease. *Nat Med*, 9, 653-60.
- CARPENTER, B., NEHME, R., WARNE, T., LESLIE, A. G. & TATE, C. G. 2016. Structure of the adenosine A(2A) receptor bound to an engineered G protein. *Nature*, 536, 104-7.
- CESCA, M., BIZZARO, F., ZUCCHETTI, M. & GIAVAZZI, R. 2013. Tumor Delivery of Chemotherapy Combined with Inhibitors of Angiogenesis and Vascular Targeting Agents. *Front Oncol*, 3, 259.
- CHEN, J. F., ELTZSCHIG, H. K. & FREDHOLM, B. B. 2013. Adenosine receptors as drug targets--what are the challenges? *Nat Rev Drug Discov*, 12, 265-86.
- CHEN, J. F., HUANG, Z., MA, J., ZHU, J., MORATALLA, R., STANDAERT, D., MOSKOWITZ, M. A., FINK, J. S. & SCHWARZSCHILD, M. A. 1999. A(2A) adenosine receptor deficiency attenuates brain injury induced by transient focal ischemia in mice. *J Neurosci*, 19, 9192-200.
- CHUNG, A. S., LEE, J. & FERRARA, N. 2010. Targeting the tumour vasculature: insights from physiological angiogenesis. *Nat Rev Cancer*, 10, 505-14.
- CIAU-UITZ, A., WALMSLEY, M. & PATIENT, R. 2000. Distinct origins of adult and embryonic blood in *Xenopus*. *Cell*, 102, 787-96.
- CIAU-UITZ, A., WANG, L., PATIENT, R. & LIU, F. 2013. ETS transcription factors in hematopoietic stem cell development. *Blood Cells Mol Dis*, 51, 248-55.
- CLARK, A. N., YOUKEY, R., LIU, X., JIA, L., BLATT, R., DAY, Y. J., SULLIVAN, G. W., LINDEN, J. & TUCKER, A. L. 2007. A1 adenosine receptor activation promotes angiogenesis and release of VEGF from monocytes. *Circ Res*, 101, 1130-8.
- COBANOGLU, M. C., SAYGIN, Y. & SEZERMAN, U. 2011. Classification of GPCRs using family specific motifs. *IEEE/ACM Trans Comput Biol Bioinform*, 8, 1495-508.
- CONN, P. J., CHRISTOPOULOS, A. & LINDSLEY, C. W. 2009. Allosteric modulators of GPCRs: a novel approach for the treatment of CNS disorders. *Nat Rev Drug Discov*, 8, 41-54.
- COOPER, S. 2003. Rethinking synchronization of mammalian cells for cell cycle analysis. *Cell Mol Life Sci*, 60, 1099-106.
- CORADA, M., MORINI, M. F. & DEJANA, E. 2014. Signaling pathways in the specification of arteries and veins. *Arterioscler Thromb Vasc Biol*, 34, 2372-7.

## Bibliography

---

- CVICEK, V., GODDARD, W. A., 3RD & ABROL, R. 2016. Structure-Based Sequence Alignment of the Transmembrane Domains of All Human GPCRs: Phylogenetic, Structural and Functional Implications. *PLoS Comput Biol*, 12, e1004805.
- DELACRETAZ, E. 2006. Clinical practice. Supraventricular tachycardia. *N Engl J Med*, 354, 1039-51.
- DEMIR, R., YABA, A. & HUPPERTZ, B. 2010. Vasculogenesis and angiogenesis in the endometrium during menstrual cycle and implantation. *Acta Histochem*, 112, 203-14.
- DESMET, C. J., GALLENNE, T., PRIEUR, A., REYAL, F., VISSER, N. L., WITTNER, B. S., SMIT, M. A., GEIGER, T. R., LAOUKILI, J., ISKIT, S., RODENKO, B., ZWART, W., EVERS, B., HORLINGS, H., AJOUAOU, A., ZEVENHOVEN, J., VAN VLIET, M., RAMASWAMY, S., WESSELS, L. F. & PEEPER, D. S. 2013. Identification of a pharmacologically tractable Fra-1/ADORA2B axis promoting breast cancer metastasis. *Proc Natl Acad Sci U S A*, 110, 5139-44.
- DOME, B., HENDRIX, M. J., PAKU, S., TOVARI, J. & TIMAR, J. 2007. Alternative vascularization mechanisms in cancer: Pathology and therapeutic implications. *Am J Pathol*, 170, 1-15.
- DORE, A. S., ROBERTSON, N., ERREY, J. C., NG, I., HOLLENSTEIN, K., TEHAN, B., HURRELL, E., BENNETT, K., CONGREVE, M., MAGNANI, F., TATE, C. G., WEIR, M. & MARSHALL, F. H. 2011. Structure of the adenosine A(2A) receptor in complex with ZM241385 and the xanthines XAC and caffeine. *Structure*, 19, 1283-93.
- DORSAM, R. T. & GUTKIND, J. S. 2007. G-protein-coupled receptors and cancer. *Nat Rev Cancer*, 7, 79-94.
- DREWES, G., EBNETH, A., PREUSS, U., MANDELKOW, E. M. & MANDELKOW, E. 1997. MARK, a novel family of protein kinases that phosphorylate microtubule-associated proteins and trigger microtubule disruption. *Cell*, 89, 297-308.
- DRURY, A. N. & SZENT-GYORGYI, A. 1929. The physiological activity of adenine compounds with especial reference to their action upon the mammalian heart. *J Physiol*, 68, 213-37.
- DUSSEAU, J. W. & HUTCHINS, P. M. 1988. Hypoxia-induced angiogenesis in chick chorioallantoic membranes: a role for adenosine. *Respir Physiol*, 71, 33-44.
- DUSSEAU, J. W., HUTCHINS, P. M. & MALBASA, D. S. 1986. Stimulation of angiogenesis by adenosine on the chick chorioallantoic membrane. *Circ Res*, 59, 163-70.
- ECKLE, T., FAIGLE, M., GRENZ, A., LAUCHER, S., THOMPSON, L. F. & ELTZSCHIG, H. K. 2008. A2B adenosine receptor dampens hypoxia-induced vascular leak. *Blood*, 111, 2024-35.
- ECKLE, T., HARTMANN, K., BONNEY, S., REITHEL, S., MITTELBRONN, M., WALKER, L. A., LOWES, B. D., HAN, J., BORCHERS, C. H., BUTTRICK, P. M., KOMINSKY, D. J., COLGAN, S. P. & ELTZSCHIG, H. K. 2012. Adora2b-elicited Per2 stabilization promotes a HIF-dependent metabolic switch crucial for myocardial adaptation to ischemia. *Nat Med*, 18, 774-82.

## Bibliography

---

- EISENSTEIN, A. & RAVID, K. 2014. G protein-coupled receptors and adipogenesis: a focus on adenosine receptors. *J Cell Physiol*, 229, 414-21.
- ELTZSCHIG, H. K. 2009. Adenosine: an old drug newly discovered. *Anesthesiology*, 111, 904-15.
- ELTZSCHIG, H. K., SITKOVSKY, M. V. & ROBSON, S. C. 2012. Purinergic signaling during inflammation. *N Engl J Med*, 367, 2322-33.
- ESCUDERO, C., ROBERTS, J. M., MYATT, L. & FEOKTISTOV, I. 2014. Impaired adenosine-mediated angiogenesis in preeclampsia: potential implications for fetal programming. *Front Pharmacol*, 5, 134.
- EVERS, B., SCHUT, E., VAN DER BURG, E., BRAUMULLER, T. M., EGAN, D. A., HOLSTEGE, H., EDSER, P., ADAMS, D. J., WADE-MARTINS, R., BOUWMAN, P. & JONKERS, J. 2010. A high-throughput pharmaceutical screen identifies compounds with specific toxicity against BRCA2-deficient tumors. *Clin Cancer Res*, 16, 99-108.
- FEIGL, E. O. 2004. Berne's adenosine hypothesis of coronary blood flow control. *Am J Physiol Heart Circ Physiol*, 287, H1891-4.
- FEOKTISTOV, I., BIAGGIONI, I. & CRONSTEIN, B. N. 2009. Adenosine receptors in wound healing, fibrosis and angiogenesis. *Handb Exp Pharmacol*, 383-97.
- FEOKTISTOV, I., GOLDSTEIN, A. E., RYZHOV, S., ZENG, D., BELARDINELLI, L., VOYNO-YASENETSKAYA, T. & BIAGGIONI, I. 2002. Differential expression of adenosine receptors in human endothelial cells: role of A2B receptors in angiogenic factor regulation. *Circ Res*, 90, 531-8.
- FEOKTISTOV, I., RYZHOV, S., GOLDSTEIN, A. E. & BIAGGIONI, I. 2003. Mast cell-mediated stimulation of angiogenesis: cooperative interaction between A2B and A3 adenosine receptors. *Circ Res*, 92, 485-92.
- FERRARINI, P. L., CALDERONE, V., CAVALLINI, T., MANERA, C., SACCOMANNI, G., PANI, L., RUIU, S. & GESSA, G. L. 2004. Synthesis and biological evaluation of 1,8-naphthyridin-4(1H)-on-3-carboxamide derivatives as new ligands of cannabinoid receptors. *Bioorg Med Chem*, 12, 1921-33.
- FERRARINI, P. L., MORI, C., MANERA, C., MARTINELLI, A., MORI, F., SACCOMANNI, G., BARILI, P. L., BETTI, L., GIANNACCINI, G., TRINCAVELLI, L. & LUCACCHINI, A. 2000. A novel class of highly potent and selective A1 adenosine antagonists: structure-affinity profile of a series of 1,8-naphthyridine derivatives. *J Med Chem*, 43, 2814-23.
- FREDHOLM, B. B., AP, I. J., JACOBSON, K. A., KLOTZ, K. N. & LINDEN, J. 2001. International Union of Pharmacology. XXV. Nomenclature and classification of adenosine receptors. *Pharmacol Rev*, 53, 527-52.
- FREDHOLM, B. B., AP, I. J., JACOBSON, K. A., LINDEN, J. & MULLER, C. E. 2011. International Union of Basic and Clinical Pharmacology. LXXXI. Nomenclature and classification of adenosine receptors--an update. *Pharmacol Rev*, 63, 1-34.

## Bibliography

---

- FREDHOLM, B. B., CHEN, J. F., MASINO, S. A. & VAUGEOIS, J. M. 2005. Actions of adenosine at its receptors in the CNS: insights from knockouts and drugs. *Annu Rev Pharmacol Toxicol*, 45, 385-412.
- FREDRIKSSON, R., LAGERSTROM, M. C., LUNDIN, L. G. & SCHIOTH, H. B. 2003. The G-protein-coupled receptors in the human genome form five main families. Phylogenetic analysis, paralogon groups, and fingerprints. *Mol Pharmacol*, 63, 1256-72.
- FREDRIKSSON, R. & SCHIOTH, H. B. 2005. The repertoire of G-protein-coupled receptors in fully sequenced genomes. *Mol Pharmacol*, 67, 1414-25.
- GAO, Z., NI, Y., SZABO, G. & LINDEN, J. 1999. Palmitoylation of the recombinant human A1 adenosine receptor: enhanced proteolysis of palmitoylation-deficient mutant receptors. *Biochem J*, 342 ( Pt 2), 387-95.
- GESSI, S., CATTABRIGA, E., AVITABILE, A., GAFA, R., LANZA, G., CAVAZZINI, L., BIANCHI, N., GAMBARI, R., FEO, C., LIBONI, A., GULLINI, S., LEUNG, E., MAC-LENNAN, S. & BOREA, P. A. 2004. Elevated expression of A3 adenosine receptors in human colorectal cancer is reflected in peripheral blood cells. *Clin Cancer Res*, 10, 5895-901.
- GHIMIRE, G., HAGE, F. G., HEO, J. & ISKANDRIAN, A. E. 2013. Regadenoson: a focused update. *J Nucl Cardiol*, 20, 284-8.
- GREILLIER, L., TOMASINI, P. & BARLESI, F. 2016. Bevacizumab in the treatment of nonsquamous non-small cell lung cancer: clinical trial evidence and experience. *Ther Adv Respir Dis*.
- GUO, S. & DIPIETRO, L. A. 2010. Factors affecting wound healing. *J Dent Res*, 89, 219-29.
- HABECK, H., ODENTHAL, J., WALDERICH, B., MAISCHEIN, H., SCHULTE-MERKER, S. & TUBINGEN SCREEN, C. 2002. Analysis of a zebrafish VEGF receptor mutant reveals specific disruption of angiogenesis. *Curr Biol*, 12, 1405-12.
- HARLAND, R. M. 1991. In situ hybridization: an improved whole-mount method for *Xenopus* embryos. *Methods Cell Biol*, 36, 685-95.
- HART, M. L., GRENZ, A., GORZOLLA, I. C., SCHITTENHELM, J., DALTON, J. H. & ELTZSCHIG, H. K. 2011. Hypoxia-inducible factor-1alpha-dependent protection from intestinal ischemia/reperfusion injury involves ecto-5'-nucleotidase (CD73) and the A2B adenosine receptor. *J Immunol*, 186, 4367-74.
- HASKO, G., LINDEN, J., CRONSTEIN, B. & PACHER, P. 2008. Adenosine receptors: therapeutic aspects for inflammatory and immune diseases. *Nat Rev Drug Discov*, 7, 759-70.
- HEADRICK, J. P., ASHTON, K. J., ROSEMEYER, R. B. & PEART, J. N. 2013. Cardiovascular adenosine receptors: expression, actions and interactions. *Pharmacol Ther*, 140, 92-111.
- HELBLING, P. M., SAULNIER, D. M. & BRANDLI, A. W. 2000. The receptor tyrosine kinase EphB4 and ephrin-B ligands restrict angiogenic growth of embryonic veins in *Xenopus laevis*. *Development*, 127, 269-78.

## Bibliography

---

- HELBLING, P. M., TRAN, C. T. & BRANDLI, A. W. 1998. Requirement for EphA receptor signaling in the segregation of *Xenopus* third and fourth arch neural crest cells. *Mech Dev*, 78, 63-79.
- HUROWITZ, E. H., MELNYK, J. M., CHEN, Y. J., KOUROS-MEHR, H., SIMON, M. I. & SHIZUYA, H. 2000. Genomic characterization of the human heterotrimeric G protein alpha, beta, and gamma subunit genes. *DNA Res*, 7, 111-20.
- JACOBSON, K. A. 2009. Introduction to adenosine receptors as therapeutic targets. *Handb Exp Pharmacol*, 1-24.
- JACOBSON, K. A. & GAO, Z. G. 2006. Adenosine receptors as therapeutic targets. *Nat Rev Drug Discov*, 5, 247-64.
- JACOBSON, K. A. & MULLER, C. E. 2016. Medicinal chemistry of adenosine, P2Y and P2X receptors. *Neuropharmacology*, 104, 31-49.
- JANKE, C. & BULINSKI, J. C. 2011. Post-translational regulation of the microtubule cytoskeleton: mechanisms and functions. *Nat Rev Mol Cell Biol*, 12, 773-86.
- JASSAL, B., JUPE, S., CAUDY, M., BIRNEY, E., STEIN, L., HERMJAKOB, H. & D'EUSTACHIO, P. 2010. The systematic annotation of the three main GPCR families in Reactome. *Database (Oxford)*, 2010, baq018.
- JEN, S. C. & ROVAINEN, C. M. 1994. An adenosine agonist increases blood flow and density of capillary branches in the optic tectum of *Xenopus laevis* tadpoles. *Microcirculation*, 1, 59-66.
- JI, T. H., GROSSMANN, M. & JI, I. 1998. G protein-coupled receptors. I. Diversity of receptor-ligand interactions. *J Biol Chem*, 273, 17299-302.
- JIN, S. W., HERZOG, W., SANTORO, M. M., MITCHELL, T. S., FRANTSVE, J., JUNGBLUT, B., BEIS, D., SCOTT, I. C., D'AMICO, L. A., OBER, E. A., VERKADE, H., FIELD, H. A., CHI, N. C., WEHMAN, A. M., BAIER, H. & STAINIER, D. Y. 2007. A transgene-assisted genetic screen identifies essential regulators of vascular development in vertebrate embryos. *Dev Biol*, 307, 29-42.
- JING, L., TAMPLIN, O. J., CHEN, M. J., DENG, Q., PATTERSON, S., KIM, P. G., DURAND, E. M., MCNEIL, A., GREEN, J. M., MATSUURA, S., ABLAIN, J., BRANDT, M. K., SCHLAEGER, T. M., HUTTENLOCHER, A., DALEY, G. Q., RAVID, K. & ZON, L. I. 2015. Adenosine signaling promotes hematopoietic stem and progenitor cell emergence. *J Exp Med*, 212, 649-63.
- KALIN, R. E., BANZIGER-TOBLER, N. E., DETMAR, M. & BRANDLI, A. W. 2009. An in vivo chemical library screen in *Xenopus* tadpoles reveals novel pathways involved in angiogenesis and lymphangiogenesis. *Blood*, 114, 1110-22.
- KALIN, R. E., KRETZ, M. P., MEYER, A. M., KISPERS, A., HEPNER, F. L. & BRANDLI, A. W. 2007. Paracrine and autocrine mechanisms of apelin signaling govern embryonic and tumor angiogenesis. *Dev Biol*, 305, 599-614.

## Bibliography

---

- KALLA, R. V., ZABLOCKI, J., TABRIZI, M. A. & BARALDI, P. G. 2009. Recent developments in A2B adenosine receptor ligands. *Handb Exp Pharmacol*, 99-122.
- KATRITCH, V., CHEREZOV, V. & STEVENS, R. C. 2012. Diversity and modularity of G protein-coupled receptor structures. *Trends Pharmacol Sci*, 33, 17-27.
- KATRITCH, V., CHEREZOV, V. & STEVENS, R. C. 2013. Structure-function of the G protein-coupled receptor superfamily. *Annu Rev Pharmacol Toxicol*, 53, 531-56.
- KAVALLARIS, M. 2010. Microtubules and resistance to tubulin-binding agents. *Nat Rev Cancer*, 10, 194-204.
- KELLEY, C., YEE, K., HARLAND, R. & ZON, L. I. 1994. Ventral expression of GATA-1 and GATA-2 in the *Xenopus* embryo defines induction of hematopoietic mesoderm. *Dev Biol*, 165, 193-205.
- KENAKIN, T. 2010. A holistic view of GPCR signaling. *Nat Biotechnol*, 28, 928-9.
- KOBILKA, B. K. 2007. G protein coupled receptor structure and activation. *Biochim Biophys Acta*, 1768, 794-807.
- KRISHNAN, A., ALMEN, M. S., FREDRIKSSON, R. & SCHIOTH, H. B. 2012. The origin of GPCRs: identification of mammalian like Rhodopsin, Adhesion, Glutamate and Frizzled GPCRs in fungi. *PLoS One*, 7, e29817.
- LAGERSTROM, M. C. & SCHIOTH, H. B. 2008. Structural diversity of G protein-coupled receptors and significance for drug discovery. *Nat Rev Drug Discov*, 7, 339-57.
- LEBON, G., EDWARDS, P. C., LESLIE, A. G. & TATE, C. G. 2015. Molecular Determinants of CGS21680 Binding to the Human Adenosine A2A Receptor. *Mol Pharmacol*, 87, 907-15.
- LEDENT, C., VAUGEOIS, J. M., SCHIFFMANN, S. N., PEDRAZZINI, T., EL YACOUBI, M., VANDERHAEGHEN, J. J., COSTENTIN, J., HEATH, J. K., VASSART, G. & PARMENTIER, M. 1997. Aggressiveness, hypoalgesia and high blood pressure in mice lacking the adenosine A2a receptor. *Nature*, 388, 674-8.
- LENOIR, B., WAGNER, D. R., BLACHER, S., SALA-NEWBY, G. B., NEWBY, A. C., NOEL, A. & DEVAUX, Y. 2014. Effects of adenosine on lymphangiogenesis. *PLoS One*, 9, e92715.
- LEWITT, P. A. 2008. Levodopa for the treatment of Parkinson's disease. *N Engl J Med*, 359, 2468-76.
- LINDEN, J. 2005. Adenosine in tissue protection and tissue regeneration. *Mol Pharmacol*, 67, 1385-7.
- LIPINSKI, C. A. 2004. Lead- and drug-like compounds: the rule-of-five revolution. *Drug Discov Today Technol*, 1, 337-41.
- LIU, J., ZHOU, Y., QI, X., CHEN, J., CHEN, W., QIU, G., WU, Z. & WU, N. 2016. CRISPR/Cas9 in zebrafish: an efficient combination for human genetic diseases modeling. *Hum Genet*.

## Bibliography

---

- LIU, W., CHUN, E., THOMPSON, A. A., CHUBUKOV, P., XU, F., KATRITCH, V., HAN, G. W., ROTH, C. B., HEITMAN, L. H., AP, I. J., CHEREZOV, V. & STEVENS, R. C. 2012. Structural basis for allosteric regulation of GPCRs by sodium ions. *Science*, 337, 232-6.
- LOKEY, R. S. 2003. Forward chemical genetics: progress and obstacles on the path to a new pharmacopoeia. *Current Opinion in Chemical Biology*, Volume 7, 91-96.
- LUSHINGTON, G. H., DONG, Y. & THEERTHAM, B. 2013. Chemical informatics and the drug discovery knowledge pyramid. *Comb Chem High Throughput Screen*, 16, 764-76.
- LUTTRELL, L. M. 2008. Reviews in molecular biology and biotechnology: transmembrane signaling by G protein-coupled receptors. *Mol Biotechnol*, 39, 239-64.
- MACDONALD, B. T. & HE, X. 2012. Frizzled and LRP5/6 receptors for Wnt/beta-catenin signaling. *Cold Spring Harb Perspect Biol*, 4.
- MACZKOWIAK, F., MATEOS, S., WANG, E., ROCHE, D., HARLAND, R. & MONSORO-BURQ, A. H. 2010. The Pax3 and Pax7 paralogs cooperate in neural and neural crest patterning using distinct molecular mechanisms, in *Xenopus laevis* embryos. *Dev Biol*, 340, 381-96.
- MAKINEN, T., JUSSILA, L., VEIKKOLA, T., KARPANEN, T., KETTUNEN, M. I., PULKKANEN, K. J., KAUPPINEN, R., JACKSON, D. G., KUBO, H., NISHIKAWA, S., YLA-HERTTUALA, S. & ALITALO, K. 2001. Inhibition of lymphangiogenesis with resulting lymphedema in transgenic mice expressing soluble VEGF receptor-3. *Nat Med*, 7, 199-205.
- MASSIE, B. M., O'CONNOR, C. M., METRA, M., PONIKOWSKI, P., TEERLINK, J. R., COTTER, G., WEATHERLEY, B. D., CLELAND, J. G., GIVERTZ, M. M., VOORS, A., DELUCCA, P., MANSOOR, G. A., SALERNO, C. M., BLOOMFIELD, D. M., DITTRICH, H. C., INVESTIGATORS, P. & COMMITTEES 2010. Rolofylline, an adenosine A1-receptor antagonist, in acute heart failure. *N Engl J Med*, 363, 1419-28.
- MASSINK, A., GUTIERREZ-DE-TERAN, H., LENSELINK, E. B., ORTIZ ZACARIAS, N. V., XIA, L., HEITMAN, L. H., KATRITCH, V., STEVENS, R. C. & AP, I. J. 2015. Sodium ion binding pocket mutations and adenosine A2A receptor function. *Mol Pharmacol*, 87, 305-13.
- MCCALLUM, M. M., PAWLAK, A. J., SHADRICK, W. R., SIMEONOV, A., JADHAV, A., YASGAR, A., MALONEY, D. J. & ARNOLD, L. A. 2014. A fluorescence-based high throughput assay for the determination of small molecule-human serum albumin protein binding. *Anal Bioanal Chem*, 406, 1867-75.
- MILAN, D. J., PETERSON, T. A., RUSKIN, J. N., PETERSON, R. T. & MACRAE, C. A. 2003. Drugs that induce repolarization abnormalities cause bradycardia in zebrafish. *Circulation*, 107, 1355-8.
- MONTESINOS, M. C., GADANGI, P., LONGAKER, M., SUNG, J., LEVINE, J., NILSEN, D., REIBMAN, J., LI, M., JIANG, C. K., HIRSCHHORN, R., RECHT, P. A., OSTAD, E., LEVIN, R. I. & CRONSTEIN, B. N. 1997. Wound healing is accelerated by agonists of adenosine A2 (G alpha s-linked) receptors. *J Exp Med*, 186, 1615-20.

## Bibliography

---

- NAKAMURA, M. 2015. Microtubule nucleating and severing enzymes for modifying microtubule array organization and cell morphogenesis in response to environmental cues. *New Phytol*, 205, 1022-7.
- NAKATSU, M. N., DAVIS, J. & HUGHES, C. C. 2007. Optimized fibrin gel bead assay for the study of angiogenesis. *J Vis Exp*, 186.
- NEUFELD, S., PLANAS-PAZ, L. & LAMMERT, E. 2014. Blood and lymphatic vascular tube formation in mouse. *Semin Cell Dev Biol*, 31, 115-23.
- NIEUWKOOP PD, F. J. 1994. a systematical and chronological survey of the development from the fertilized egg till the end of metamorphosis. Normal table of *Xenopus laevis* (Daudin).
- NY, A., KOCH, M., SCHNEIDER, M., NEVEN, E., TONG, R. T., MAITY, S., FISCHER, C., PLAISANCE, S., LAMBRECHTS, D., HELIGON, C., TERCLAVERS, S., CIESIOLKA, M., KALIN, R., MAN, W. Y., SENN, I., WYNS, S., LUPU, F., BRANDLI, A., VLEMINCKX, K., COLLEN, D., DEWERCHIN, M., CONWAY, E. M., MOONS, L., JAIN, R. K. & CARMELIET, P. 2005. A genetic *Xenopus laevis* tadpole model to study lymphangiogenesis. *Nat Med*, 11, 998-1004.
- OCHAION, A., BAR-YEHUDA, S., COHEN, S., BARER, F., PATOKA, R., AMITAL, H., REITBLAT, T., REITBLAT, A., OPHIR, J., KONFINO, I., CHOWERS, Y., BEN-HORIN, S. & FISHMAN, P. 2009. The anti-inflammatory target A(3) adenosine receptor is over-expressed in rheumatoid arthritis, psoriasis and Crohn's disease. *Cell Immunol*, 258, 115-22.
- OLAH, M. E. & CALDWELL, C. C. 2003. Adenosine receptors and mammalian toll-like receptors: synergism in macrophages. *Mol Interv*, 3, 370-4.
- OLDHAM, W. M. & HAMM, H. E. 2008. Heterotrimeric G protein activation by G-protein-coupled receptors. *Nat Rev Mol Cell Biol*, 9, 60-71.
- OVERINGTON, J. P., AL-LAZIKANI, B. & HOPKINS, A. L. 2006. How many drug targets are there? *Nat Rev Drug Discov*, 5, 993-6.
- PANDEY, U. B. & NICHOLS, C. D. 2011. Human disease models in *Drosophila melanogaster* and the role of the fly in therapeutic drug discovery. *Pharmacol Rev*, 63, 411-36.
- PHELPS, P. T., ANTHES, J. C. & CORRELL, C. C. 2006. Characterization of adenosine receptors in the human bladder carcinoma T24 cell line. *Eur J Pharmacol*, 536, 28-37.
- PIIRAINEN, H., ASHOK, Y., NANEKAR, R. T. & JAAKOLA, V. P. 2011. Structural features of adenosine receptors: from crystal to function. *Biochim Biophys Acta*, 1808, 1233-44.
- PROTA, A. E., BARGSTEN, K., DIAZ, J. F., MARSH, M., CUEVAS, C., LINIGER, M., NEUHAUS, C., ANDREU, J. M., ALTMANN, K. H. & STEINMETZ, M. O. 2014. A new tubulin-binding site and pharmacophore for microtubule-destabilizing anticancer drugs. *Proc Natl Acad Sci U S A*, 111, 13817-21.

## Bibliography

---

- RACITI, D., REGGIANI, L., GEFFERS, L., JIANG, Q., BACCHION, F., SUBRIZI, A. E., CLEMENTS, D., TINDAL, C., DAVIDSON, D. R., KAISLING, B. & BRANDLI, A. W. 2008. Organization of the pronephric kidney revealed by large-scale gene expression mapping. *Genome Biol*, 9, R84.
- RAVELLI, R. B., GIGANT, B., CURMI, P. A., JOURDAIN, I., LACHKAR, S., SOBEL, A. & KNOSSOW, M. 2004. Insight into tubulin regulation from a complex with colchicine and a stathmin-like domain. *Nature*, 428, 198-202.
- RITCHIE, T. J. 2001. Chemoinformatics: manipulating chemical information to facilitate decision-making in drug discovery. *Drug Discov Today*, 6, 813-814.
- ROBERTS, V. S., COWAN, P. J., ALEXANDER, S. I., ROBSON, S. C. & DWYER, K. M. 2014. The role of adenosine receptors A and A signaling in renal fibrosis. *Kidney Int*.
- ROBINTON, D. A. & DALEY, G. Q. 2012. The promise of induced pluripotent stem cells in research and therapy. *Nature*, 481, 295-305.
- ROSENBAUM, D. M., RASMUSSEN, S. G. & KOBILKA, B. K. 2009. The structure and function of G-protein-coupled receptors. *Nature*, 459, 356-63.
- ROSENBERGER, P., SCHWAB, J. M., MIRAKAJ, V., MASEKOWSKY, E., MAGER, A., MOROTE-GARCIA, J. C., UNERTL, K. & ELTZSCHIG, H. K. 2009. Hypoxia-inducible factor-dependent induction of netrin-1 dampens inflammation caused by hypoxia. *Nat Immunol*, 10, 195-202.
- ROSS, E. M. & WILKIE, T. M. 2000. GTPase-activating proteins for heterotrimeric G proteins: regulators of G protein signaling (RGS) and RGS-like proteins. *Annu Rev Biochem*, 69, 795-827.
- ROUDNICKY, F., POYET, C., WILD, P., KRAMPITZ, S., NEGRINI, F., HUGGENBERGER, R., ROGLER, A., STOHR, R., HARTMANN, A., PROVENZANO, M., OTTO, V. I. & DETMAR, M. 2013. Endocan is upregulated on tumor vessels in invasive bladder cancer where it mediates VEGF-A-induced angiogenesis. *Cancer Res*, 73, 1097-106.
- RYZHOV, S., MCCALED, J. L., GOLDSTEIN, A. E., BIAGGIONI, I. & FEOKTISTOV, I. 2007. Role of adenosine receptors in the regulation of angiogenic factors and neovascularization in hypoxia. *J Pharmacol Exp Ther*, 320, 565-72.
- SACHIDANANDAN, C., YEH, J. R., PETERSON, Q. P. & PETERSON, R. T. 2008. Identification of a novel retinoid by small molecule screening with zebrafish embryos. *PLoS One*, 3, e1947.
- SALMON, J. E. & CRONSTEIN, B. N. 1990. Fc gamma receptor-mediated functions in neutrophils are modulated by adenosine receptor occupancy. A1 receptors are stimulatory and A2 receptors are inhibitory. *J Immunol*, 145, 2235-40.
- SALON, J. A., LODOWSKI, D. T. & PALCZEWSKI, K. 2011. The significance of G protein-coupled receptor crystallography for drug discovery. *Pharmacol Rev*, 63, 901-37.

## Bibliography

---

- SALVATORE, C. A., TILLEY, S. L., LATOUR, A. M., FLETCHER, D. S., KOLLER, B. H. & JACOBSON, M. A. 2000. Disruption of the A(3) adenosine receptor gene in mice and its effect on stimulated inflammatory cells. *J Biol Chem*, 275, 4429-34.
- SCHENONE, M., DANCİK, V., WAGNER, B. K. & CLEMONS, P. A. 2013. Target identification and mechanism of action in chemical biology and drug discovery. *Nat Chem Biol*, 9, 232-40.
- SCHMITT, S. M., GULL, M. & BRANDLI, A. W. 2014. Engineering *Xenopus* embryos for phenotypic drug discovery screening. *Adv Drug Deliv Rev*, 69-70, 225-46.
- SCHUERMANN, A., HELKER, C. S. & HERZOG, W. 2014. Angiogenesis in zebrafish. *Semin Cell Dev Biol*, 31, 106-14.
- SCHULTE, G. & LEVY, F. O. 2007. Novel aspects of G-protein-coupled receptor signalling--different ways to achieve specificity. *Acta Physiol (Oxf)*, 190, 33-8.
- SCHULZ, M. M., REISEN, F., ZGRAGGEN, S., FISCHER, S., YUEN, D., KANG, G. J., CHEN, L., SCHNEIDER, G. & DETMAR, M. 2012. Phenotype-based high-content chemical library screening identifies statins as inhibitors of in vivo lymphangiogenesis. *Proc Natl Acad Sci U S A*, 109, E2665-74.
- SHARP, D. J. & ROSS, J. L. 2012. Microtubule-severing enzymes at the cutting edge. *J Cell Sci*, 125, 2561-9.
- SHETH, S., BRITO, R., MUKHERJEA, D., RYBAK, L. P. & RAMKUMAR, V. 2014. Adenosine receptors: expression, function and regulation. *Int J Mol Sci*, 15, 2024-52.
- SHIH, T. & LINDLEY, C. 2006. Bevacizumab: an angiogenesis inhibitor for the treatment of solid malignancies. *Clin Ther*, 28, 1779-802.
- SMRCKA, A. V. 2008. G protein betagamma subunits: central mediators of G protein-coupled receptor signaling. *Cell Mol Life Sci*, 65, 2191-214.
- SNYDER, S. H., KATIMS, J. J., ANNAU, Z., BRUNS, R. F. & DALY, J. W. 1981. Adenosine receptors and behavioral actions of methylxanthines. *Proc Natl Acad Sci U S A*, 78, 3260-4.
- STACKER, S. A., WILLIAMS, S. P., KARNEZIS, T., SHAYAN, R., FOX, S. B. & ACHEN, M. G. 2014. Lymphangiogenesis and lymphatic vessel remodelling in cancer. *Nat Rev Cancer*, 14, 159-72.
- SUN, D., SAMUELSON, L. C., YANG, T., HUANG, Y., PALIEGE, A., SAUNDERS, T., BRIGGS, J. & SCHNERMANN, J. 2001. Mediation of tubuloglomerular feedback by adenosine: evidence from mice lacking adenosine 1 receptors. *Proc Natl Acad Sci U S A*, 98, 9983-8.
- TENG, B., LEDENT, C. & MUSTAFA, S. J. 2008. Up-regulation of A 2B adenosine receptor in A 2A adenosine receptor knockout mouse coronary artery. *J Mol Cell Cardiol*, 44, 905-14.
- TESMER, J. J. 2016. Hitchhiking on the heptahelical highway: structure and function of 7TM receptor complexes. *Nat Rev Mol Cell Biol*, 17, 439-50.

## Bibliography

---

- THIELE, A., KRONSTEIN, R., WETZEL, A., GERTH, A., NIEBER, K. & HAUSCHILDT, S. 2004. Regulation of adenosine receptor subtypes during cultivation of human monocytes: role of receptors in preventing lipopolysaccharide-triggered respiratory burst. *Infect Immun*, 72, 1349-57.
- TITUS, S. A., BEACHAM, D., SHAHANE, S. A., SOUTHALL, N., XIA, M., HUANG, R., HOOTEN, E., ZHAO, Y., SHOU, L., AUSTIN, C. P. & ZHENG, W. 2009. A new homogeneous high-throughput screening assay for profiling compound activity on the human ether-a-go-go-related gene channel. *Anal Biochem*, 394, 30-8.
- TYNDALL, J. D. & SANDILYA, R. 2005. GPCR agonists and antagonists in the clinic. *Med Chem*, 1, 405-21.
- UNAL, H. & KARNIK, S. S. 2012. Domain coupling in GPCRs: the engine for induced conformational changes. *Trends Pharmacol Sci*, 33, 79-88.
- VASQUEZ, R. J., HOWELL, B., YVON, A. M., WADSWORTH, P. & CASSIMERIS, L. 1997. Nanomolar concentrations of nocodazole alter microtubule dynamic instability in vivo and in vitro. *Mol Biol Cell*, 8, 973-85.
- VITZTHUM, H., WEISS, B., BACHLEITNER, W., KRAMER, B. K. & KURTZ, A. 2004. Gene expression of adenosine receptors along the nephron. *Kidney Int*, 65, 1180-90.
- WANG, Y., ZHANG, H., GIGANT, B., YU, Y., WU, Y., CHEN, X., LAI, Q., YANG, Z., CHEN, Q. & YANG, J. 2016. Structures of a diverse set of colchicine binding site inhibitors in complex with tubulin provide a rationale for drug discovery. *FEBS J*, 283, 102-11.
- WEI, C. J., LI, W. & CHEN, J. F. 2011. Normal and abnormal functions of adenosine receptors in the central nervous system revealed by genetic knockout studies. *Biochim Biophys Acta*, 1808, 1358-79.
- WEIS, S. M. & CHERESH, D. A. 2011. Tumor angiogenesis: molecular pathways and therapeutic targets. *Nat Med*, 17, 1359-70.
- WHEELER, G. N. & BRANDLI, A. W. 2009. Simple vertebrate models for chemical genetics and drug discovery screens: lessons from zebrafish and *Xenopus*. *Dev Dyn*, 238, 1287-308.
- WISE, A., GEARING, K. & REES, S. 2002. Target validation of G-protein coupled receptors. *Drug Discov Today*, 7, 235-46.
- WOOTEN, D., CHRISTOPOULOS, A. & SEXTON, P. M. 2013. Emerging paradigms in GPCR allostery: implications for drug discovery. *Nat Rev Drug Discov*, 12, 630-44.
- WORZFELD, T., WETTSCHURECK, N. & OFFERMANN, S. 2008. G(12)/G(13)-mediated signalling in mammalian physiology and disease. *Trends Pharmacol Sci*, 29, 582-9.
- XU, F., WU, H., KATRITCH, V., HAN, G. W., JACOBSON, K. A., GAO, Z. G., CHEREZOV, V. & STEVENS, R. C. 2011. Structure of an agonist-bound human A2A adenosine receptor. *Science*, 332, 322-7.

## Bibliography

---

- YAAR, R., JONES, M. R., CHEN, J. F. & RAVID, K. 2005. Animal models for the study of adenosine receptor function. *J Cell Physiol*, 202, 9-20.
- YAMAGUCHI, D., TERAYAMA, R., OMURA, S., TSUCHIYA, H., SATO, T., ICHIKAWA, H. & SUGIMOTO, T. 2014. Effect of adenosine A1 receptor agonist on the enhanced excitability of spinal dorsal horn neurons after peripheral nerve injury. *Int J Neurosci*, 124, 213-22.
- YAN, L. & MULLER, C. E. 2004. Preparation, properties, reactions, and adenosine receptor affinities of sulfophenylxanthine nitrophenyl esters: toward the development of sulfonic acid prodrugs with peroral bioavailability. *J Med Chem*, 47, 1031-43.
- YANG, J. N., BJORKLUND, O., LINDSTROM-TORNQVIST, K., LINDGREN, E., ERIKSSON, T. M., KAHLSTROM, J., CHEN, J. F., SCHWARZSCHILD, M. A., TOBLER, I. & FREDHOLM, B. B. 2009. Mice heterozygous for both A1 and A(2A) adenosine receptor genes show similarities to mice given long-term caffeine. *J Appl Physiol (1985)*, 106, 631-9.
- YUAN, G., GEDEON, N. G., JANKINS, T. C. & JONES, G. B. 2015. Novel approaches for targeting the adenosine A2A receptor. *Expert Opin Drug Discov*, 10, 63-80.
- ZEZULA, J. & FREISSMUTH, M. 2008. The A(2A)-adenosine receptor: a GPCR with unique features? *Br J Pharmacol*, 153 Suppl 1, S184-90.
- ZHOU, J. & GIANNAKAKOU, P. 2005. Targeting microtubules for cancer chemotherapy. *Curr Med Chem Anticancer Agents*, 5, 65-71.
- ZHU, W., LEE, C. Y., JOHNSON, R. L., WICHTERMAN, J., HUANG, R. & DEPAMPHILIS, M. L. 2011. An image-based, high-throughput screening assay for molecules that induce excess DNA replication in human cancer cells. *Mol Cancer Res*, 9, 294-310.

## Acknowledgements

I would like to thank the following persons who contributed in many different ways towards the successful completion of my PhD thesis project.

**Prof. Dr. André Brändli**, I would like to express my sincere gratitude to you for accepting me in your laboratory and for your continuous support during my research work. Your guidance helped me to understand different biological processes, and showed me how to think about what questions are worth asking in biomedical. Thank you for your constructive advice with regard to my experimental work and being so helpful in correcting my thesis. I wholeheartedly express that your guidance proved pivotal for the success of my project and your immense knowledge improved my scientific vision tremendously.

**Prof. Dr. Michael Detmar & Dr. Adriana Primorac** (Institute of Pharmaceutical Sciences, ETH Zurich, Switzerland), I would like to thank both you for agreeing to conduct the endothelial cell sprouting and proliferation experiments, which provided essential insight into the *in vitro* activities of the test compounds.

**Prof. Dr. Raffaella Giavazzi & Dr. Valentina Scarlato**, (Mario Negri Institute for Pharmacological Research, Milan, Italy), thank you for testing our lead compounds on cancer cell lines and in mouse xenograft models. This data will be included in a future publication.

**Stefan Schmitt**, for the many intellectual conversations covering various topics, for stimulating discussions, and for successfully collaborating with me on several other unrelated research projects.

**Drs. Bernd Uhl & Angela Kurz**, for being so helpful during the planning and execution of the FACS experiments and the subsequent data analysis.

**Sabine D'Avis**, for excellent technical assistance, for taking care of reagent orders, for maintaining the frog colony, and for always offering a helpful hand.

**Kerstin Kraus**, for helping me to recover lost orders (which happened a lot), for making phone calls to arrange appointments with the German authorities, and for correcting my terrible German whenever needed.

## Acknowledgements

---

I also want to thank **Prof. Dr. Ulrich Pohl** and the many other colleagues I got to meet during my years at the Walter-Brendel-Zentrum für Experimentelle Medizin. Their help, support, and friendship made all the difference!

Last but not the least; I would like to express my sincere gratitude to my family: my mother **Salma Rasheed**, my father **Mian Abdul Rasheed**, my brothers, my sister and my beloved wife **Maseerah**. Their prayers, persistent support, and regular words of encouragement had made everything so much easier during the execution of the project work, and I therefore dedicate this work to them.

## Deklaration

Ich erkläre an Eides statt,

dass ich die vorliegende Dissertation mit dem Thema:

***In vivo* pharmacological profiling in *Xenopus* embryos defines a subset of A<sub>1</sub> adenosine receptor-selective antagonists with potent anti-angiogenic activities**

selbständig verfasst, mich ausser der angegebenen keiner weiteren Hilfsmittel bedient und alle Erkenntnisse, die aus dem Schrifttum ganz oder annähernd übernommen sind, als solche kenntlich gemacht und nach ihrer Herkunft unter Bezeichnung der Fundstelle einzeln nachgewiesen habe.

Ich erkläre des Weiteren, dass die hier vorgelegte Dissertation nicht in gleicher oder in ähnlicher Form bei einer anderen Stelle zur Erlangung eines akademischen Grades eingereicht wurde.

München, den 11.07.2017

Mazhar Gull

## Appendix

### Abbreviation

7CH	7-Chloro-4-hydroxy-[1,8] naphthyridine
7CN	7-chloro-4-hydroxy-2-phenyl-1, 8-naphthyridine
7MN	7-Methyl-2-phenyl-1, 8-naphthyridin-4(1 <i>H</i> )-one (7-MN)
7 TM	7 transmembrane
Ado	Adenosine
ADA	Adenosine deaminase
ADP	Adenosine diphosphate
ADME	Absorption, distribution, metabolism, and excretion
AGTR	Angiotensin receptors
ALH	Anterior lymph heart
ALS	Anterior lymph sac
AMP	Adenosine monophosphate
Ang	Angiopietin
ARs	Adenosine receptors
ATP	Adenosine triphosphate
AURK	Aurora kinase
bFGF	Fibroblast factor
cAMP	Cyclic AMP
CBS	Colchicine-binding site
CCR	Chemokine receptors
CNR	Cannabinoid
CPA	Cyclopentyladenosine
CRD	Cysteine-rich domains
CT	Connecting tubule
DEPX	1, 3-Diethyl-8-phenylxanthine
DPPX,	1, 3-Dipropyl-8- phenylxanthine
DMPX	1, 3-Dimethyl-8-phenylxanthine
DMSO	Dimethyl sulfoxide
DPSPX	1, 3-Dipropyl-8-(sulfophenyl) xanthine
DT	Distal tubule
EC	Extracellular
EC <sub>50</sub>	Half of effective concentration
EC <sub>max</sub>	Concentration with maximum effect
ECL	Extracellular loop

## Appendix

---

ECD	Extracellular domains
EDNR	Endothelin
ENTPD1	Ectonucleoside triphosphate diphosphohydrolase 1
ERK	Extracellular signal-regulated kinase
FA	Formamide
FCF	Fetal Calf serum
FCM	Flow cytometer
FDA	Food and Drug Administration
FDZs	Frizzled receptors
FGF	Fibroblast growth factor
FSHR	Follicle stimulating hormone receptor
GAIN	GPCR autoproteolysis-inducing domains
G proteins	Guanosine nucleotide-binding proteins
GEFs	Guanine-nucleotide exchange factors
GIRK	G-protein-coupled inwardly rectifying potassium
GPCRs	Guanylyl – nucleotide - binding protein-coupled receptors
GRKs	GPCR kinases
GPS	GPCR proteolytics
GRMs	Metabotropic glutamate receptors
HAS	Human serum albumin
HB	Hybridization buffer
hERG	Human ether-a-go-go-related gene
HIF	Hypoxia-inducible factor
Hpf	Hours post fertilization
HUVECs	Human umbilical vein endothelial cells
ICL	Intercellular loop
IL	Interleukin
IP <sub>3</sub>	Inositol-triphosphate
IT	Intermediate tubule
ISVs	Intersomitic veins
JNK	C-jun N-terminal kinase
KCl	Potassium chloride
LC <sub>50</sub>	Half of lethal concentration
LECs	Lymphatic endothelial cells
MAB	Maleic Acid buffer
MAPK	Mitogen-activated protein kinase
MCD	Mitotic cell death

## Appendix

---

MCHR	Melanin-concentrating hormone receptors
MgSO <sub>4</sub>	Magnesium sulfate
MMR	Marc's Modified Ringers
NaCl	Sodium chloride
Noc	Nocodazole
NPY	Neuropeptide
P2Y	Purinergic receptors
PBS	Phosphate buffered saline
PCVs	Posterior cardinal veins
PET	Positron emission tomography
PDE	Phosphodiesterases
PI	Propidium Iodide
PI3	Phosphoinositide 3-kinase
PIP	Phosphatidylinositol bisphosphate
PLC	Phospholipase C
PLVs	Posterior lymph vessels
PT	Proximal tubule
PTW	PBS tween 20
RCC	Renal cell carcinoma
RHO	Rhodopsin
RT	Room temperature
S1P	Sphingosine-1-phosphate
SAR	Structure activity relationship
SSC	Saline-sodium citrate
SMC	Smooth muscles cell
T2R	Taste 2 receptors
TM	Transmembrane
TSP	Thrombospondin
VDA	Vascular disruption agents
VFD	Venus fly trap domains
VEGF	Vascular endothelial growth factor
VVNs	Vitelline vein networks

# Mazhar Gull

## Curriculum Vitae

### Academic Education

2010-present	<b>Graduate Student in Natural Sciences.</b> Walter Brendel Centre of Experimental Medicine, Ludwig Maximilians University Munich, Planegg-Martinsried, Germany
2008-2009	<b>Master of Science: Molecular Biology.</b> University of Skövde, Skövde, Sweden
2005-2007	<b>Master of Science: Biological Sciences.</b> Quaid-i-Azam University, Islamabad, Pakistan
2002-2004	<b>Bachelor of Science: Biological Sciences.</b> Government College University, Lahore, Pakistan

### PhD Thesis

Title	<i>In vivo</i> pharmacological profiling in <i>Xenopus</i> embryos defines a subset of A <sub>1</sub> adenosine receptor-selective antagonists with potent anti-angiogenic activities
Supervisor	Prof. Dr. André Brändli
Institution	Walter Brendel Centre of Experimental Medicine, Ludwig Maximilians University Munich, Planegg-Martinsried, Germany

### Master Thesis

Title	Collective chemotaxis requires contact dependent polarity
Supervisor	Prof. Dr. Roberto Mayor
Institution	Department of Cell & Developmental Biology, University College London, United Kingdom

### Research Skills

Software	MS Office, Sigma Plot, Graph Pad, Prism, ImageJ, Adobe Photoshop & Illustrator, Lasergene
Molecular Biology	DNA and RNA isolation, spectrophotometric quantification, reverse transcription and Real-Time PCR, cloning of fusion protein and "site directed" mutagenesis, genome modification (via TALENs and CRISPR/Cas) sequencing, genotyping
Cell and Developmental Biology	Cell culture, Whole mount <i>in situ</i> hybridization, use of morpholoni induced translational regulation, immunohistological staining, FACS, Confocal and fluorescent microscopy, <i>in vitro</i> fertilization, microinjection

*In Vivo & in vitro* experience Handling and implementation of *Xenopus* as a disease model for drug discovery. Potency testing of compounds using cell culture and *Xenopus* embryos

---

### Languages

Urdu	Native speaker
English	Fluent
German	B1.1

---

### Projects Worked On

- Systematic mapping of human renal diseases genes in *Xenopus* embryos
- GPR56 involvement in kidney organogenesis (*Xenopus* embryos)
- *Xenopus* embryos as a model for rare inherited renal disease polycystic kidney disease (PKD2)
- *Xenopus* embryos as a model for hair cell toxicity screen in collaboration with Stefan Schmitt

---

### Publications

- SCHMITT, S. M., GULL, M. & BRANDLI, A. W. 2014. Engineering *Xenopus* embryos for phenotypic drug discovery screening. *Adv Drug Deliv Rev*, 69-70, 225-246.
- DIETZEL, S., PIRCHER, J., NEKOLLA, A. K., GULL, M., BRANDLI, A. W., POHL, U. & REHBERG, M. 2014. Label-free determination of hemodynamic parameters in the microcirculation with third harmonic generation microscopy. *PLoS One*, 9, e99615.
- SAUERT, K., KAHNERT, S., ROOSE, M., GULL, M., BRANDLI, A. W., RYFFEL, G. U. & WALDNER, C. 2012. Heat-shock mediated overexpression of HNF1beta mutations has differential effects on gene expression in the *Xenopus* pronephric kidney. *PLoS One*, 7, e33522.
- THEVENEAU, E., MARCHANT, L., KURIYAMA, S., GULL, M., MOEPPS, B., PARSONS, M. & MAYOR, R. 2010. Collective chemotaxis requires contact-dependent cell polarity. *Dev Cell*, 19, 39-53.